

UC Santa Cruz

UC Santa Cruz Electronic Theses and Dissertations

Title

Structural and Therapeutic Investigations of Human Lipoxygenase

Permalink

<https://escholarship.org/uc/item/34p7m3mg>

Author

Hoobler, Eric Kerstan

Publication Date

2013

Peer reviewed|Thesis/dissertation

UNIVERSITY OF CALIFORNIA

SANTA CRUZ

**STRUCTURAL AND THERAPEUTIC INVESTIAGIONS OF HUMAN
LIPOXYGENASE**

A dissertation submitted in partial satisfaction
of the requirements for the degree of

DOCTOR OF PHILOSOPHY

in

CHEMISTRY

By

Eric Kerstan Hoobler

March 2013

The Dissertation of Eric Kerstan
Hoobler is approved:

Professor Roberto A. Bogomolni, chair

Professor Theodore R. Holman

Professor Ólöf Einarsdóttir

Tyrus Miller
Vice Provost and Dean of Graduate Studies

Copyright © by

Eric Hoobler

2013

Table of contents

List of Figures.....	iv
List of Tables.....	v
Abstract.....	vi
Acknowledgements.....	viii
Chapter 1 Introduction.....	1
Chapter 2 Investigations into the PLAT domain and the allosteric binding site of human epithelial 15-lipoxygenase-2.....	26
Chapter 3 Discovery of a novel dual fungal cyp51/human 5-lipoxygenase inhibitor: Implications for anti-seborrhoeic dermatitis therapy.....	63
Chapter 4 Pseudoperoxidase investigations of hydroperoxides and inhibitors of human lipoxygenases.....	100

List of figures

Chapter 1

Figure 1.1.....15

Chapter 2

Figure 2.1.....47

Figure 2.2.....48

Figure 2.3.....49

Figure 2.4.....50

Figure 2.5.....51

Figure 2.6.....52

Chapter 3

Figure 3.1.....82

Figure 3.2.....83

Figure 3.3.....84

Figure 3.4.....85

Chapter 4

Figure 4.1.....116

Figure 4.2.....117

List of tables

Chapter 2

Table 2.1.....	53
Table 2.2.....	54
Table 2.3.....	55
Table 2.4.....	56
Table 2.5.....	57

Chapter 3

Table 3.1.....	86
Table 3.2.....	87
Table 3.3.....	88
Table 3.4.....	89
Table 3.5.....	90

Chapter 4

Table 4.1.....	118
Table 4.2.....	119
Table 4.3.....	120
Table 4.4.....	121

Abstract

STRUCTURAL AND THERAPEUTIC INVESTIAGIONS OF HUMAN LIPOXYGENASE

Eric K. Hoobler

The research in this dissertation describes the investigations of potential therapeutics as well as structural and allosteric properties of human lipoxygenases. Lipoxygenases (LOX) are a ubiquitous enzyme found in plants and mammals, of which are responsible for regulation of inflammation in humans. Uncontrolled inflammation in humans may result in various types of cancers and inflammatory diseases, for which LOX is implicated. This has prompted the Holman lab to explore a diverse range on potential therapeutic targets in hopes of discovery of novel selective LOX inhibitors, while concurrently investigating the structural and kinetic properties of the enzyme.

Through use of conventional kinetic and structural studies we investigated the role of the polycystin-1 lipoxygenase alpha-toxin (PLAT) domain's role in enzyme catalysis and allosteric regulation. Previous studies had implicated the PLAT domain as being a critical aspect of the allosteric binding site. This theory was explored through extensive investigations into the resulting effects elicited by removal of the PLAT domain from human epithelial 15-lipoxygenase-2 (15-LOX-2). In chapter 2 we

present our findings supporting our previous concept, that indeed the PLAT domain plays a key role in the allosteric properties of 15-LOX-2.

Chapter 3 describes collaboration with the National Institutes Chemical Genomic Center, where we report the discovery of a novel dual inhibitor targeting fungal sterol 14 α -demethylase (CYP51 or Erg11) and human 5-lipoxygenase (5-LOX) with improved potency against 5-LOX due to its reduction of the iron center by its phenylenediamine core. The phenylenediamine core was then translated into the structure of ketoconazole, a highly effective anti-fungal medication for seborrheic dermatitis, to generate a novel compound, ketaminazole. Ketaminazole was found to be a potent dual selective inhibitor against human 5-LOX and CYP51 in vitro.

Understanding the mode of action of lipoxygenase (LOX) inhibitors is critical to determining their efficacy in the cell. The pseudoperoxidase assay is an important tool for establishing if an inhibitor is reductive in nature. In chapter 4, we evaluate the effectiveness of two distinct pseudoperoxidase methods in characterizing known inhibitor's redox properties; the "234 nm" decomposition and xylenol orange assay. In addition, we identified rapid inactivation occurring with particular inhibitors in the pseudoperoxidase assay. To account for the resulting inaccuracy attributed to this inhibitor dependent inactivation, we modified the pre-existing "234 nm" assay allowing for observation of this inactivation.

Acknowledgements

First I would like to thank my dissertation advisor, Professor Theodore Holman, for all of his support; encouragement and helping me develop a strong foundation in the field of biochemistry. Second I would like to thank the chair of my committee, Professor Roberto Bogomolni, and committee member Professor Ólöf Einarsson, whom have been great assets throughout my education within the graduate program.

I am extremely grateful to all the past and present members of the Holman lab, who helped with direction and motivation: Josh Deschamps, Aaron Weckler, Victor Kenyon, Stephen Perry, Netra Joshi, Christopher J. Smyrniotis, Kenny Ikea, Brian Jameson, Charles Holz.

I would also like to thank all of my closest friends that have allowed life outside the lab to be full of great experiences and memories: Forest, Josh, Clint, Bob, Mark, Doug, Kari, Micah, Zack H., Zack S., Aaron, Victor, and Steve.

Finally I would like to thank my family for their continued support through these years, especially my wife Carly for here patience and dedication. I wanted to say thanks to my sisters; Sonya, Jenny and Rebecca for their love and support. I would also like to thank my father for all his guidance and wisdom, he has shared with me allowing me to excel and weather the tough times.

Chapter 1

Introduction

1.1 Lipoxygenase

Lipoxygenase (LOX) plays an essential role in processing polyunsaturated fatty acids containing a cis-double bond in both plants, fungi, and animals, which initiates the biosynthesis of important mediators of physiological processes [1,2,3]. LOXs consist of a family of iron-containing metalloenzymes, which utilize a non-heme catalytic center to catalyze the dioxygenation of 1,4-cis,cis-pentadiene-containing polyunsaturated fatty acids (e.g., linoleic acid (LA) and arachidonic acid (AA)) to form hydroperoxy-fatty acids. These hydroperoxy-polyunsaturated fatty acids regulate the inflammatory response in humans [4], and are implicated in a variety of human diseases, such as asthma, psoriasis, atherosclerosis and cancer [5,6,7].

LOX activates the substrate for incorporation of dioxygen into 1,4-cis,cis-pentadiene-containing fatty acids, which generates the chiral (E,Z) conjugated hydroperoxide product [8,9,10]. LOX catalytic cycle is facilitated through use of its iron center. The resting state of the enzyme is in the ferrous oxidation state and is inactive. Activation occurs upon oxidation of iron to its ferric state, through use of concurrent reduction of one equivalence of the hydroperoxy-fatty acid product, reflecting product feedback activation. The activated ferric ion oxidizes the 1,4-diene

of the substrate to a pentadienyl radical that reacts with dioxygen to yield the S-configuration of the hydroperoxide product [11] (**Figure 1.1**).

1.1.2 Mammalian LOX

The nomenclature for denoting mammalian LOXs reflects the prototypical tissue of their occurrence and oxidized carbon of their respective hydroperoxyeicosatetraenoic acid (HPETE) product, from AA, with 5-, 12-, and 15-LOX being the predominant isozymes. Interestingly, LOXs generating a particular hydroperoxidation product do not necessarily demonstrate high sequence homology, as witnessed with human reticulocyte 15-LOX-1 having 25% identity to soybean LOX-1, 35% identity to human epidermal 15-LOX-2, and 80% identity to rabbit reticulocyte 15-LOX, yet all generate predominately 15-HPETE [12].

The biochemistry of human LOX's role in maintaining inflammatory response homeostasis is complicated by their diverse tissue and cellular localization [1,2,13]. 5-LOX activation of leukocytes triggers the upregulation of leukotriene production, which provokes bronchioconstriction [14,15,16] and linked to certain types of cancer [17,18,19] and asthma [7,15]. Reticulocyte 15-LOX-1 has been shown to oxidize membrane lipids during red blood cell maturation [20,21], and has been implicated in colorectal [22,23], atherosclerosis [24], and prostate cancer [25,26,27]. 15-LOX-1 is also associated with both resolving and promoting human disease, as witnessed by its down-regulation in colorectal cancer progression and up-regulation in prostate cancer progression. Epithelial 15-LOX-2 is found to be expressed in hair, prostate, lung, and

cornea [28,29] and its down-regulation is correlated with progression of prostate cancer [30,31]. Epidermis 12-(R)-LOX is expressed in the skin and, if mutated, has been shown to result in non-bullous congenital ichthyosiform erythroderma [32]. Up-regulation of platelet-type 12-(S)-LOX affects platelet adhesion and prostate cancer metastasis [26]. It has also been implicated in skin disease [33], pancreatic [34], breast [35,36], diabetes [37] and blood coagulation [38] and platelet activation [39,40].

1.2 Allostery

Allosteric regulation of protein activity is a common phenomenon in biology, one of the most fundamental examples is hemoglobin, an iron-containing oxygen transport metalloprotein found within red blood cells. The quaternary structure of hemoglobin of most vertebrates is an assembly of four globular protein subunits. Individual subunits are shown to influence O₂ binding properties of adjacent neighbors via cooperative allostery [41]. Allostery can be reflected via alterations in substrate specificity, as seen with ribonucleotide reductase (RNR) [42]. RNR synthesizes all four deoxyribonucleoside triphosphates (dNTPs) through reduction of the 2'-OH of the respective ribonucleotide, and the ability of RNR to allosterically regulate substrate specificity enables it to maintain homeostatic balance of all four dNTPs. This rapid adaptation to changes in dNTP requirements allows for proportionate amounts of each nucleotide to be present, ensuring efficient DNA replication and repair [42,43]. Allosteric regulation is an essential property in nature,

allowing for the delicate modulation of enzymatic activity and/or substrate specificity to occur, both characteristics found in the LOX family of enzymes.

1.2.1 5-LOX ATP and Ca²⁺ allosteric properties

Allosteric regulation of enzymes is a critical process in biochemistry [44,45,46] and has recently emerged as an increasingly important aspect of LOX activity [47]. Allosteric regulation of lipoxygenase was first demonstrated with 5-LOX, which was shown to possess secondary binding sites for both ATP and Ca²⁺ [67]. Kinetic studies have demonstrated that calcium is required for catalytic activity, while the binding of ATP synergistically increases the catalytic activity of calcium-bound enzyme [49,50,51], 100 μM ATP was sufficient to elicit maximal effect [52]. The ATP and Ca²⁺ rate enhancement resulted in a 5-fold activation for the human LOX [53] and up to 300-fold activation for the rat 5-LOX [55]. It was determined that hydrolysis of the phosphodiester bond within ATP had no influence on activation, as reflected by equal effects provoked by ADP and AMP [53,54]. The N-terminal domain of LOX assumes a β-barrel structure, commonly referred to as the polycystin-1, lipoxygenase, alpha-toxin (PLAT) domain (i.e. the beta domain). The PLAT domain of 5-LOX was found to be highly negatively charged and Ca²⁺ was proposed to neutralize the charge in concert with interactions by the head groups of phosphate in the phosphatidyl membrane [56]. Ca²⁺ also appears to increase the hydrophobicity of the domain via exposing tryptophans 13 and 75 [57].

1.2.2 15-LOX allostery

Continued exploration in the field of LOX uncovered a divergent allosteric effect in the family of 15-LOX isozymes. Soybean lipoxygenase-1 (soybean LOX-1) and reticulocyte human 15-lipoxygenase (15-LOX-1) have been shown to contain allosteric sites, as demonstrated employing by the synthetic fatty acid oleyl sulfate (OS) in kinetic studies [58]. This work demonstrated that OS binds with considerable affinity to an allosteric binding site on both soybean LOX-1 ($K_D = 0.6 \mu\text{M}$) and 15-LOX-1 ($K_D = 0.4 \mu\text{M}$). This is seen by an increase in the kinetic isotope effect (KIE) of both enzymes in a saturating manner, mirroring their inhibition curves [58]. Further stopped-flow experiments demonstrated that binding of OS to sLO-1 did not interfere with enzyme activation, indicating that the allosteric site was not in the active site [59].

The role of the allosteric site was further refined by the discovery in the Holman laboratory that LOX products, such as 13-(S)-hydroxyoctadecadienoic acid (13-HODE), could bind to the allosteric site of both 15-LOX-1 and human epithelial 15-LOX-2 (15-LOX-2) and change the substrate specificity with respect to AA and linoleic acid (LA) [60,61]. The substrate specificity was shown to be pH dependent for 15-LOX-2, which was hypothesized to be due to a change in allosteric effector binding. A docking model was proposed, placing the allosteric binding pocket between the PLAT domain (i.e. the beta domain) [60,61] and the catalytic domain of 15-LOX-2. Specifically, the docking model suggested that the carboxylic acid of the

13-HODE interacted with a histidine at the bottom of the cleft between the two domains [60].

1.2.3 PLAT domain background

Plant and animal LOX isozymes demonstrate a conserved fundamental structure consisting of a single polypeptide chain which folds into two distinct domains, the catalytic domain often referred to as the C-terminal domain, and the N-terminal domain (PLAT). The PLAT domain is a conserved tertiary structure in various other membrane or lipid-associated proteins [62]. As mentioned previously, the catalytic domain contains a non-heme iron center while the PLAT domain has been shown to facilitate membrane binding [63,64,65]. Later studies revealed that truncation of the PLAT domain from human 12-LOX resulted in higher population of oligomers [63]. In addition, Kuhn and collaborators demonstrated that the removal of the PLAT domain triggered an increased frequency of auto-inactivation for rabbit 15-LOX-1 [66].

1.2.4 Homology modeling and No PLAT construct

The biochemical mechanism for allostery in LOX is still unknown, but a few hypotheses have been proposed. The extensive research conducted by the Holman lab in the characterization of LOX allosteric product feed-back, prompted exploration of homology models in hopes of revealing probable allosteric sites for biochemical targeting. As mentioned above, the cleft between the two domains was proposed to contain the allosteric site. We identified residue H627 as appropriately positioned to

bind the carboxylic moiety of 13-HPODE, which was further stabilized through a bifurcated hydrogen bond with residue R407 and Y408 [60,61]. This hypothesis was supported by earlier work implicating the PLAT domain as a fatty acid binding site, due to the localization of a substrate-linked photoreactive-azido group between the two domains when probing the 15-LOX catalytic site [48].

In order to test our hypothesis as to the location of the allosteric site, the PLAT domain was explored through extensive experimentation. PLAT domain mutants for human 15-LOX-2, were generated in hope of unraveling the origins of the allosteric regulation of LOX; in addition the mutant H627A, which replaced a histidine proposed to facilitate product binding. 15-LOX-2 No PLAT mutant was used to investigate membrane binding, oligomerization, auto-inactivation, and most importantly, what effect had been elicited with regard to allosteric properties. Structural data were obtained with circular dichroism, size exclusion chromatography, small angle x-ray, dynamic light scattering, and Western blotting. Kinetic data was gathered observing lipid and O₂ metabolism via steady state kinetics, competitive substrate capture HPLC analytical methods, and LTQ analysis for product specificity.

1.3 5-LOX biochemistry

Immune and inflammatory responses are mediated by leukotrienes (LTs), which serve a primary role in respiratory and cardiovascular diseases [4,5,54]. The precursor for LT biosynthesis is arachidonic acid (AA), which is stored in membrane-

phospholipids and released by phospholipase A2 (cPLA2) to be metabolized by 5-LOX in conjunction with 5-LOX-activating protein (FLAP). Reflective of the fact that 5-LOX catalyzes the rate limiting step in the biosynthesis of LTs, it serves as an ideal candidate for therapeutic intervention.

The incorporation of molecular oxygen into AA by 5-LOX generates 5(S)-hydroperoxy-6-trans-8,11,14-cis-eicosatetraenoic acid (5-HPETE), which is immediately reduced to the alcohol by glutathione reductase. 5LOX has a second activity converting the hydroperoxide of 5-HPETE to an unstable epoxide product, LTA₄. The unstable epoxide product LTA₄ is an intermediate to the production of LTB₄ by LTA₄ hydrolase, or is conjugated by LTC₄ synthase to glutathione to produce LTC₄. Upon LTC₄ release into the extracellular environment, amino-acid cleavage (g-glutamyl and glycine) can occur yielding LTD₄ and then LTE₄. LTC₄, LTD₄ and LTE₄ are often referred to as cysteinyl-LTs (cys-LTs), reflecting the presence of a cysteinyl residue within their structure.

The various LTs elicit distinct downstream responses mediated through selective receptors; LTB₄ interfaces with BLT1 and BLT2 receptors, CysLT1 and CysLT2 receptors interact with cys-LTs [68,69]. G-Protein Coupled Receptors (GPCRs) are also referred to as seven-transmembrane domain receptors, and G protein-linked receptors (GPLR) amplify signal transduction pathways. GPCRs mediate 5-H(P)ETE and 5-oxo-ETE responses, and have been implicated in asthma, allergic diseases, cancer, and cardiovascular disease [4,5,70].

Leukocyte activation is stimulated by LTB₄. It acts as a chemotactic and chemokinetic mediator, which triggers migration and activation of granulocytes/T cells and adherence of granulocytes to vessel walls, causing degranulation and release of cathelicidin LL-37 and superoxide [71]. This process, which results in the phagocytic activation of neutrophils and macrophages, as well as stimulation of immunoglobulins by lymphocytes [72,73], highlights the regulation of the immune response by LTB₄ in inflammatory diseases, such as arthritis, asthma and atherosclerosis [74]. Cys-LTs instigate smooth muscle contraction, mucus secretion, plasma extravasation, vasoconstriction, recruitment of eosinophils [72] and fibrocyte proliferation [75]. Imbalance in the homeostasis of Cys-LTs is linked to asthma, allergic rhinitis [7,15], chronic inflammation and regulation of the adaptive immune response [76].

1.3.1 5-LOX therapeutics

Reflecting the importance of 5-LOX in LT production in homeostasis, alternative methods for regulating as well as probing its biochemistry are essential for furthering our understanding on how to alleviate physiological imbalances [71-76]. Current compounds (inhibitors) employed for addressing elevated LT levels include: Zylflo (zileuton), a 5-LOX inhibitor, Xolair (omalizumab), a humanized antibody targeting the IgE receptor, MK-591, a FLAP inhibitor which stops 5-LOX activation, and Accolate (zafirlukast), a LT receptor antagonist [4,78-81].

There are three typical classifications for human 5-LOX inhibitors, reductive, iron chelative and active site binding inhibitors [4,14,82]. Zileuton contains an N-hydroxyurea, which is proposed to chelate to the enzyme's active site ferric ion and reduce it to the inactive ferrous ion [14,78]. In general, chelation/reduction is not considered an optimal mode of inhibition for a therapeutic because metal chelation tends to be a promiscuous behavior to other metalloproteins, and reductive inhibitors can be chemically inactivated in the cell [82]. Nevertheless, Zileuton has been shown to not only be selective for 5-LOX but also to be efficacious in the cell [83-84].

Interestingly, many of the chelative inhibitors, such as nordihydroguaiaretic acid (NDGA) [85,86] and Zileuton, are also reductive due to the facile nature of inner sphere electron reduction. Catechol moieties, present in NDGA, are postulated to reduce the ferric ion to the inactive ferrous state, concomitant with the oxidation of the catechol to semiquinone. This mechanism has been shown to occur with catechol dioxygenase, a metalloenzyme, whose catechol substrate is activated to the semiquinone by the active site ferric ion [86-88]. In contrast, the phenylenediamine derivatives do not possess chelators so their mode of action is most likely through long-range electron transfer, although yet no direct proof currently exists.

A novel 5-LOX inhibitor chemotype, phenylenediamine, was discovered while screening for LOX inhibitors in our lab. One unique property of the 5-LOX inhibitor chemotype, which we have characterized in this thesis, is that it employs redox chemistry similar to the commercially available 5-LOX inhibitor zileuton [78,84]. A

variety of the 80+ compounds within the Structure activity relationship (SAR) screen were evaluated using the pseudoperoxidase assay for redox properties. Extensive investigation was conducted to determine the chemotypes selectivity amongst the various LOX isozymes (5-LOX, 12-LOX, 15-LOX-1, and 15-LOX-2), in addition to COX 1 and COX 2. Human blood potency trials were conducted as well to determine efficacy. A known anti-fungal ketoconazole contained a similar scaffold and was modified to include the phenylenediamine core; this compound was then screened against the various LOX isozymes, COX 1, 2, and human and fungal sterol 14 α -demethylase (CYP51).

1.3.2 Determination of inhibitor mode of action

Discovery of novel drug targets is followed by a variety of analytical techniques to identify the mode of action of the compounds. For LOX this is accomplished through use of fundamental enzyme kinetics to evaluate whether the enzyme is a competitive, noncompetitive, mixed, or uncompetitive inhibitor. In particular, use of steady-state kinetics, which employs evaluation of inhibition curves at various substrate concentrations, allows one to measure the K_i values. A competitive inhibitor raises the K_m value for its substrate, with no change in the apparent V_{max} . An uncompetitive inhibitor will lower the apparent V_{max} , yet not affect the apparent K_m value for its substrate. Mixed inhibition is where both the apparent V_{max} and apparent K_m values change. Mixed-type inhibition has often been observed for LOX inhibitors, as reflected by modification of both the apparent V_{max} and K_m , yielding a K_i (catalytic

site binding) distinct from K_i (allosteric site binding). This common mode of LOX inhibition is most likely a result of its allosteric properties, because inhibitor binding to the allosteric site would affect catalysis. Inhibitors of LOX have frequently been shown to act through a reductive mechanism, namely, where the drug transfers one electron to the enzyme's catalytic iron center, converting it to the inactive iron (II) state; this property is characterized in detail in the following section.

1.3.3 Pseudoperoxidase assay

Understanding of the reductive properties of a particular inhibitor is important due to possible toxicity issues that may arise, such as triggering methemoglobin formation [89,90]. Not all reductive inhibitors display high toxicity, such as seen for AA-861 [91], and several topically active inhibitors (ionapalene [92]) display positive clinical results with no major toxicity indicated. In addition, reductive moieties, such as hydroxamic acids and hydroxyurea, act as radical scavengers as well, with the commercially available Zileuton containing a hydroxyurea motif [78].

One of the main methods for determining if an inhibitor is a reductive inhibitor is the pseudoperoxidase assay. This assay is an O_2 independent reaction, where lipoxygenase catalyzes fatty acid hydroperoxide decomposition with a reductant present to oxidize the iron back to its ferric form. A variety of reductive inhibitors can serve as substrates in this pseudoperoxidase reaction, such as N-hydroxyureas, hydroxybenzofurans, hydroxamic acids, hydroxylamines, and catechols [4,14,82]. The activity of these inhibitors is derived by their ability to reduce the Fe(III) enzyme

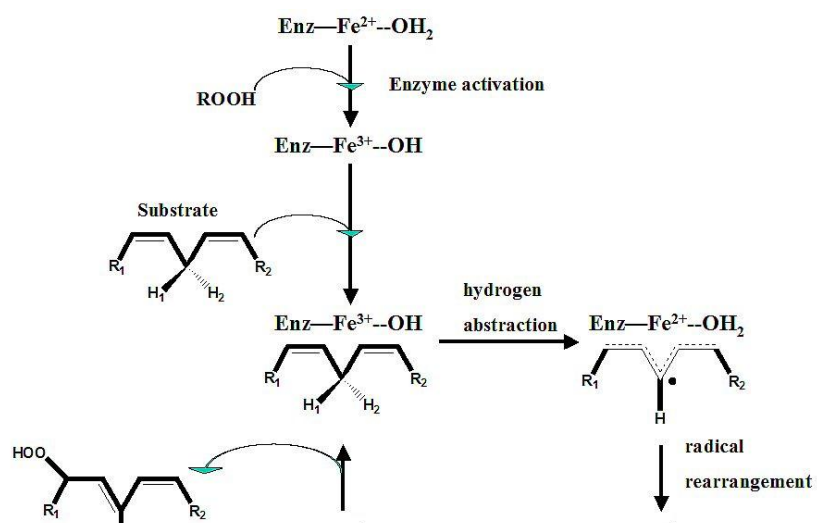
to the inactive Fe(II) state. This reaction involves a one-electron reduction of the fatty acid hydroperoxide, rather than the standard peroxidase reaction of two-electron reduction. The proposed products of this pseudoperoxidase reaction are an alkoxide radical and an inhibitor radical [82,93]. In the literature, these reductive inhibitors are more effective substrates for 5-LOX than the other LOX isozymes [93,94].

1.4 Scope of Dissertation

This dissertation summarizes three distinct investigations of lipoxygenase. Chapter 2 examines LOX allostery through the comparison of various modifications of 15-LOX-2 via extensive structural and kinetic experimentation. In particular, we have focused on a mutant with no PLAT domain to gain insight into its involvement in allostery and enzyme function. Chapter 3 presents structure activity investigations for a novel phenylenediamine inhibitor of 5-LOX. Over 80 distinct alterations to the core structure were examined, with one having the phenylenediamine core translated into the ketoconazole structure, a known anti-fungal. This novel compound demonstrates dual CYP51/5-LOX inhibitory properties, which could have ramifications for anti-fungal therapies. Chapter 4 investigates the pseudoperoxidase activity of LOX and examines the accuracy of the assay to characterize reductive inhibitors. We evaluated various isozymes, 5-LOX, 12-LOX, 15-LOX-1, and 15-LOX-2, using the colorimetric as well as UV spectroscopic pseudoperoxidase assay and found that both techniques are accurate in determining the reductant properties of most of the inhibitors.

Figures 1.5

Figure 1.1. The LOX reaction scheme.



1.5 References

1. Grechkin, A., Recent Developments in Biochemistry of the Plant Lipoxygenase Pathway. *Prog. Lipid Res.* **1998**, 37 (5), 317-352.
2. Funk, C. D., Prostaglandins and leukotrienes: Advances in eicosanoid biology [Review]. *Science* **2001**, 294 (5548), 1871-1875.
3. Yamamoto, S.; Suzuki, H.; Ueda, N., Arachidonate 12-lipoxygenases. *Prog Lipid Res* **1997**, 36 (1), 23-41.
4. Ford-Hutchinson, A. W.; Gresser, M.; Young, R. N., 5-Lipoxygenase. *Annu. Rev. Biochem* **1994**, 63, 383-417.
5. Kuhn, H.; Chaitidis, P.; Roffeis, J.; Walther, M., Arachidonic Acid metabolites in the cardiovascular system: the role of lipoxygenase isoforms in atherogenesis with particular emphasis on vascular remodeling. *J Cardiovasc Pharmacol* **2007**, 50 (6), 609-20.
6. Pace-Asciak, C. R.; Asotra, S., Biosynthesis, catabolism, and biological properties of HPETEs, hydroperoxide derivatives of arachidonic acid. *Free Radical Biology & Medicine* **1989**, 7 (4), 409-33.
7. Radmark, O.; Samuelsson, B., 5-lipoxygenase: regulation and possible involvement in atherosclerosis. *Prostaglandins Other Lipid Mediat* **2007**, 83 (3), 162-74.
8. Veldink, G. A.; Vliegthart, J. F. G., Lipoxygenases, Nonheme Iron-Containing Enzymes. *Adv. Inorg. Biochem.* **1984**, 6, 139-161.
9. Nelson, M. J.; Seitz, S. P., The Structure and Function of Lipoxygenase. *Curr. Op. Struc. Bio.* **1994**, 4 (6), 878-884.
10. Solomon, E. I.; Zhou, J.; Neese, F.; Pavel, E. G., New Insights from Spectroscopy into the structure/function relationships of lipoxygenases. *Chem. Biol.* **1997**, 4 (11), 795-808.
11. Gardner, H. W., Soybean Lipoxygenase-1 Enzymatically Forms Both (9S)-and (13S)-Hydroperoxides From Linoleic Acid by a pH-Dependent Mechanism. *Biochim. Biophys. Acta* **1989**, 1001, 274-281.

12. Walther, M.; Hofheinz, K.; Vogel, R.; Roffeis, J.; Kühn, H., The N-terminal β -barrel domain of mammalian lipoxygenases including mouse 5-lipoxygenase is not essential for catalytic activity and membrane binding but exhibits regulatory functions. *Archives of Biochemistry and Biophysics* **2011**, 516 (1), 1-9.
13. Jisaka, M.; Kim, R. B.; Boeglin, W. E.; Nanney, L. B.; Brash, A. R., Molecular cloning and functional expression of a phorbol ester-inducible 8S-lipoxygenase from mouse skin. *J Biol Chem* **1997**, 272 (39), 24410-6.
14. Pergola, C.; Werz, O., 5-Lipoxygenase inhibitors: a review of recent developments and patents. *Expert Opinion on Therapeutic Patents* **2010**, 20 (3), 355-375.
15. Brock, T. G., Regulating leukotriene synthesis: the role of nuclear 5-lipoxygenase. *J Cell Biochem* **2005**, 96 (6), 1203-11.
16. Newcomer, M. E.; Gilbert, N. C., Location, location, location: compartmentalization of early events in leukotriene biosynthesis. *J Biol Chem* **2010**, 285 (33), 25109-14.
17. Ghosh, J., Inhibition of arachidonate 5-lipoxygenase triggers prostate cancer cell death through rapid activation of c-Jun N-terminal kinase. *Biochem Biophys Res Commun* **2003**, 307 (2), 342-9.
18. Ghosh, J.; Myers, C. E., Inhibition of arachidonate 5-lipoxygenase triggers massive apoptosis in human prostate cancer cells. *Proc Natl Acad Sci U S A* **1998**, 95 (22), 13182-7.
19. Nakano, H.; Inoue, T.; Kawasaki, N.; Miyataka, H.; Matsumoto, H.; Taguchi, T.; Inagaki, N.; Nagai, H.; Satoh, T., Synthesis and biological activities of novel antiallergic agents with 5-lipoxygenase inhibiting action. *Bioorg. Med. Chem.* **2000**, 8 (2), 373-380.
20. van Leyen, K.; Duvoisin, R. M.; Engelhardt, H.; Wiedmann, M., A function for lipoxygenase in programmed organelle degradation. *Nature* **1998**, 395 (6700), 392-5.
21. Rapoport, S. M.; Schewe, T., The maturational breakdown of mitochondria in reticulocytes. *Biochim Biophys Acta* **1986**, 864 (3-4), 471-95.
22. Jones, R.; Adel-Alvarez, L. A.; Alvarez, O. R.; Broaddus, R.; Das, S., Arachidonic acid and colorectal carcinogenesis. *Mol Cell Biochem* **2003**, 253 (1-2), 141-9.

23. Kelavkar, U. P.; Cohen, C.; Kamitani, H.; Eling, T. E.; Badr, K. F., Concordant induction of 15-lipoxygenase-1 and mutant p53 expression in human prostate adenocarcinoma: correlation with Gleason staging. *Carcinogenesis* **2000**, 21 (10), 1777-87.
24. Shureiqi, I.; Lippman, S. M., Lipoxygenase modulation to reverse carcinogenesis. *Cancer Res* **2001**, 61 (17), 6307-12.
25. Hsi, L. C.; Wilson, L. C.; Eling, T. E., Opposing effects of 15-lipoxygenase-1 and -2 metabolites on MAPK signaling in prostate. Alteration in peroxisome proliferator-activated receptor gamma. *J Biol Chem* **2002**, 277 (43), 40549-56.
26. Shappell, S. B.; Manning, S.; Boeglin, W. E.; Guan, Y. F.; Roberts, R. L.; Davis, L.; Olson, S. J.; Jack, G. S.; Coffey, C. S.; Wheeler, T. M.; Breyer, M. D.; Brash, A. R., Alterations in lipoxygenase and cyclooxygenase-2 catalytic activity and mRNA expression in prostate carcinoma. *Neoplasia* **2001**, 3, 287-303.
27. Shappell, S. B.; Olson, S. J.; Hannah, S. E.; Manning, S.; Roberts, R. L.; Masumori, N.; Jisaka, M.; Boeglin, W. E.; Vader, V.; Dave, D. S.; Shook, M. F.; Thomas, T. Z.; Funk, C. D.; Brash, A. R.; Matusik, R. J., Elevated expression of 12/15-lipoxygenase and cyclooxygenase-2 in a transgenic mouse model of prostate carcinoma. *Cancer Res* **2003**, 63 (9), 2256-67.
28. Brash, A. R.; Boeglin, W. E.; Chang, M. S., Discovery of a second 15S-lipoxygenase in humans. *Proc Natl Acad Sci U S A* **1997**, 94 (12), 6148-52.
29. Gonzalez, A. L.; Roberts, R. L.; Massion, P. P.; Olson, S. J.; Shyr, Y.; Shappell, S. B., 15-Lipoxygenase-2 expression in benign and neoplastic lung: an immunohistochemical study and correlation with tumor grade and proliferation. *Hum Pathol* **2004**, 35 (7), 840-9.
30. Suraneni, M. V.; Schneider-Broussard, R.; Moore, J. R.; Davis, T. C.; Maldonado, C. J.; Li, H.; Newman, R. A.; Kusewitt, D.; Hu, J.; Yang, P.; Tang, D. G., Transgenic expression of 15-lipoxygenase 2 (15-LOX2) in mouse prostate leads to hyperplasia and cell senescence. *Oncogene* **2010**, 29 (30), 4261-75.
31. Tang, D. G.; Bhatia, B.; Tang, S.; Schneider-Broussard, R., 15-lipoxygenase 2 (15-LOX2) is a functional tumor suppressor that regulates human prostate epithelial cell differentiation, senescence, and growth (size). *Prostaglandins Other Lipid Mediat* **2007**, 82 (1-4), 135-46.

32. Jobard, F.; Lefevre, C.; Karaduman, A.; Blanchet-Bardon, C.; Emre, S.; Weissenbach, J.; Ozguc, M.; Lathrop, M.; Prud'homme, J. F.; Fischer, J., Lipoxygenase-3 (ALOXE3) and 12(R)-lipoxygenase (ALOX12B) are mutated in non-bullous congenital ichthyosiform erythroderma (NCIE) linked to chromosome 17p131. *Hum Mol Genet* **2002**, 11 (1), 107-13.
33. Hussain, H.; Shornick, L. P.; Shannon, V. R.; Wilson, J. D.; Funk, C. D.; Pentland, A. P.; Holtzman, M. J., Epidermis contains platelet-type 12-lipoxygenase that is overexpressed in germinal layer keratinocytes in psoriasis. *Am J Physiol* **1994**, 266 (1 Pt 1), C243-53.
34. Ding, X. Z.; Iversen, P.; Cluck, M. W.; Knezetic, J. A.; Adrian, T. E., Lipoxygenase inhibitors abolish proliferation of human pancreatic cancer cells. *Biochemical and Biophysical Research Communications* **1999**, 261 (1), 218-223.
35. Connolly, J. M.; Rose, D. P., Enhanced angiogenesis and growth of 12-lipoxygenase gene-transfected MCF-7 human breast cancer cells in athymic nude mice. *Cancer Lett* **1998**, 132 (1-2), 107-12.
36. Natarajan, R.; Nadler, J., Role of lipoxygenases in breast cancer. *Front. Biosci.* **1998**, 3, E81-88.
37. Ma, K.; Nunemaker, C. S.; Wu, R.; Chakrabarti, S. K.; Taylor-Fishwick, D. A.; Nadler, J. L., 12-Lipoxygenase Products Reduce Insulin Secretion and β -Cell Viability in Human Islets. *Journal of Clinical Endocrinology and Metabolism* **2010**, 95 (2), 887-93.
38. Thomas, C. P.; Morgan, L. T.; Maskrey, B. H.; Murphy, R. C.; Kuhn, H.; Hazen, S. L.; Goodall, A. H.; Hamali, H. A.; Collins, P. W.; O'Donnell, V. B., Phospholipid-esterified eicosanoids are generated in agonist-activated human platelets and enhance tissue factor-dependent thrombin generation. *Journal of Biological Chemistry* **2010**, 285 (10), 6891-903.
39. Holinstat, M.; Boutaud, O.; Apopa, P. L.; Vesci, J.; Bala, M.; Oates, J. A.; Hamm, H. E., Protease-activated receptor signaling in platelets activates cytosolic phospholipase A₂alpha differently for cyclooxygenase-1 and 12-lipoxygenase catalysis. *Arterioscler Thromb Vasc Biol* **2011**, 31 (2), 435-42.
40. Kaur, G.; Jalagadugula, G.; Mao, G.; Rao, A. K., RUNX1/core binding factor A2 regulates platelet 12-lipoxygenase gene (ALOX12): studies in human RUNX1 haplodeficiency. *Blood* **2010**, 115 (15), 3128-35.

41. Saffran, W. A.; Gibson, Q. H., The effect of pH on carbon monoxide binding to Menhaden hemoglobin. Allosteric transitions in a root effect hemoglobin. *Journal of Biological Chemistry* **1978**, 253 (9), 3171-3179.
42. Nordlund, P.; Reichard, P., Ribonucleotide reductases. *Annu Rev Biochem* **2006**, 75, 681-706.
43. Reichard, P., Ribonucleotide reductases: the evolution of allosteric regulation. *Arch Biochem Biophys* **2002**, 397 (2), 149-55.
44. Karginov, A. V.; Ding, F.; Kota, P.; Dokholyan, N. V.; Hahn, K. M., Engineered allosteric activation of kinases in living cells. *Nature biotechnology* **2010**, 28 (7), 743-747.
45. Cui, L.; Zhang, X.; Yang, R.; Liu, L.; Wang, L.; Li, M.; Du, W., Baicalein is neuroprotective in rat MCAO model: role of 12/15-lipoxygenase, mitogen-activated protein kinase and cytosolic phospholipase A2. *Pharmacol Biochem Behav* **2010**, 96 (4), 469-75.
46. Rouzer, C. A.; Samuelsson, B., The importance of hydroperoxide activation for the detection and assay of mammalian 5-lipoxygenase. *FEBS Lett* **1986**, 204 (2), 293-6.
47. Ivanov, I.; Shang, W.; Toledo, L.; Masgrau, L.; Svergun, D. I.; Stehling, S.; Gómez, H.; Di Venere, A.; Mei, G.; Lluch, J. M.; Skrzypczak-Jankun, E.; González-Lafont, À.; Kühn, H., Ligand-induced formation of transient dimers of mammalian 12/15-lipoxygenase: A key to allosteric behavior of this class of enzymes? *Proteins: Structure, Function, and Bioinformatics* **2012**, 80 (3), 703-712.
48. Falgoutyret, J. P.; Denis, D.; Macdonald, D.; Hutchinson, J. H.; Riendeau, D., Characterization of the arachidonate and ATP binding sites of human 5-lipoxygenase using photoaffinity labeling and enzyme immobilization. *Biochemistry* **1995**, 34 (41), 13603-11.
49. Hogaboom, G. K.; Cook, M.; Newton, J. F.; Varrichio, A.; Shorr, R. G.; Sarau, H. M.; Crooke, S. T., Purification, characterization, and structural properties of a single protein from rat basophilic leukemia (RBL-1) cells possessing 5-lipoxygenase and leukotriene A4 synthetase activities. *Mol Pharmacol* **1986**, 30 (6), 510-519.
50. Shimizu, T.; Izumi, T.; Seyama, Y.; Tadokoro, K.; Radmark, O.; Samuelsson, B., Characterization of leukotriene A4 synthase from murine mast cells: evidence for its

identity to arachidonate 5-lipoxygenase. *Proc Natl Acad Sci U S A* **1986**, 83 (12), 4175-4179.

51. Maskrey, B. H.; Bermudez-Fajardo, A.; Morgan, A. H.; Stewart-Jones, E.; Dioszeghy, V.; Taylor, G. W.; Baker, P. R.; Coles, B.; Coffey, M. J.; Kuhn, H.; O'Donnell, V. B., Activated platelets and monocytes generate four hydroxyphosphatidylethanolamines via lipoxygenase. *J Biol Chem* **2007**, 282 (28), 20151-63.

52. Skorey, K. I.; Gresser, M. J., Calcium is not required for 5-lipoxygenase activity at high phosphatidyl choline vesicle concentrations. *Biochemistry* **1998**, 37 (22), 8027-8034.

53. Percival, M. D.; Denis, D.; Riendeau, D.; Gresser, M. J., Investigation of the mechanism of non-turnover-dependent inactivation of purified human 5-lipoxygenase. *European Journal of Biochemistry* **1992**, 210 (1), 109-117.

54. Matsumoto, T.; Funk, C. D.; Radmark, O.; Hoog, J. O.; Jornvall, H.; Samuelsson, B., Molecular cloning and amino acid sequence of human 5-lipoxygenase. *Adv Prostaglandin Thromboxane Leukot Res* **1989**, 19, 466-9.

55. Balcarek, J. M.; Theisen, T. W.; Cook, M. N.; Varrichio, A.; Hwang, S. M.; Strohsacker, M. W.; Crooke, S. T., Isolation and characterization of a cDNA clone encoding rat 5-lipoxygenase. *Journal of Biological Chemistry* **1988**, 263 (27), 13937-13941.

56. Kulkarni, S.; Das, S.; Funk, C. D.; Murray, D.; Cho, W., Molecular basis of the specific subcellular localization of the C2-like domain of 5-lipoxygenase. *J Biol Chem* **2002**, 277 (15), 13167-74.

57. Pande, A. H.; Qin, S.; Tatulian, S. A., Membrane fluidity is a key modulator of membrane binding, insertion, and activity of 5-lipoxygenase. *Biophysical journal* **2005**, 88 (6), 4084-4094.

58. Mogul, R.; Holman, T. R., Inhibition studies of soybean and human 15-lipoxygenases with long-chain alkenyl sulfate substrates. *Biochemistry* **2001**, 40 (14), 4391-4397.

59. Ruddat, V. C.; Whitman, S.; Holman, T. R.; Bernasconi, C. F., Stopped-flow kinetic investigations of the activation of soybean lipoxygenase-1 and the influence of inhibitors on the allosteric site. *Biochemistry* **2003**, 42 (14), 4172-4178.

60. Wecksler, A. T.; Kenyon, V.; Garcia, N. K.; Deschamps, J. D.; van der Donk, W. A.; Holman, T. R., Kinetic and structural investigations of the allosteric site in human epithelial 15-lipoxygenase-2. *Biochemistry* **2009**, 48 (36), 8721.
61. Wecksler, A. T.; Kenyon, V.; Deschamps, J. D.; Holman, T. R., Substrate specificity changes for human reticulocyte and epithelial 15-lipoxygenases reveal allosteric product regulation. *Biochemistry* **2008**, 47 (28), 7364-75.
62. Michel, A. A. Y.; Steinhilber, D.; Werz, O., Development of a method for expression and purification of the regulatory C2-like domain of human 5-lipoxygenase. *Protein Expression and Purification* **2008**, 59 (1), 110-116.
63. Aleem, A. M.; Jankun, J.; Dignam, J. D.; Walther, M.; Kuhn, H.; Svergun, D. I.; Skrzypczak-Jankun, E., Human platelet 12-lipoxygenase, new findings about its activity, membrane binding and low-resolution structure. *J Mol Biol* **2008**, 376 (1), 193-209.
64. Di Venere, A.; Salucci, M. L.; van Zadelhoff, G.; Veldink, G.; Mei, G.; Rosato, N.; Finazzi-Agro, A.; Maccarrone, M., Structure-to-function relationship of mini-lipoxygenase, a 60-kDa fragment of soybean lipoxygenase-1 with lower stability but higher enzymatic activity. *J Biol Chem* **2003**, 278 (20), 18281-8.
65. Dainese, E.; Angelucci, C. B.; Sabatucci, A.; De Filippis, V.; Mei, G.; Maccarrone, M., A novel role for iron in modulating the activity and membrane-binding ability of a trimmed soybean lipoxygenase-1. *The FASEB Journal* **2010**, 24 (6), 1725-1736.
66. Walther, M.; Anton, M.; Wiedmann, M.; Fletterick, R.; Kuhn, H., The N-terminal domain of the reticulocyte-type 15-lipoxygenase is not essential for enzymatic activity but contains determinants for membrane binding. *J. Biol. Chem.* **2002**, 277 (30), 27360-27366.
67. Romanov, S.; Wiesner, R.; Myagkova, G.; Kuhn, H.; Ivanov, I., Affinity labeling of the rabbit 12/15-lipoxygenase using azido derivatives of arachidonic acid. *Biochemistry* **2006**, 45 (11), 3554-62.
68. Maekawa, A.; Kanaoka, Y.; Xing, W.; Austen, K. F., Functional recognition of a distinct receptor preferential for leukotriene E4 in mice lacking the cysteinyl leukotriene 1 and 2 receptors. *Proceedings of the National Academy of Sciences* **2008**, 105 (43), 16695-16700.

69. Brink, C.; Dahlén, S.-E.; Drazen, J.; Evans, J. F.; Hay, D. W. P.; Nicosia, S.; Serhan, C. N.; Shimizu, T.; Yokomizo, T., International Union of Pharmacology XXXVII. Nomenclature for Leukotriene and Lipoxin Receptors. *Pharmacological Reviews* **2003**, 55 (1), 195-227.
70. Grant, G. E.; Rokach, J.; Powell, W. S., 5-Oxo-ETE and the OXE receptor. *Prostaglandins & Other Lipid Mediators* **2009**, 89 (3-4), 98-104.
71. Wan, M.; Sabirsh, A.; Wetterholm, A.; Agerberth, B.; Haeggström, J. Z., Leukotriene B₄ triggers release of the cathelicidin LL-37 from human neutrophils: novel lipid-peptide interactions in innate immune responses. *The FASEB Journal* **2007**, 21 (11), 2897-2905.
72. Claesson, H. E.; Dahlén, S. E., Asthma and leukotrienes: antileukotrienes as novel anti-asthmatic drugs. *Journal of Internal Medicine* **1999**, 245 (3), 205-227.
73. Peters-Golden, M., Expanding roles for leukotrienes in airway inflammation. *Current Allergy and Asthma Reports* **2008**, 8 (4), 367-373.
74. Bäck, M.; Sakata, K.; Qiu, H.; Haeggström, J. Z.; Dahlén, S.-E., Endothelium-dependent vascular responses induced by leukotriene B₄. *Prostaglandins & Other Lipid Mediators* **2007**, 83 (3), 209-212.
75. Austen, K. F., Additional functions for the cysteinyl leukotrienes recognized through studies of inflammatory processes in null strains. *Prostaglandins & Other Lipid Mediators* **2007**, 83 (3), 182-187.
76. Vannella, K. M.; McMillan, T. R.; Charbeneau, R. P.; Wilke, C. A.; Thomas, P. E.; Toews, G. B.; Peters-Golden, M.; Moore, B. B., Cysteinyl Leukotrienes Are Autocrine and Paracrine Regulators of Fibrocyte Function. *The Journal of Immunology* **2007**, 179 (11), 7883-7890.
77. Samuelsson, B., Leukotrienes: Mediators of Immediate Hypersensitivity Reactions and Inflammation. *Science* **1983**, 220 (4597), 568-575.
78. Carter, G. W.; Young, P. R.; Albert, D. H.; Bouska, J.; Dyer, R.; Bell, R. L.; Summers, J. B.; Brooks, D. W., 5-lipoxygenase inhibitory activity of zileuton. *J Pharmacol Exp Ther* **1991**, 256 (3), 929-37.
79. Ducharme, Y.; Blouin, M.; Brideau, C.; Châteauneuf, A.; Gareau, Y.; Grimm, E. L.; Juteau, H. l. n.; Laliberté, S. b.; MacKay, B.; Massé, F. d. r.; Ouellet, M.; Salem,

- M.; Styhler, A.; Friesen, R. W., The Discovery of Setileuton, a Potent and Selective 5-Lipoxygenase Inhibitor. *ACS Medicinal Chemistry Letters* **2010**, 1 (4), 170-174.
80. Hutchinson, J. H.; Li, Y.; Arruda, J. M.; Baccei, C.; Bain, G.; Chapman, C.; Correa, L.; Darlington, J.; King, C. D.; Lee, C.; Lorrain, D.; Prodanovich, P.; Rong, H.; Santini, A.; Stock, N.; Prasit, P.; Evans, J. F., 5-Lipoxygenase-Activating Protein Inhibitors: Development of 3-[3-tert-Butylsulfanyl-1-[4-(6-methoxy-pyridin-3-yl)-benzyl]-5-(pyridin-2-ylmethoxy)-1H-indol-2-yl]-2,2-dimethyl-propionic Acid (AM103). *Journal of Medicinal Chemistry* **2009**, 52 (19), 5803-5815.
81. Koeberle, A.; Zettl, H.; Greiner, C.; Wurglics, M.; Schubert-Zsilavec, M.; Werz, O., Pirinixic Acid Derivatives as Novel Dual Inhibitors of Microsomal Prostaglandin E2 Synthase-1 and 5-Lipoxygenase. *Journal of Medicinal Chemistry* **2008**, 51 (24), 8068-8076.
82. Falgoutyret, J. P.; Hutchinson, J. H.; Riendeau, D., Criteria for the identification of non-redox inhibitors of 5-lipoxygenase. *Biochemical Pharmacology* **1993**, 45 (4), 978-81.
83. Bell, R. L.; Young, P. R.; Albert, D.; Lanni, C.; Summers, J. B.; Brooks, D. W.; Rubin, P.; Carter, G. W., The discovery and development of zileuton: an orally active 5-lipoxygenase inhibitor. *Int J Immunopharmacol* **1992**, 14 (3), 505-10.
84. McGill, K. A.; Busse, W. W., Zileuton. *The Lancet* **1996**, 348 (9026), 519-524
85. Walenga, R. W.; Showell, H. J.; Feinstein, M. B.; Becker, E. L., Parallel inhibition of neutrophil arachidonic acid metabolism and lysosomal enzyme secretion by nordihydroguaiaretic acid. *Life Sciences* **1980**, 27 (12), 1047-1053.
86. Kemal, C.; Louis-Flamberg, P.; Krupinski-Olsen, R.; Shorter, A. L., Reductive inactivation of soybean lipoxygenase 1 by catechols: a possible mechanism for regulation of lipoxygenase activity. *Biochemistry* **1987**, 26 (22), 7064-72.
87. Pham, C.; Jankun, J.; Skrzypczak-Jankun, E.; Flowers, R. A.; Funk, M. O., Structural and thermochemical characterization of lipoxygenase-catechol complexes. *Biochemistry* **1998**, 37 (51), 17952-17957.
88. Nelson, M. J.; Brennan, B. A.; Chase, D. B.; Cowling, R. A.; Grove, G. N.; Scarrow, R. C., Structure and Kinetics of Formation of Catechol Complexes of Ferric Soybean Lipoxygenase-1. *Biochemistry* **1995**, 34 (46), 15219-15229.

89. Hlasta, D. J.; Casey, F. B.; Ferguson, E. W.; Gangell, S. J.; Heimann, M. R.; Jaeger, E. P.; Kullnig, R. K.; Gordon, R. J., 5-Lipoxygenase inhibitors: the synthesis and structure-activity relationships of a series of 1-phenyl-3-pyrazolidinones. *Journal of Medicinal Chemistry* **1991**, 34 (5), 1560-1570.
90. Cucurou, C.; Battioni, J. P.; Thang, D. C.; Nam, N. H.; Mansuy, D., Mechanisms of inactivation of lipoxygenases by phenidone and BW755C. *Biochemistry* **1991**, 30 (37), 8964-8970.
91. Ashida, Y.; Saijo, T.; Kuriki, H.; Makino, H.; Terao, S.; Maki, Y., Pharmacological profile of AA-861, A 5-lipoxygenase inhibitor. *Prostaglandins* **1983**, 26 (6), 955-972.
92. Lassus, A.; and Forsstrom, S., A dimethoxynaphthalene derivative (RS-43179 gel) compared with 0.025% fluocinolone acetonide gel in the treatment of psoriasis. *British Journal of Dermatology* **1985**, 113, 103-106,
93. Musser, J. H.; Kreft, A. F., 5-Lipoxygenase: properties, pharmacology, and the quinolinyl(bridged)aryl class of inhibitors. *Journal of Medicinal Chemistry* **1992**, 35 (14), 2501-2524.
94. Riendeau, D.; Falgueyret, J. P.; Guay, J.; Ueda, N.; Yamamoto, S., Pseudoperoxidase Activity of 5-Lipoxygenase Stimulated by Potent Benzofuranol and N-Hydroxyurea Inhibitors of the Lipoxygenase Reaction. *Biochem. J.* **1991**, 274, 287-292.

Chapter 2

Investigations into the PLAT domain and the allosteric binding site of human epithelial 15-lipoxygenase-2

2.1 Introduction

The inflammatory response in humans is regulated by fatty acid signaling cascades, which are initiated by the oxidation of polyunsaturated fatty acids. Three classes of enzymes catalyze this oxidation: cyclooxygenase (COX) [1]; cytochrome P450 [2]; and lipoxygenase (LOX) [3], which is the focus of this study. Lipoxygenases (LOX) are a family of iron-containing metalloenzymes that utilize a non-heme catalytic center to incorporate molecular oxygen into a variety of fatty acids. There are three main LOXs of pharmacological importance, 5-LOX, 12-LOX and 15-LOX, which are named according to the position on arachidonic acid (AA) where the oxygen reacts [4]. The peroxidation of AA by different LOXs results in position-specific hydroperoxyeicosatetraenoic acid (HPETE) products [5], which are responsible for maintaining the homeostasis of the inflammatory response [6], and have also been implicated in many human diseases, such as asthma [7], psoriasis [8], atherosclerosis [9], cancer [10], heart disease [11,12] and diabetes [13], to name a few. Allosteric regulation of enzymes is a critical process in biochemistry [14,15,16], and has recently emerged as an important aspect of LOX activity [17,18,19]. As

mentioned above, there are numerous LOX isozymes involved in the complex process of inflammation, and allosteric regulation could play a role in the inflammation response. The first discovery of allosteric regulation of LOX was identified with human leukocyte 5-LOX, where ATP and Ca^{2+} were shown to increase enzymatic activity significantly [20-23]. This was followed by the discovery that soybean LOX-1 and reticulocyte human 15-LOX-1 (15-LOX-1) could be allosterically inhibited by the synthetic fatty sulfate, oleyl sulfate (OS) [24]. OS is bound with considerable affinity to an allosteric binding site on both soybean LOX-1 ($K_D = 0.6 \mu\text{M}$) and 15-LOX-1 ($K_D = 0.4 \mu\text{M}$). This was seen by steady-state inhibition kinetics, an increase in their kinetic isotope effects (KIE) and by stopped-flow kinetics. These results demonstrated that OS binding to soybean LOX-1 did not interfere with enzyme activation [25]. The role of the allosteric site was further refined by the discovery that LOX products, such as 13-(S)-hydroxyoctadecadienoic acid (13-(S)-HODE), could bind to the allosteric site of both 15-LOX-1 and human epithelial 15-LOX-2 (15-LOX-2) and change the substrate specificity with respect to AA and linoleic acid (LA) [17,18]. The substrate specificity was shown to be pH dependent for 15-LOX-2, which was hypothesized to be due to a change in allosteric effector binding. A docking model was proposed, placing the allosteric binding pocket between the polycystin-1 lipoygenase alpha-toxin (PLAT) domain (i.e. the beta domain) [17] and the catalytic domain of 15-LOX-2. Specifically, the docking model suggested that the

carboxylic acid of 13-(S)-HODE interacted with His627 at the bottom of the cleft between the two domains [18].

Additional studies have indicated that C₁₈ and C₂₀ fatty acid substrates have distinct responses to pH. This observation was confirmed with steady-state kinetics, where the k_{cat} and k_{cat}/K_M of (γ)-linolenic acid (GLA) (C₁₈) are decreased with increasing pH, while the same kinetic parameters of arachidonic acid (AA), dihomo (γ) linolenic acid (DGLA), eicosadienoic acid (EDA) and eicosapentaenoic acid (EPA) (C₂₀) are increased with increasing pH [19]. It was also discovered that addition of the C₁₈ lipid products, 13-(S)-HODE and 13-(S)-HOTrE(γ), mirror the k_{cat}/K_M pH effect, with an increase in the AA/GLA ratio and are partially additive, with the AA/GLA k_{cat}/K_M ratio increasing from 0.62 (pH 7.5 and no products added) to 6.8 (pH 8.5 and 15 μ M product added), an 11-fold increase. In addition, these two allosteric effectors, 13-(S)-HODE and 13-(S)-HOTrE(γ), display hyperbolic kinetics with similar K_i values, $9.8 \pm 0.2 \mu$ M and $4.9 \pm 0.7 \mu$ M, respectively [19]. However, the K_i of 13-(S)-HODE is pH dependent and the effect of 13-(S)-HODE on the K_M is 2.1 fold greater than that of 13-(S)-HOTrE(γ).

Previous studies on the role of the PLAT domain of LOX suggested that it is important for membrane association of various LOX isozymes [26-30]. PLAT domain truncation proteins, such as the soybean LOX-1^{NoPLAT}, rabbit 15-LOX^{NoPLAT}, 15-LOX-1^{NoPLAT}, 15-LOX-2^{NoPLAT}, human platelet 12-LOX^{NoPLAT} (12-LOX^{NoPLAT}), all displayed a reduction in liposome affinity; however, mouse leukocyte 5-

LOX^{NoPLAT} displayed no change in affinity, possibly due to a compensatory effect on membrane binding produced by its association with the 5-LOX activating protein (FLAP) [26-30]. It was also found that loss of activity accompanied PLAT domain removal for almost all the LOX isozymes investigated, except soybean LOX-1^{NoPLAT}, the activity of which increased upon partial trypsin cleavage [30]. Interestingly, not only was the absolute activity decreased for rabbit 15-LOX^{NoPLAT} and human 15-LOX-1^{NoPLAT}, but their rates of auto-inactivation increased as well [26,27]. In the present study, we have further investigated the role of the PLAT domain in both the allosteric effect and catalysis of 15-LOX-2. The results indicate that the PLAT domain has a minimal role on enzyme activity, yet is directly involved in the allosteric properties.

2.2 Results and discussion

2.2.1 Protein purification and metal content.

Methods developed for structural genomics studies of eukaryotic proteins were applied to the expression and purification of 15-LOX-2 and 15-LOX-2^{NoPLAT} [19]. Briefly, the His₆-MBP-fusion protein (16 hrs growth, 20° C and no IPTG) was passed over an IMAC column. After cleavage with TEV protease [34] and subtractive IMAC, approximately 30 mg of 90% pure protein (SDS-PAGE) was isolated; the purity is comparable to that previously achieved using the SF9 expression system [33]. However, ICP-MS data indicated that the pure 15-LOX-2 and 15-LOX-2^{NoPLAT} had iron content ranging from 25-45%, which is higher than previous 15-LOX-2

preparations [17,18,24]. The unique benefits of this expression and purification method were its high yield in *E. coli* and increased metal content, yielding a highly active protein.

2.2.2 Characterization of steady-state kinetics with arachidonic acid and gamma linoleic acid.

To investigate the elicited effect resulting from removal of the PLAT domain, steady-state kinetics were conducted with 15-LOX-2^{NoPLAT} (normalized to metal content) at 22° C in 25 mM HEPES, 150 mM NaCl, pH 7.5, using both AA and GLA as substrates (**Table 1.1**). The k_{cat} value was previously determined to be $1.5 \pm 0.03 \text{ s}^{-1}$ for AA and $1.8 \pm 0.03 \text{ s}^{-1}$ for GLA for 15-LOX-2 [19]. A slight loss in activity was observed for 15-LOX-2^{NoPLAT} with a k_{cat} value of $0.75 \pm 0.03 \text{ s}^{-1}$ for AA, and $0.99 \pm 0.04 \text{ s}^{-1}$ for GLA [19]. The loss in k_{cat} after removal of the PLAT domain is consistent with previous results of Kuhn and coworkers, however, they observed a smaller decrease in k_{cat} (AA) for rabbit 15-LOX^{NoPLAT} of 22% [26]. Additional works discovered that the mouse leukocyte 5-LOX^{NoPLAT} (D114) only retained 9% of its native k_{cat} ; this increased inactivation is attributed to the higher instability of 5-LOX [27]. The k_{cat}/K_M value of 15-LOX-2 for GLA has been shown to be $0.40 \pm 0.04 (\mu\text{M}^{-1} \text{ s}^{-1})$ for AA, and $0.64 \pm 0.01 (\mu\text{M}^{-1} \text{ s}^{-1})$ [19], whereas we measured for 15-LOX-2^{NoPLAT} a k_{cat}/K_M value of $0.21 \pm 0.02 (\mu\text{M}^{-1} \text{ s}^{-1})$ for AA, and $0.16 \pm 0.02 (\mu\text{M}^{-1} \text{ s}^{-1})$ for GLA. The decrease in the k_{cat}/K_M value after the removal of the PLAT domain is also consistent with the previous results of Kuhn and coworkers, however, these

authors recorded a larger decrease in the catalytic efficiency for AA, 87% versus 47%, for 15-LOX^{NoPLAT} and 5-LOX^{NoPLAT}, respectively [26,27]. In comparing the substrate specificity of 15-LOX-2^{NoPLAT}, it is observed that the $(k_{cat})^{AA}/(k_{cat})^{GLA}$ does not change much relative to 15-LOX-2, 0.76 ± 0.06 and 0.83 ± 0.03 , respectively. However, the $(k_{cat}/K_M)^{AA}/(k_{cat}/K_M)^{GLA}$ ratio is different, with a ratio of 1.3 ± 0.3 for 15-LOX-2^{NoPLAT} and a ratio of 0.62 ± 0.04 for 15-LOX-2. These data indicate that the removal of the PLAT domain shifts the substrate preference of the rate of substrate capture for 15-LOX-2^{NoPLAT} towards AA.

2.2.3 CD half-transition temperature determination.

To explore the structural alterations resulting from the removal of the PLAT domain, thermal stabilities were measured. As seen in Figure 1, both 15-LOX-2 and 15-LOX-2^{NoPLAT} undergo a loss in secondary structure with a two-state unfolding transition, with a T_{50} between 40-45° C for both proteins. These data indicate that the stability of the truncated protein to be approximately the same as the wild-type protein (**Figure 2.1**) and that their differences are not due to large scale thermal stability differences.

2.2.4 Substrate specificity pH profile using the competitive substrate capture method.

Previously, it was proposed, using homology modeling, that the allosteric site in 15-LOX-2 was in a cleft between the PLAT and catalytic domains and that the pH-dependent substrate specificity was due to the protonation of His627 at the bottom of

the allosteric site [17,18]. To further explore whether the PLAT domain or His627 were responsible for giving rise to the pH effect, the CSC method was employed to evaluate the various enzymes pH profile. The competitive substrate capture ratio of substrate turnover for 15-LOX-2^{NoPLAT} was determined using an AA:LA reaction mixture (25 mM HEPES, pH 7.5, and pH 8.5, 22° C). It was found that the $(k_{cat}/K_M)^{AA}/(k_{cat}/K_M)^{LA}$ ratio for 15-LOX-2^{NoPLAT} was 2.5 ± 0.2 at pH 7.5 and 3.6 ± 0.3 at pH 8.5 (**Table 2.2**). The AA metabolism dependence on pH was comparable between 15-LOX-2 and the 15-LOX-2^{NoPLAT}, indicating that the PLAT domain makes essentially no contribution to the pH effect. As mentioned above, we hypothesized that the allosteric effector molecule will bind in the cleft between the two domains of 15-LOX-2, with His627 being critical for interaction with the carboxylate group on the effector molecule. In order to test this hypothesis, His627 was mutated to alanine and its pH dependence of the substrate specificity investigated. The $(k_{cat}/K_M)^{AA}/(k_{cat}/K_M)^{LA}$ ratio was determined to be 1.8 ± 0.1 at pH 7.5 and 3.1 ± 0.1 at pH 8.5, for the mutant protein, 15-LOX-2^{H627A}. These results indicate that His627 does not contribute to the pH dependence of the $(k_{cat}/K_M)^{AA}/(k_{cat}/K_M)^{LA}$ ratio, as was hypothesized previously [17,18]. It should be noted that the CSC AA/LA ratio was different from that measured by steady-state kinetics, which is common in these measurements due to the changing concentrations of both 15-(S)-HPETE and 13-(S)-HPODE in the CSC reaction mixtures.

2.2.5 Effect of pH on the steady-state substrate specificity kinetics of 15-LOX-2.

To probe the pH dependence of 15-LOX-2 further, steady-state kinetics pH profiles were conducted on 15-LOX-2^{NoPLAT} with AA and GLA. Previously conducted pH kinetic data for 15-LOX-2 indicated that as pH increases, AA becomes a more efficiently processed substrate, increasing both k_{cat} (1.5 ± 0.03 to 2.0 ± 0.04) and k_{cat}/K_M (0.40 ± 0.04 to 0.76 ± 0.07), with increase in pH from 7.5 to 8.5 [17,18,19]. However, for 15-LOX-2^{NoPLAT} only the AA k_{cat}/K_M increases from 0.21 ± 0.02 to 0.29 ± 0.08 with increasing pH. Essentially no pH effect was elicited on k_{cat} , 0.75 ± 0.03 to 0.72 ± 0.04 in the case of 15-LOX-2^{NoPLAT}, yielding a $(k_{cat})^{pH8.5}/(k_{cat})^{pH7.5}$ ratio of 0.96 ± 0.09 . Thus the pH effect on 15-LOX-2^{NoPLAT} is attributed to increased efficiency in substrate capture for AA (k_{cat}/K_M), unlike for 15-LOX-2, where an increase in both product release (k_{cat}) and substrate capture (k_{cat}/K_M) occurred. This pH effect is best viewed in the expression $(k_{cat}/K_M)^{pH8.5}/(k_{cat}/K_M)^{pH7.5}$, where 15-LOX-2 and 15-LOX-2^{NoPLAT} displayed a relatively conserved response, with values of 1.9 ± 0.2 and 1.4 ± 0.5 , respectively (**Table 2.3**). These data indicate that removal of the PLAT domain eliminates the k_{cat} (product release) pH effect, but that k_{cat}/K_M (substrate capture) is still affected by pH.

2.2.6 Effect of 13-(S)-HOTrE (γ) and 13-(S)-HODE on GLA steady-state substrate kinetics.

Previously it was discovered that there is a different allosteric effect between 13-(S)-HODE and 13-(S)-HOTrE(γ) upon 15-LOX-2, with GLA as the substrate [19].

These data demonstrated that 15-LOX-2 exhibited a hyperbolic inhibitory response to increasing amounts of 13-(S)-HOTrE(γ) with a K_i (the strength of binding) of $4.9 \pm 0.7 \mu\text{M}$, an α (the change in K_M) of 3.5 ± 0.2 and a β (the change in k_{cat}) of 1.2 ± 0.02 [19]. These studies were conducted with 15-LOX-2^{NoPLAT} and in place of a hyperbolic inhibitory response; we observed poor competitive inhibition with GLA upon increasing amounts of 13-(S)-HOTrE(γ). The $K_M(\text{app})$ for GLA was increased from $6.3 \mu\text{M}$ to $\sim 7.0 \mu\text{M}$ (**Figure 2.2**), and a decrease in k_{cat}/K_M from $0.16 \mu\text{M}^{-1}\text{s}^{-1}$ to $\sim 0.14 \mu\text{M}^{-1}\text{s}^{-1}$ (**Figure 2.3**) was observed. These data indicate a severely reduced allosteric effect for 15-LOX-2^{NoPLAT} elicited upon introduction of 13-(S)-HOTrE(γ), generating a linear fit K_i value of $218 \pm 38 \mu\text{M}$, whereas 15-LOX-2 previously displayed hyperbolic kinetics with a K_i of $4.9 \pm 0.7 \mu\text{M}$ [19].

Previous examination of 13-(S)-HODE with 15-LOX-2 demonstrated a conserved response relative to 13-(S)-HOTrE(γ), where an inhibitory hyperbolic fit was observed, with an α value of 7.3 ± 0.06 , a β value of 1.2 ± 0.02 and a K_i value of $9.8 \pm 0.2 \mu\text{M}$ [19]. Divergent from the results with 13-(S)-HOTrE(γ) and 15-LOX-2^{NoPLAT}, increasing amounts of 13-(S)-HODE with 15-LOX-2^{NoPLAT} evoked a hyperbolic inhibitor effect, allowing for evaluation of the microscopic rate constants. These data revealed an α value of 4.9 ± 1.9 and a K_i value of $6.1 \pm 1.7 \mu\text{M}$ from the K_M plot (**Figure 2.4**) for the 15-LOX-2^{NoPLAT}, indicating similar but reduced allostery for 15-LOX-2^{NoPLAT} relative to 15-LOX-2. The 15-LOX-2^{NoPLAT} displayed a β value of 1.6 ± 0.2 (**Figure 2.5**), which highlights the conserved 13-(S)-HODE allosteric response for

both 15-LOX-2 and 15-LOX-2^{NoPLAT}. The fact that 13-(S)-HODE elicits an allosteric effect on 15-LOX-2^{NoPLAT} but 13-(S)-HOTrE(γ) does not, is difficult to explain. Our group previously determined that 13-(S)-HODE and 13-(S)-HOTrE(γ) have different 15-LOX-2 binding properties, with 13-(S)-HODE binding being pH dependent, while 13-(S)-HOTrE(γ) binding is not. These 15-LOX-2 data indicate that the two allosteric effectors may bind to the same site with different constraints or they may bind to distinct sites. The stronger allosteric effect elicited by 13-(S)-HODE with 15-LOX-2 may reflect a more stable or distinct binding interaction versus that of 13-(S)-HOTrE(γ), which is partially intact within the 15-LOX-2^{NoPLAT}. These data clearly demonstrate that the PLAT domain is involved in the allosteric properties yet is not solely responsible; in the case of 13-(S)-HODE it may only play a minor role in the catalysis of GLA oxidation. The 15-LOX-2^{NoPLAT} allosteric data indicate that the PLAT domain affects the allostery of 13-(S)-HOTrE(γ), however, it does not significantly affect the allostery of 13-(S)-HODE. Considering that the structure of 13-(S)-HODE only differs from 13-(S)-HOTrE(γ) by one less double-bond, it is unclear if the PLAT domain alters the structure of the catalytic domain to differentially affect its allosteric response between the two LOX products or if the 13-(S)-HOTrE(γ) binding site is completely abolished with the removal of the PLAT domain. If it is the former and the PLAT domain stabilizes the catalytic domain, it is a subtle effect because the structures of the two LOX products are so similar and the

overall stability of 15-LOX-2^{NoPLAT} is comparable to 15-LOX-2, as witnessed by the similar thermal stabilities.

2.2.7 Effect of 13-(S)-HODE on AA steady-state substrate kinetics.

Previous reports have highlighted an activation of 15-LOX-2 AA catalysis upon 13-(S)-HODE addition as reflected by an increase in the k_{cat}/K_M of AA for 15-LOX-2 ($0.40 \pm 0.02 \mu\text{M}^{-1}\text{s}^{-1}$ to $0.66 \pm 0.07 \mu\text{M}^{-1}\text{s}^{-1}$) [19]. To further investigate the effect of PLAT domain removal on 13-(S)-HODE allostery, we conducted steady-state kinetics on 15-LOX-2^{NoPLAT} with 13-(S)-HODE. The kinetic parameters of 15-LOX-2^{NoPLAT} with AA and 15 μM 13-(S)-HODE added are listed in **Table 2.4**. These data show a very distinct response associated with the truncation, specifically, 13-(S)-HODE was shown to inhibit 15-LOX-2^{NoPLAT}, decreasing the k_{cat}/K_M of AA from $0.21 \pm 0.02 \mu\text{M}^{-1}\text{s}^{-1}$ to $0.14 \pm 0.01 \mu\text{M}^{-1}\text{s}^{-1}$ (**Table 2.4**). These findings are better displayed by the relative differences in the $(k_{cat}/K_M)^{\text{w/ 13-(S)-HODE}}/(k_{cat}/K_M)^{\text{w/o 13-(S)-HODE}}$ ratio, with a value of 1.7 ± 0.2 for 15-LOX-2 and a value of 0.69 ± 0.1 for 15-LOX-2^{NoPLAT}. Examination of the 13-(S)-HODE effect on k_{cat} revealed no effect for 15-LOX-2^{NoPLAT}, with a $(k_{cat})^{\text{w/ 13-(S)-HODE}}/(k_{cat})^{\text{w/o 13-(S)-HODE}}$ of 0.99 ± 0.05 , while a ratio of 0.87 ± 0.03 was observed for 15-LOX-2 [19]. These data indicate an altered allosteric response for 15-LOX-2^{NoPLAT} catalysis of AA oxidation in the presence of 13-(S)-HODE. Considering that the removal of the PLAT domain had limited effect on GLA catalysis with 13-(S)-HODE present, but a dramatic effect on GLA catalysis in the presence of 13-(S)-HOTrE(γ). We interpret the 13-(S)-HODE/AA data as supporting

the hypothesis that the allosteric site is still present in the catalytic domain, but that removal of the PLAT domain alters its binding selectivity and resulting effect on catalysis. Continued research is underway to further understand the location and the behavior of the allosteric site of 15-LOX-2.

2.2.8 Size-exclusion chromatography.

Recently, it was proposed that a monomer-dimer equilibrium could account for the rabbit 12/15-LOX allosteric effect induced by 13-(S)-HODE [37]. A similar hypothesis has been proposed for COX, that its substrate specificity is affected by an allosteric-induced conformational heterodimer [38]. To investigate the oligomeric state of 15-LOX-2, we conducted SEC experiments to evaluate the monomer-oligomer equilibrium for 15-LOX-2 and 15-LOX-2^{NoPLAT}. The 15-LOX-2 chromatogram displayed two major peaks, with the first peak (24 min.) corresponding to the void volume of the column and indicating a very high order oligomer. The second major peak (42 min.) corresponds to the monomer species, with bovine serum albumin (67 kDa) as a standard (**Table 2.5**). A minor peak was observed in between these two predominate peaks, suggesting a smaller oligomer, possibly a dimer or tetramer. A similar SEC trace was found for 15-LOX-2^{NoPLAT}, however, the dimer/tetramer peak is increased in amplitude such that all three peaks are of similar area (**Table 2.5**). These data suggest that removal of the PLAT domain leads to higher oligomeric states at high concentrations (50 μ M), an observation previously reported for 12-LOX [28]. Considering that 15-LOX-2^{NoPLAT} does not manifest a

large allosteric effect, the higher oligomeric states do not appear to be the allosterically activated state of the protein. However, these measurements were conducted at concentrations significantly greater than that of the kinetic experiments, so it is difficult to assume that these higher oligomeric states would exist at the lower concentrations.

2.2.9 Dependence of CD spectra on protein concentration.

Considering that the above data indicate that 15-LOX-2^{NoPLAT} has a higher propensity to aggregate than 15-LOX-2, the concentration dependence on the CD spectra of 15-LOX-2 and 15-LOX-2^{NoPLAT} was investigated. The CD data for both 15-LOX-2 and 15-LOX-2^{NoPLAT} demonstrate a loss in their 210 nm signal (α -helical secondary structure), relative to the 220 nm signal (β -sheet secondary structure), upon increasing their protein concentrations from approximately 2 to 18 μ M. Plotting the 220/210 nm ratio demonstrated comparable concentration dependence for the two proteins, with 15-LOX-2^{NoPLAT} showing a slightly smaller effect at the highest concentration (**Figure 2.6**). This result indicates an increase in the β sheet structure relative to α -helical structure with increasing protein concentration for both 15-LOX-2 and 15-LOX-2^{NoPLAT}. The 220/210 nm ratio decreased upon dilution of both 15-LOX-2 and 15-LOX-2^{NoPLAT}, indicating the structural change was reversible. Similar effects have been seen previously, an increase in α -helical structure with increasing protein concentration [39]; for example an increase in oligomerization of tyrosine hydrolase upon incubation with tetrahydrobiopterin triggers a loss in 210 nm intensity

[40,41,42]. Since this structural change occurs with both 15-LOX-2 and 15-LOX-2^{NoPLAT}, the change presumably originates in the catalytic domain. Finally, the change in the 220/210 ratio was not induced upon the addition of 13-(S)-HODE. This data indicates that this structural change is not related to the allosteric effect, considering it is observed for both 15-LOX-2 and 15-LOX-2^{NoPLAT} and that 13-(S)-HODE had no effect.

2.3 Conclusion

In summary, the removal of the PLAT domain resulted in an active 15-LOX-2^{NoPLAT}, retaining 50% of its catalytic rate for both AA and GLA. However, 15-LOX-2^{NoPLAT} displayed an unaltered K_M value for AA, whereas the K_M for GLA roughly doubled, indicating that the PLAT domain influences substrate specificity. The CD melt temperature measurements revealed identical profiles for 15-LOX-2 and 15-LOX-2^{NoPLAT}, indicating no significant effect on protein stability resulting from the PLAT domain removal. Competitive substrate capture (CSC) and steady-state experiments indicated that the pH dependence of AA/LA substrate specificity remained intact for 15-LOX-2^{NoPLAT} and 15-LOX-2^{H627A}, suggesting the origin of the pH sensitivity is centered in the catalytic domain. However, the removal of the PLAT domain did affect allostery, with the 13-(S)-HOTrE(γ) hyperbolic inhibition of GLA oxidation and the 13-(S)-HODE activation of AA being completely abolished. Interestingly, 13-(S)-HODE still displayed an allosteric effect with 15-LOX-2^{NoPLAT}, similar in nature to previous work on 15-LOX-2 with GLA. These data suggest that

the allosteric site is located in the catalytic domain but that removal of the PLAT domain affects both the binding constraints and catalytic effects of the allosteric site. Finally, the SEC and CD experiments do not support the hypothesis that loss of allostery for 15-LOX-2^{NoPLAT} is due to a loss in 15-LOX-2 oligomerization. However, further experiments are required to rule out this hypothesis. In summary, these data demonstrate that the PLAT domain is non-essential for enzyme activity and stability, but does play a role in allosteric regulation. Continued efforts are underway to refine our understanding of the allosteric properties of 15-LOX-2.

2.4 Acknowledgements

The clones used in these studies were produced by Dr. Brian Fox, Dr. Russell L. Wrobel and Mr. Karl W. Nichols (from the Center for Eukaryotic Structural Genomics) and for discussions on the preparation of lipoxygenase fusion proteins.

2.5 Materials and methods

2.5.1 Materials.

All commercial fatty acids (Sigma-Aldrich Chemical Company, and NuCheck) were stored at -80°C for a maximum of 6 months. LOX products were generated by reacting substrate with the appropriate LOX isozyme (13-(S)-HPODE from soybean LOX-1 and LA, 15-(S)-HPETE from soybean LOX-1 and AA). Products were generated in the following manner. An assay of 500 μL of 50-100 μM substrate was run to completion, reactions were quenched with 5 mL acetic acid, extracted three times with 100 mL of dichloromethane, evaporated to dryness, and reconstituted in MeOH for HPLC purification. The products were HPLC purified using an isocratic elution of 75% MeOH: 25% H_2O : 0.1% acetic acid. All products were tested with enzyme to show that no residual substrate was present, as well as tested using analytical HPLC. The reduced products were purified in a similar fashion; however, trimethylphosphite was added to selectively reduce the peroxide to the alcohol moiety. All other chemicals were reagent grade or better and used without further purification.

2.5.2 Overexpression and purification of lipoxygenase isozymes and mutants.

Human reticulocyte 15-lipoxygenase-1 (15-LOX-1) was expressed as N-terminally, His6-tagged proteins and purified to greater than 90% purity [31,32]. Human prostate epithelial 15-lipoxygenase-2 (15-LOX-2), without a His6-tag, and 15-LOX-2^{H627A} were expressed and purified as previously published [19,33]. The 15-

LOX-2^{H627A} mutation was generated with a QuickChange protocol (5'-CCTATCCGGATGAGGCCTTCACAGAGGAG-3'), and confirmed by sequencing.

Purification of the 15-LOX-2 PLAT domain truncation mutant (15-LOX-2^{NoPLAT}) was carried out using a construct encoding a fusion protein consisting of an N-terminal His8-tag fused to maltose. The parent plasmid used in these studies, pVP68K, is available from the Protein Structure Initiative Materials Repository, <http://www.psimr.asu.edu>. The 15-LOX-2^{NoPLAT} fusion was expressed using the pVP68K-Ndelta188 plasmid in *Escherichia coli* BL21 (DE3). For expression of protein, the host cells were grown to 0.6 OD at 37° C, the cells were then induced by dropping the temperature to 20° C and grown overnight (16 h). The cells were harvested in 2 L fractions at a velocity of 5,000 g, followed by snap freezing in liquid nitrogen. The cell pellets were resuspended in buffer A (25 mM HEPES, pH 8, containing 150 mM NaCl) and lysed using a Power Laboratory Press. The cellular lysate was centrifuged at 40,000 g for 25 min, and the supernatant was loaded onto an NTA-Ni affinity column. The column was washed with 15 mM imidazole in buffer A, followed by elution with 250 mM imidazole in buffer A (no NaCl). 15-LOX-2^{NoPLAT} fractions were collected and pooled together and then dialyzed for 1 h against 25 mM HEPES, pH 7.5. The protein was then removed from the dialysis bag and cleaved with His6-TEV protease for 1.5 h, followed by second dialysis for 1 h in 25 mM HEPES, pH 6.5, containing 150 mM NaCl. The cleaved 15-LOX-2^{NoPLAT} sample was then passed through tandem NTA Nickel and Amylose columns equilibrated in

buffer A containing 15 mM imidazole, and fractions with greater than 90% purity, as judged by SDS-PAGE, were pooled. In this purification protocol, the His6-tagged TEV and uncleaved His8-MBP-15-LOX-2^{NoPLAT} fusion protein were bound to the columns. The resulting 15-LOX-2^{NoPLAT} was concentrated by ultrafiltration (30 kDa molecular mass cut-off), combined with glycerol to 20% (v/v) and then snap-frozen in liquid nitrogen. The TEV protease was used as previously described [34]. Overexpression and purification of soybean LOX-1 followed a protocol outlined previously [31]. All enzymes were purified to greater than 90% purity, as evaluated by SDS-PAGE. Iron content of 15-LOX-2 and 15-LOX-2^{NoPLAT} were determined with a Thermo Element XR inductively coupled plasma mass spectrometer (ICP-MS), using cobalt or scandium (EDTA) for 15-LOX-2 and 15-LOX-2^{NoPLAT}, respectively, as an internal standard. Iron concentrations were compared to standard iron solutions.

2.5.3 Steady-state kinetic measurements and pH profile.

Lipoxygenase rates were determined by following the formation of the conjugated diene product at 234 nm ($\epsilon = 25,000 \text{ M}^{-1} \text{ cm}^{-1}$) with a Perkin-Elmer Lambda 40 UV/visible spectrometer. All reactions were 2 mL in volume and constantly stirred using a magnetic stir bar in 25 mM HEPES, 150 mM NaCl, pH 7.5 or 8.5, at 22° C, with substrate concentrations ranging from 1 μM to 30 μM . Assays were initiated by the addition of 15-LOX-2 and 15-LOX-2^{NoPLAT} (200-500 nM, normalized to iron content), and all substrate concentrations were quantitatively determined by allowing

the enzymatic reaction to go to completion. Kinetic data were obtained by recording initial enzymatic rates at each substrate concentration, which were then fitted to the Michaelis-Menten equation using KaleidaGraph (Synergy) to determine the k_{cat} and k_{cat}/K_M values [17,18,35,36,].

2.5.4 CD half-transition temperature measurements.

Protein unfolding was monitored by CD measurements at 220 nm using an AVIV CD Spectrometer model 62DS in a 0.1 cm quartz cuvette. Each sample consisted of 5 μ M enzyme in a volume of 200 μ L, solubilized in 25 mM HEPES 150 mM NaCl, pH 7.5, for evaluation of 15-LOX-2 and 15-LOX-2^{NoPLAT}. Measurements were made between 10-80° C at intervals of 5° C except close to T_{50} , where the intervals were decreased to 2° C. Each temperature recording was after a 10 min equilibration period.

2.5.5 Allosteric effects of 13-(S)-HODE and 13-(S)-HOTrE(γ) on AA and GLA metabolism.

Lipoxygenase rates were determined by following the methodology outlined within the previous outlined steady-state kinetic measurement section. Products (13-(S)-HODE and 13-(S)-HOTrE(γ)) were evaluated at 5, 15, and 30 μ M concentrations for 15-LOX-2^{NoPLAT}, with substrate GLA. The allosteric properties of 13-(S)-HODE on AA catalysis were investigated at 15 μ M. K_i and K_i' were evaluated for GLA metabolism for both enzymes, with 13-(S)-HODE and 13-(S)-HOTrE(γ), to investigate the mode of action.

2.5.6 Size-Exclusion Chromatography.

Size-exclusion chromatography (SEC) was conducted to evaluate whether removal of the PLAT domain altered the distribution of monomer and oligomer species of 15-LOX-2. Samples were prepared in 25 mM HEPES, pH 7.5, at 4° C. 300 µL injections of 35 µM 15-LOX-2 and 50 µM 15-LOX-2^{NoPLAT} were made onto a GE Superdex 200 on a Biorad FPLC. The samples were run at 4° C in 25 mM HEPES, pH 7.5, containing 150 mM NaCl, at a flow rate of 0.33 mL/min. Calibration of the column to identify monomer elution time was accomplished through use of Bovine Serum Albumin (BSA). BSA was selected due to its similar molecular weight, globular nature, and almost exclusive (95%) monomer state. Monomer protein resolution time was determined for the BSA control in 50 mM Tris buffer, pH 7, containing 150 mM NaCl with a 300 µL injection of a 8 mg/mL sample, at a flow rate of 0.33 mL/min.

2.5.7 CD protein concentration profile.

Changes in CD signals at 210 and 220 nm, were recorded at various protein concentrations using a AVIV CD Spectrometer model 62DS in a 0.1 cm quartz cuvette. Each sample consisted of 200 µL of 25 mM HEPES, pH 7.5, at 22° C, for evaluation of 15-LOX-2 and 15-LOX-2^{NoPLAT}. Protein concentration profiles ranged from 2.2 - 17.5 µM and 1.6 - 25 µM for 15-LOX-2 and 15-LOX-2^{NoPLAT}, respectively.

2.6 Figures

Figure 2.1 CD half-transition temperature (T_{50}) measurement for 15-LOX-2 (●, red circles) and 15-LOX-2^{NoPLAT} (■, blue squares). Enzyme assay was performed in 25 mM HEPES buffer (pH 7.5) between 10-80° C.

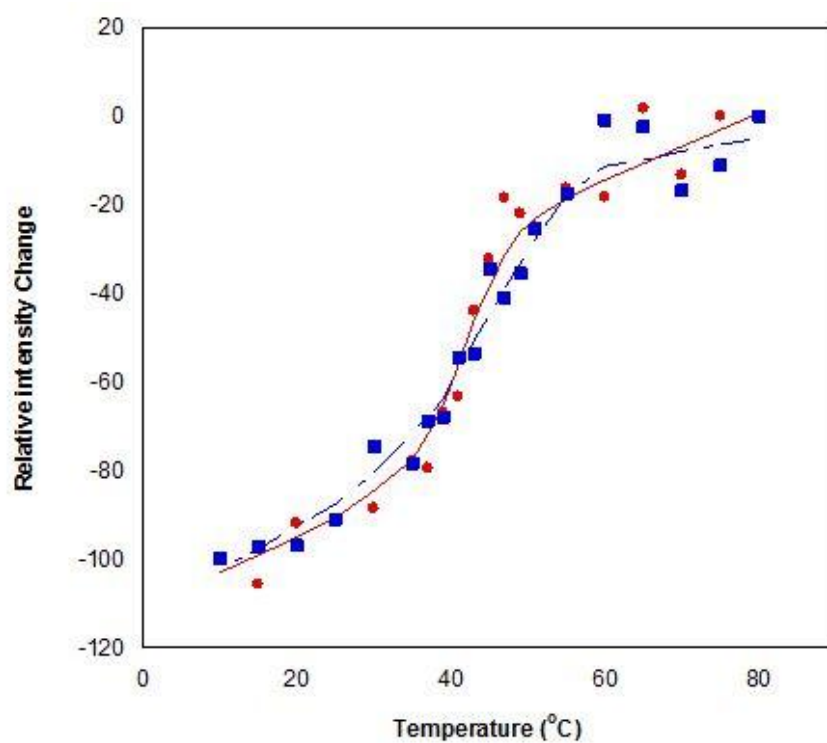


Figure 2.2 Steady-steady kinetics of allosteric effects of 13-(S)-HOTrE (γ) on GLA metabolism. Enzymatic assays were performed with GLA substrate in 25 mM HEPES, 150 mM NaCl buffer (pH 7.5), at 22° C.

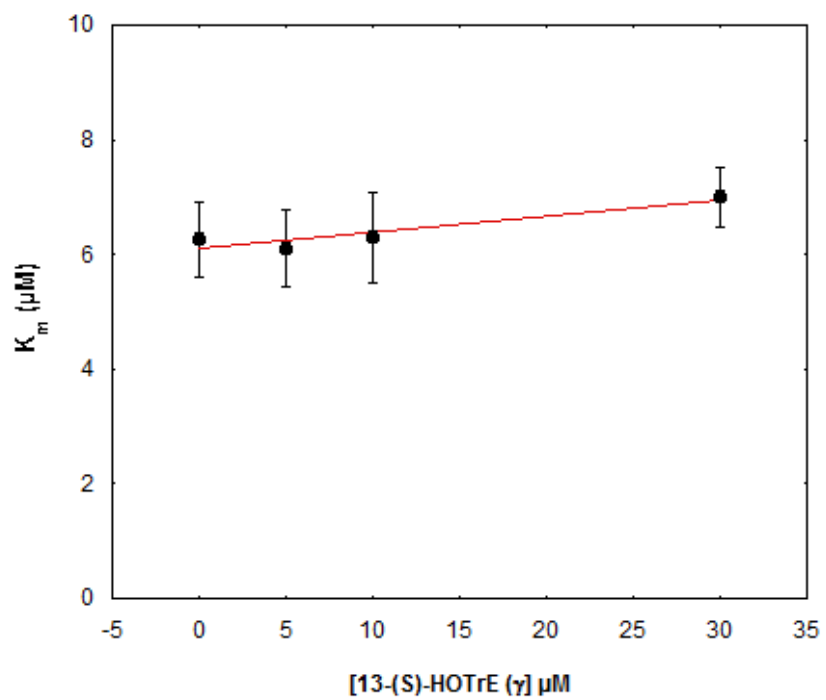


Figure 2.3 Steady-steady kinetics of allosteric effects of 13-(S)-HOTrE (γ) on GLA metabolism. Enzymatic assays were performed with GLA substrate in 25 mM HEPES, 150 mM NaCl buffer (pH 7.5), at 22° C.

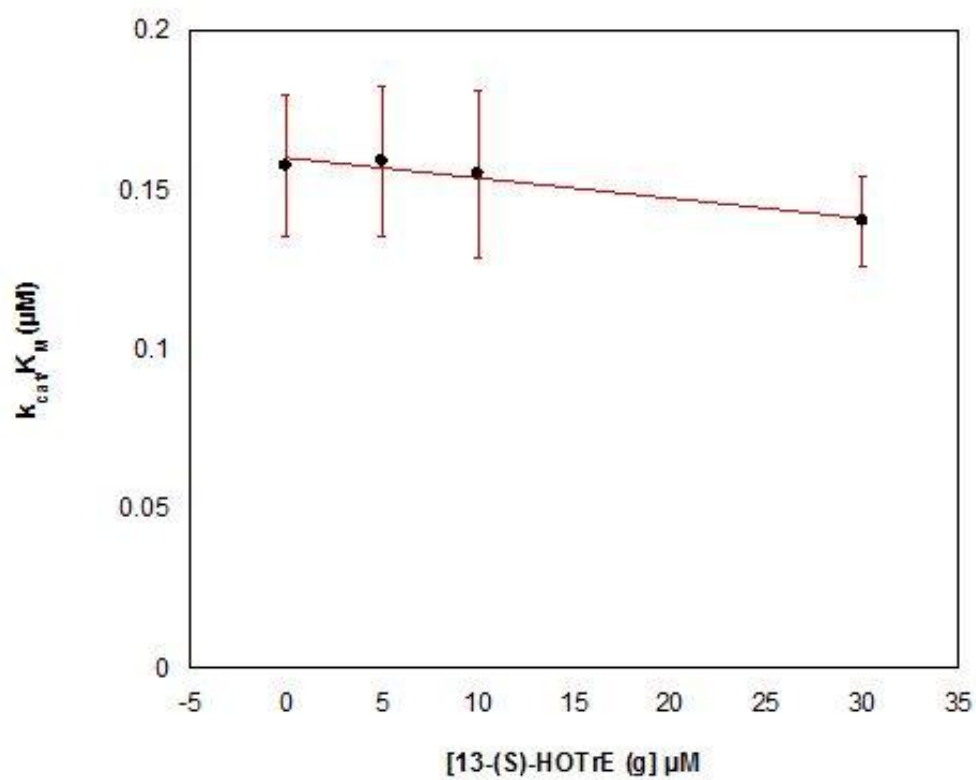


Figure 2.4 Steady-steady kinetics of the allosteric effects of 13-(S)-HODE on GLA metabolism. Enzymatic assays were performed with GLA substrate in 25 mM HEPES, 150 mM NaCl buffer (pH 7.5), at 22° C.

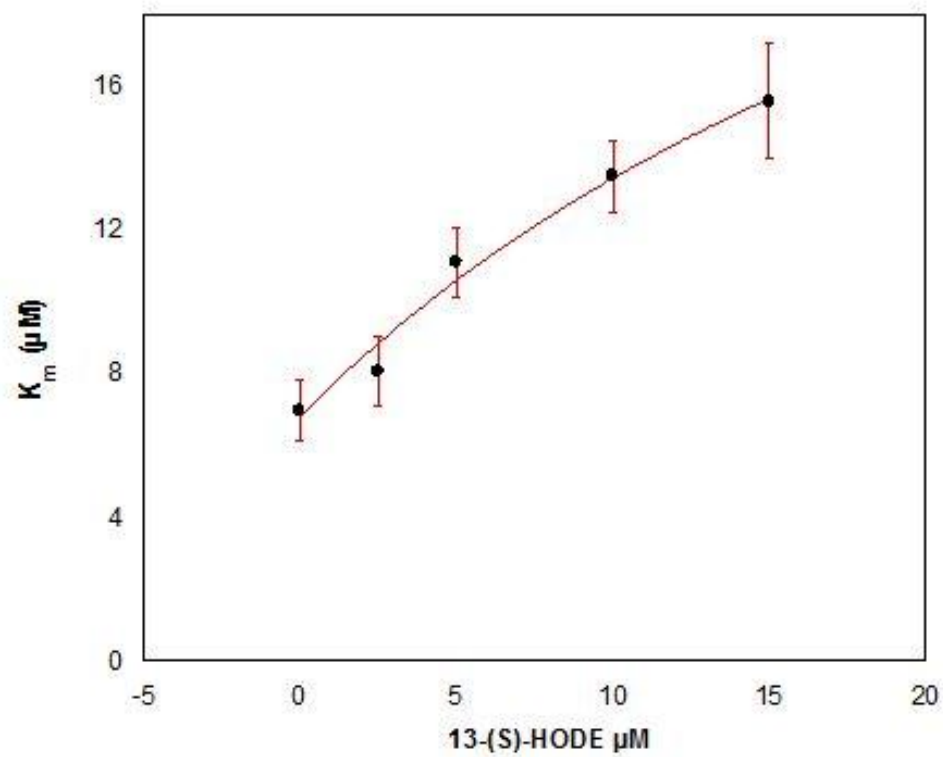


Figure 2.5 Steady-steady kinetics of the allosteric effects of 13-(S)-HODE on GLA metabolism. Enzymatic assays were performed with GLA substrate in 25 mM HEPES, 150 mM NaCl buffer (pH 7.5), at 22° C.

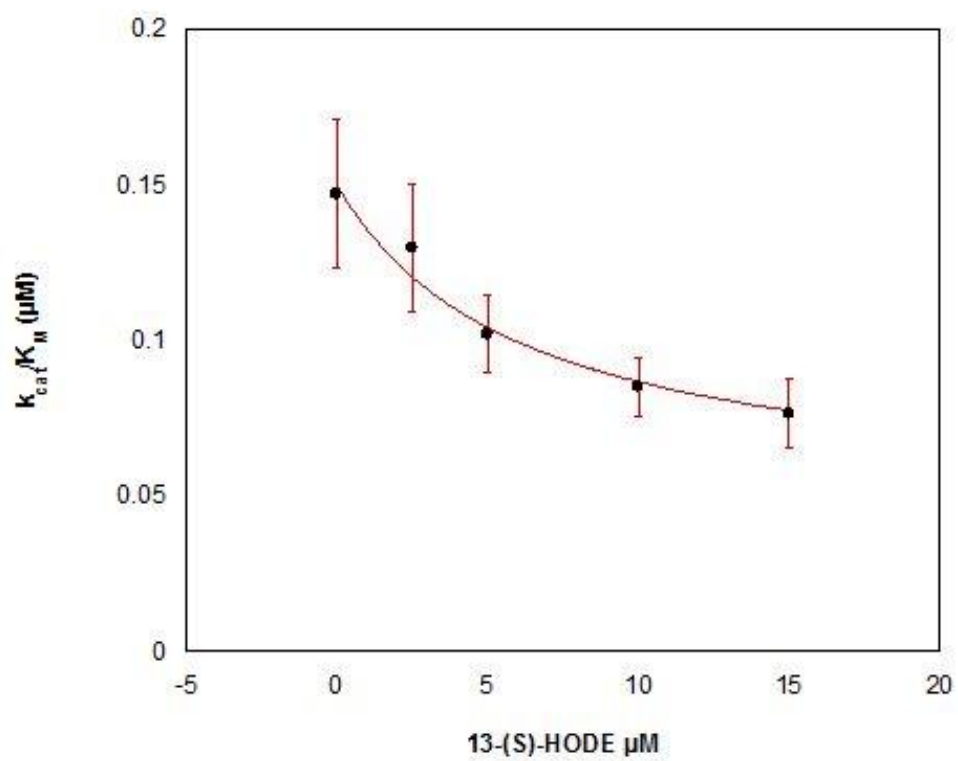
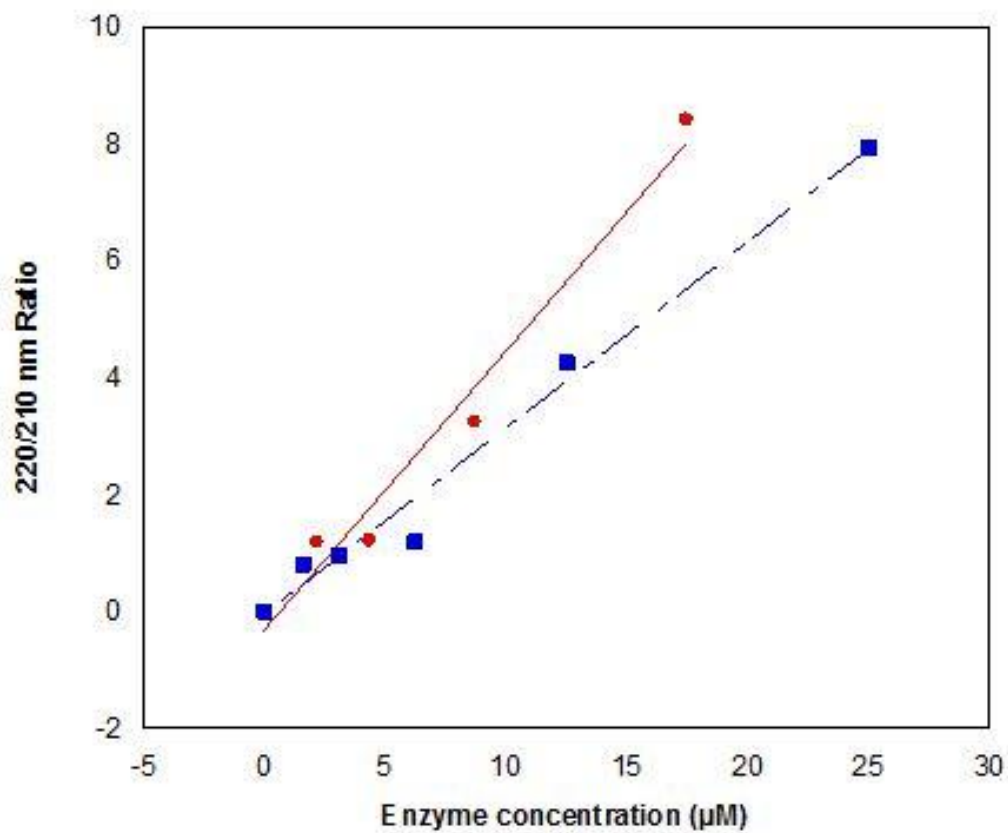


Figure 2.6 CD spectral changes in 220/210 nm ratio resulting from increased protein concentration of 15-LOX-2 (red circles) and 15-LOX-2^{NoPLAT} (blue squares) (25 mM HEPES, 150 mM NaCl, pH 7.5, 22° C).



2.7 Tables

Table 2.1 Kinetic values for 15-LOX-2 and 15-LOX-2^{NoPLAT} with AA and LA as substrates. Enzymatic reactions were performed in 25 mM HEPES buffer at 30° C.

^a [19]

Substrate	AA	GLA	AA	GLA
Enzyme	15-LOX-2 ^a	15-LOX-2 ^a	15-LOX-2 ^{NoPLAT}	15-LOX-2 ^{NoPLAT}
k_{cat} (s ⁻¹)	1.5 ± 0.03	1.8 ± 0.03	0.75 ± 0.03	0.99 ± 0.04
$(k_{cat})^{AA}/(k_{cat})^{GLA}$	0.83 ± 0.02		0.76 ± 0.04	
K_M (μM)	3.8 ± 0.4	2.8 ± 0.1	3.6 ± 0.3	6.3 ± 0.7
k_{cat}/K_M (μM ⁻¹ s ⁻¹)	0.40 ± 0.02	0.64 ± 0.03	0.21 ± 0.02	0.16 ± 0.02
$(k_{cat}/K_M)^{AA}/(k_{cat}/K_M)^{GLA}$	0.62 ± 0.04		1.3 ± 0.2	

Table 2.2 pH dependence of the substrate specificity $(k_{cat}/K_M)^{AA}/(k_{cat}/K_M)^{LA}$ for 15-LOX-2, 15-LOX-2^{NoPLAT}, and 15-LOX-2^{H627A}, using the competitive substrate capture method. Enzymatic assays were performed at 1 μ M substrate in 25 mM HEPES buffer (pH 7.5, 8.5), at 22° C.

Enzyme	pH	$(k_{cat}/K_M)^{AA}/(k_{cat}/K_M)^{LA}$
15-LOX-2	pH 7.5	2.1 \pm (0.1)
15-LOX-2	pH 8.5	3.4 \pm (0.3)
15-LOX-2 ^{NoPLAT}	pH 7.5	2.5 \pm (0.2)
15-LOX-2 ^{NoPLAT}	pH 8.5	3.6 \pm (0.3)
15-LOX-2 ^{H627A}	pH 7.5	1.8 \pm 0.1
15-LOX-2 ^{H627A}	pH 8.5	3.1 \pm 0.1

Table 2.3_ Steady steady kinetics of pH dependence on AA metabolism. Enzymatic assays were performed with AA substrate in 25 mM HEPES, 150 mM NaCl buffer (pH 7.5, and pH 8.5), at 22° C.
^a [19]

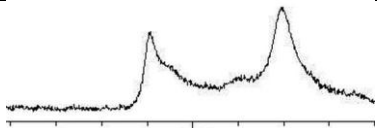
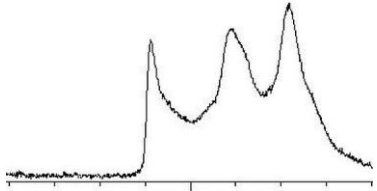
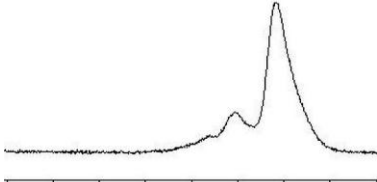
Substrate	pH 7.5	pH 8.5	pH 7.5	pH 8.5
Enzyme	15-LOX-2 ^a	15-LOX-2 ^a	15-LOX-2 ^{NoPLAT}	15-LOX-2 ^{NoPLAT}
k_{cat} (s ⁻¹)	1.5 ± 0.03	2.0 ± 0.04	0.75 ± 0.03	0.72 ± 0.04
$(k_{cat})^{pH8.5}/(k_{cat})^{pH7.5}$	1.3 ± 0.04		0.96 ± 0.07	
K_M (μM)	3.8 ± 0.3	2.6 ± 0.2	3.6 ± 0.3	2.5 ± 0.5
k_{cat}/K_M (μM ⁻¹ s ⁻¹)	0.40 ± 0.03	0.76 ± 0.06	0.21 ± 0.02	0.29 ± 0.06
$(k_{cat}/K_M)^{pH8.5}/(k_{cat}/K_M)^{pH7.5}$	1.9 ± 0.2		1.4 ± 0.3	

Table 2.4 Steady steady kinetics of allosteric regulation by 13-(S)-HODE on AA metabolism. Enzymatic assays were performed with AA substrate in 25 mM HEPES, 150 mM NaCl buffer (pH 7.5), at 22° C.

^a [19]

Product	None	13-(S)-HODE	none	13-(S)-HODE
Enzyme	15-LOX-2 ^a	15-LOX-2 ^a	15-LOX-2 NoPLAT	15-LOX-2 NoPLAT
k_{cat} (s ⁻¹)	1.5 ± 0.03	1.3 ± 0.02	0.75 ± 0.03	0.74 ± 0.01
$\frac{(k_{cat})^{w/13-(S)-HODE}}{(k_{cat})^{w/o13-(S)-HODE}}$	0.87 ± 0.02		0.99 ± 0.04	
K_M (μM)	3.8 ± 0.3	2.0 ± 0.3	3.6 ± 0.3	5.1 ± 0.3
k_{cat}/K_M (μM ⁻¹ s ⁻¹)	0.40 ± 0.03	0.66 ± 0.01	0.21 ± 0.02	0.14 ± 0.01
$\frac{(k_{cat}/K_M)^{w/13-(S)-HODE}}{(k_{cat}/K_M)^{w/o13-(S)-HODE}}$	1.7 ± 0.2		0.69 ± 0.1	

Table 2.5 Size Exclusion Chromatography of 15-LOX-2 and 15-LOX-2^{NoPLAT} (25 mM HEPES, 150mM NaCl, pH 7.5, 4° C). The monomer control sample, BSA (50 mM Tris buffer, pH 7, 150 mM NaCl, 4° C), is also shown.

Enzyme	pH	Chromatograph
15-LOX-2	pH 7.5	
15-LOX-2 ^{No PLAT}	pH 7.5	
BSA	pH 7	

2.7 References

1. Vane, J. R.; Bakhle, Y. S.; Botting, R. M., Cyclooxygenases 1 and 2. *Annu Rev Pharmacol Toxicol* **1998**, 38, 97-120.
2. Capdevila, J. H.; Falck, J. R.; Estabrook, R. W., Cytochrome P450 and the arachidonate cascade. *FASEB J* **1992**, 6 (2), 731-736.
3. Haeggstrom, J. Z.; Wetterholm, A., Enzymes and receptors in the leukotriene cascade. *Cell Mol Life Sci* **2002**, 59 (5), 742-753.
4. Yamamoto, S., Mammalian lipoxygenases : molecular structures and functions. *Biochim. Biophys. Acta* **1992**, 1128 (2-3), 117-131.
5. Solomon, E. I.; Zhou, J.; Neese, F.; Pavel, E. G., New Insights from Spectroscopy into the structure/function relationships of lipoxygenases. *Chem. Biol.* **1997**, 4 (11), 795-808.
6. Serhan, C. N., Lipoxin biosynthesis and its impact in inflammatory and vascular events. *Biochim Biophys Acta* **1994**, 1212 (1), 1-25.
7. Nakano, H.; Inoue, T.; Kawasaki, N.; Miyataka, H.; Matsumoto, H.; Taguchi, T.; Inagaki, N.; Nagai, H.; Satoh, T., Synthesis and biological activities of novel antiallergic agents with 5-lipoxygenase inhibiting action. *Bioorg. Med. Chem.* **2000**, 8 (2), 373-380.
8. Fogh, K.; Kragballe, K., Eicosanoids in inflammatory skin diseases. *Prostaglandins & other lipid mediators* **2000**, 63 (1-2), 43.
9. Capra, V.; Bäck, M.; Barbieri, S. S.; Camera, M.; Tremoli, E.; Rovati, G. E., Eicosanoids and Their Drugs in Cardiovascular Diseases: Focus on Atherosclerosis and Stroke. *Medicinal research reviews* **2012**.
10. Rao, C. V.; Janakiram, N. B.; Mohammed, A., Lipoxygenase and Cyclooxygenase Pathways and Colorectal Cancer Prevention. *Current colorectal cancer reports* **2012**, 1-9.
11. Yeung, J.; Apopa, P. L.; Vesci, J.; Kenyon, V.; Rai, G.; Jadhav, A.; Simeonov, A.; Holman, T. R.; Maloney, D. J.; Boutaud, O., Protein kinase C regulation of 12-lipoxygenase-mediated human platelet activation. *Molecular pharmacology* **2012**, 81 (3), 420-430.

12. Ikei, K. N.; Yeung, J.; Apopa, P. L.; Ceja, J.; Vesci, J.; Holman, T. R.; Holinstat, M., Investigations of human platelet-type 12-lipoxygenase: role of lipoxygenase products in platelet activation. *Journal of Lipid Research* **2012**.
13. Weaver, J. R.; Holman, T. R.; Imai, Y.; Jadhav, A.; Kenyon, V.; Maloney, D. J.; Nadler, J. L.; Rai, G.; Simeonov, A.; Taylor-Fishwick, D. A., Integration of pro-inflammatory cytokines, 12-lipoxygenase and NOX-1 in pancreatic islet beta cell dysfunction. *Molecular and Cellular Endocrinology* **2012**.
14. Karginov, A. V.; Ding, F.; Kota, P.; Dokholyan, N. V.; Hahn, K. M., Engineered allosteric activation of kinases in living cells. *Nature biotechnology* **2010**, 28 (7), 743-747.
15. Huang, Z.; Zhu, L.; Cao, Y.; Wu, G.; Liu, X.; Chen, Y.; Wang, Q.; Shi, T.; Zhao, Y.; Wang, Y., ASD: a comprehensive database of allosteric proteins and modulators. *Nucleic acids research* **2011**, 39 (suppl 1), D663-D669.
16. Prasannan, C. B.; Tang, Q.; Fenton, A. W., Allosteric regulation of human liver pyruvate kinase by peptides that mimic the phosphorylated/dephosphorylated N-terminus. *Methods in Molecular Biology (Clifton, NJ)* **2012**, 796, 335-349.
17. Wecksler, A. T.; Kenyon, V.; Deschamps, J. D.; Holman, T. R., Substrate specificity changes for human reticulocyte and epithelial 15-lipoxygenases reveal allosteric product regulation. *Biochemistry* **2008**, 47 (28), 7364-75.
18. Wecksler, A. T.; Kenyon, V.; Garcia, N. K.; Deschamps, J. D.; van der Donk, W. A.; Holman, T. R., Kinetic and structural investigations of the allosteric site in human epithelial 15-lipoxygenase-2. *Biochemistry* **2009**, 48 (36), 8721.
19. Yoshi, N; Hoobler, E. K.; Perry, S.; Holman, T. R.; Investigations into the allosteric and pH effect on substrate specificity of human epithelial 15-lipoxygenase-2. *Biochemistry* In submission
20. Falgueyret, J. P.; Denis, D.; Macdonald, D.; Hutchinson, J. H.; Riendeau, D., Characterization of the arachidonate and ATP binding sites of human 5-lipoxygenase using photoaffinity labeling and enzyme immobilization. *Biochemistry* **1995**, 34 (41), 13603-11.
21. Hogaboom, G. K.; Cook, M.; Newton, J. F.; Varrichio, A.; Shorr, R. G.; Sarau, H. M.; Crooke, S. T., Purification, characterization, and structural properties of a single protein from rat basophilic leukemia (RBL-1) cells possessing 5-lipoxygenase and leukotriene A4 synthetase activities. *Mol Pharmacol* **1986**, 30 (6), 510-519.

22. Rouzer, C. A.; Samuelsson, B., The importance of hydroperoxide activation for the detection and assay of mammalian 5-lipoxygenase. *FEBS Lett* **1986**, 204 (2), 293-6.
23. Shimizu, T.; Izumi, T.; Seyama, Y.; Tadokoro, K.; Radmark, O.; Samuelsson, B., Characterization of leukotriene A4 synthase from murine mast cells: evidence for its identity to arachidonate 5-lipoxygenase. *Proc Natl Acad Sci U S A* **1986**, 83 (12), 4175-4179.
24. Mogul, R.; Holman, T. R., Inhibition studies of soybean and human 15-lipoxygenases with long-chain alkenyl sulfate substrates. *Biochemistry* **2001**, 40 (14), 4391-4397
25. Ruddat, V. C.; Whitman, S.; Holman, T. R.; Bernasconi, C. F., Stopped-flow kinetic investigations of the activation of soybean lipoxygenase-1 and the influence of inhibitors on the allosteric site. *Biochemistry* **2003**, 42 (14), 4172-4178.
26. Walther, M.; Anton, M.; Wiedmann, M.; Fletterick, R.; Kuhn, H., The N-terminal domain of the reticulocyte-type 15-lipoxygenase is not essential for enzymatic activity but contains determinants for membrane binding. *J. Biol. Chem.* **2002**, 277 (30), 27360-27366.
27. Walther, M.; Hofheinz, K.; Vogel, R.; Roffeis, J.; Kühn, H., The N-terminal β -barrel domain of mammalian lipoxygenases including mouse 5-lipoxygenase is not essential for catalytic activity and membrane binding but exhibits regulatory functions. *Archives of Biochemistry and Biophysics* **2011**, 516 (1), 1-9.
28. Aleem, A. M.; Jankun, J.; Dignam, J. D.; Walther, M.; Kuhn, H.; Svergun, D. I.; Skrzypczak-Jankun, E., Human platelet 12-lipoxygenase, new findings about its activity, membrane binding and low-resolution structure. *J Mol Biol* **2008**, 376 (1), 193-209.
29. Dainese, E.; Angelucci, C. B.; Sabatucci, A.; De Filippis, V.; Mei, G.; Maccarrone, M., A novel role for iron in modulating the activity and membrane-binding ability of a trimmed soybean lipoxygenase-1. *The FASEB Journal* **2010**, 24 (6), 1725-1736.
30. Di Venere, A.; Salucci, M. L.; van Zadelhoff, G.; Veldink, G.; Mei, G.; Rosato, N.; Finazzi-Agro, A.; Maccarrone, M., Structure-to-function relationship of mini-lipoxygenase, a 60-kDa fragment of soybean lipoxygenase-1 with lower stability but higher enzymatic activity. *J Biol Chem* **2003**, 278 (20), 18281-8.

31. Holman, T. R.; Zhou, J.; Solomon, E. I., Spectroscopic and functional characterization of a ligand coordination mutant of soybean lipoxygenase-1: first coordination sphere analogue of human 15-lipoxygenase. *Journal of the American Chemical Society* **1998**, 120 (48), 12564-12572.
32. Sloane, D. L.; Leung, R.; Barnett, J.; Craik, C. S.; Sigal, E., Conversion of Human 15-Lipoxygenase to an Efficient 12-Lipoxygenase - The Side-Chain Geometry of Amino Acids 417 and 418 Determine Positional Specificity. *Prot. Eng.* **1995**, 8 (3), 275-282.
33. Deschamps, J. D.; Gautschi, J. T.; Whitman, S.; Johnson, T. A.; Gassner, N. C.; Crews, P.; Holman, T. R., Discovery of platelet-type 12-human lipoxygenase selective inhibitors by high-throughput screening of structurally diverse libraries. *Bioorganic & Medicinal Chemistry* **2007**, 15 (22), 6900-8.
34. Blommel, P. G.; Fox, B. G., A combined approach to improving large-scale production of tobacco etch virus protease. *Protein expression and purification* **2007**, 55 (1), 53-68.
35. Wecksler, A. T.; Jacquot, C.; van der Donk, W. A.; Holman, T. R., Mechanistic Investigations of Human Reticulocyte 15- and Platelet 12-Lipoxygenases with Arachidonic Acid. *Biochemistry* **2009**, 48, 6259-6267.
36. Segraves, E. N.; Holman, T. R., Kinetic investigations of the rate-limiting step in human 12- and 15-lipoxygenase. *Biochemistry* **2003**, 42 (18), 5236-43.
37. Ivanov, I.; Shang, W.; Toledo, L.; Masgrau, L.; Svergun, D. I.; Stehling, S.; Gómez, H.; Di Venere, A.; Mei, G.; Lluch, J. M.; Skrzypczak-Jankun, E.; González-Lafont, À.; Kühn, H., Ligand-induced formation of transient dimers of mammalian 12/15-lipoxygenase: A key to allosteric behavior of this class of enzymes? *Proteins: Structure, Function, and Bioinformatics* **2012**, 80 (3), 703-712.
38. Yuan, C.; Sidhu, R. S.; Kuklev, D. V.; Kado, Y.; Wada, M.; Song, I.; Smith, W. L., Cyclooxygenase Allosterism, Fatty Acid-mediated Cross-talk between Monomers of Cyclooxygenase Homodimers. *Journal of Biological Chemistry* **2009**, 284 (15), 10046-10055.
39. O'Neil, K. T.; DeGrado, W. F., A thermodynamic scale for the helix-forming tendencies of the commonly occurring amino acids. *Science (New York, NY)* **1990**, 250 (4981), 646.

40. Urano, F.; Hayashi, N.; Arisaka, F.; Kurita, H.; Murata, S.; Ichinose, H., Molecular Mechanism for Pterin-Mediated Inactivation of Tyrosine Hydroxylase: Formation of Insoluble Aggregates of Tyrosine Hydroxylase. *Journal of Biochemistry* **2006**, 139 (4), 625-635.
41. Wichmann, C.; Becker, Y.; Chen-Wichmann, L.; Vogel, V.; Vojtkova, A.; Herglotz, J.; Moore, S.; Koch, J.; Lausen, J.; Mäntele, W.; Gohlke, H.; Grez, M., Dimer-tetramer transition controls RUNX1/ETO leukemogenic activity. *Blood* **2010**, 116 (4), 603-613.
42. Tchan, M. C.; Choy, K. J.; Mackay, J. P.; Lyons, A. T. L.; Bains, N. P. S.; Weiss, A. S., Interfacial Asparagine Residues within an Amide Tetrad Contribute to Max Helix-Loop-Helix Leucine Zipper Homodimer Stability. *Journal of Biological Chemistry* **2000**, 275 (48), 37454-37461.

Chapter 3

Discovery of a novel dual fungal cyp51/human 5-lipoxygenase inhibitor: Implications for anti-seborrhoeic dermatitis therapy

3.1 Introduction

Human 5-lipoxygenase (5-LOX) has long been considered a possible therapeutic target for inflammatory diseases. Asthma is the principal disease target, however, numerous other diseases have been postulated in the literature as possible targets for 5-LOX inhibition, such as allergic rhinitis, chronic obstructive pulmonary disease, idiopathic pulmonary fibrosis, atherosclerosis, ischemia-reperfusion injury, atopic dermatitis and acne vulgaris [2-7]. The role of 5-LOX in acne vulgaris has been shown to be related to the production of sebum in the derma [8]. 5-LOX has also been implicated in another skin disease, seborrheic dermatitis (i.e. dandruff) [9], which is a common chronic skin disorder that affects sebum-rich areas and shares some features with psoriasis and atopic dermatitis. The pathogenesis of dandruff is complex and appears to result from interactions among scalp skin, cutaneous microflora and the cutaneous inflammation [10]. Recently, three inflammation biomarkers (IL-1 α , IL-1RA and IL-8) were associated with development of dandruff [10]. Of these markers, IL-8 was shown to be induced by the production of leukotriene B₄ (LTB₄),

indicating the involvement of 5-LOX in the cause of dandruff as LTB₄ is a product of 5-LOX [11-13].

Ketoconazole is a widely used anti-fungal agent that is currently utilized as an active ingredient in anti-dandruff shampoo [14,15]. Its mode of action is that it inhibits fungal sterol 14 α -demethylase (Erg11 or CYP51) during ergosterol biosynthesis, thus retarding fungal growth [16]. However, it has been proposed that part of its effectiveness is due to anti-inflammation activity because it also inhibits 5-LOX [17]. The anti-inflammatory effect of ketoconazole has also been seen for itraconazole, a similar anti-fungal therapeutic [18], which suggests a common theme, dual anti-fungal/anti-inflammatory for effective dandruff agents. Nevertheless, the potency of ketoconazole and itraconazole against 5-LOX is poor, with IC₅₀ values greater than 50 μ M for both molecules, which indicates potential for improvement in their anti-dandruff activity [17,18].

Numerous inhibitors for 5-LOX have been found [19-22], which can be generally classified into three categories; reductive, iron ligands and competitive/mixed inhibitors [7,23,24] (Figure 3.1); however, only one compound has been approved as a drug, Zileuton [25,26]. Zileuton is a potent and selective 5-LOX inhibitor but its mode of action is unusual for a therapeutic [24,27]. It contains an N-hydroxyurea, which is proposed to chelate to the active enzyme's ferric ion and reduce it to the inactive ferrous ion [21,27,28]. In general, chelation/reduction is not considered a viable mode of inhibition for a therapeutic because metal chelation tends toward

promiscuous behavior with other metalloproteins, and reductive inhibitors can be chemically inactivated in the cell [21,23,24]. Nevertheless, Zileuton has been shown to not only be selective for 5-LOX but also efficacious in the cell [25-27], making this class of inhibitors as a viable chemotype for 5-LOX inhibition. Other chelative inhibitors, such as nordihydroguaiaretic acid (NDGA) [29-31] are also reductive due to their facile nature of inner sphere electron reduction. NDGA contains a catechol moiety, which binds to the active site ferric ion of 5-LOX, reducing it to the ferrous ion, with the concomitant oxidation of the catechol moiety to the semiquinone. This reactivity has previously been observed with the metalloenzyme, catechol dioxygenase, the substrate (catechol) of which is activated to the semiquinone by the active site ferric ion for oxidation by molecular oxygen [30,32,33]. There is also a sub-classification of reductive inhibitors that do not chelate the active site iron. The mechanism for these inhibitors is most likely long-range electron transfer, but no direct proof has been found for this mechanism. Recent efforts by the pharmaceutical industry have focused on non-reductive inhibitors of 5-LOX, however, these appear to have been discontinued during Phase II clinical trials [3,34,35]. In the current publication, phenylenediamine derivatives are presented as highly selective, non-chelative, reductive inhibitors towards 5-LOX. One derivative, in particular, is similar to ketoconazole in structure and demonstrates dual CYP51/5-LOX inhibitory properties. This new chemical entity, which combines anti-inflammatory and

antifungal activities, is presented as a possible novel therapeutic against both the fungal and inflammatory causes of dandruff.

3.2 Results and discussion

A novel 5-LOX inhibitor chemotype, phenylenediamine, was discovered while screening for LOX inhibitors in our lab. Based on its chemical nature, the mode of inhibition was postulated to arise from reduction of the active site ferric atom. As mentioned in the introduction, reductive inhibition of lipoxygenase is a very effective mode of action, with many reductive inhibitors having sub-micromolar IC_{50} values[6,7,21,24], and is indicative of both the ease by which the active site ferric can be reduced and the importance of the oxidation state of the iron. With this in mind, the phenylenediamine parent compound (1) was modified to change its reduction potential (Table 3.1) [36]. Modifications of the phenylenediamine core, such as atom substitutions of the nitrogens with carbon or oxygen (2 and 3, respectively), or the insertion of two additional nitrogen atoms into the core phenyl of the phenylenediamine (4, 5), induced complete loss of inhibitory potency. Interestingly, substitution of only one nitrogen in the core phenyl ring (6) did not lower potency dramatically, nor did methylation of the nitrogen (7).

The pseudoperoxidase assay, which requires a reductive inhibitor, was subsequently conducted with these inhibitors to establish their reductive activity against 5-LOX (Table 1). The results demonstrated that the pseudoperoxidase activity paralleled the inhibitor potency, consistent with changes in the reductive potential of

the inhibitors. Similar alterations of the core phenylenediamine structure were previously used in a similar manner to determine the relationship between potency and reductive properties [37-40]. For comparison, Zileuton and Setileuton were screened as positive controls, with Zileuton being reductive and Setileuton being non-reductive in their method of inhibition.

Determining IC_{50} values for reductive inhibitors is challenging because their relative potency is dependent on a combination of their reactivity with the active site iron and their binding affinity. The binding affinity was investigated by changing the substituents on either side of the phenylenediamine core. As seen in Table 3.2, the chemotype core tolerated a large range of modifications, such as changing the steric bulk on either side of the phenylenediamine core. The only modification in this small set that showed a greater than 10-fold decrease in potency was inhibitor 10, which was surprising given the activity of the related oxazoles 8 and 9. The relative lack of potency dependence on inhibitor structure suggests that the active site can accommodate a variety of inhibitor shapes and sizes, consistent with the large size of the 5-LOX active site [41] and the relatively large 5-LOX inhibitors previously discovered [7,21,24].

Steady state kinetics were conducted with compound 13. Plotting K_M/V_{max} and $1/V_{max}$ versus inhibitor concentration yielded linear plots, with K_I equaling 0.58 ± 0.27 μM and K_I' equaling 1.72 ± 1.37 μM ; these are defined as the equilibrium constants of inhibitor dissociation from the enzyme and enzyme substrate complex, respectively

(Supporting Materials, Figures 3.1 and 3.2). These values reflect a mixed-type inhibition, which is common for lipoxygenase inhibitors [7,42]. Considering that compound 13 is a reductive inhibitor, as seen by the pseudoperoxidase assay, it is interesting to note that the catalytic site inhibition constant (K_I) is similar in magnitude to the IC_{50} value of 13 ($0.57 \pm 0.07 \mu\text{M}$).

Selectivity of the inhibitor chemotype was evaluated by screening a variety of LOX isozymes with a small subset of compounds (Table 3.3). Strong selectivity was displayed against 5-LOX relative to the other isozymes, with selectivity being 80-fold for 12-LOX, 75-fold for 15-LOX-1, and 30-fold for 15-LOX-2 (Table 3). The chemotype also displayed strong selectivity when assayed against cyclooxygenase (COX), with a 140-fold selectivity against COX-1 and a 240-fold selectivity against COX-2. These combined results indicate that this chemotype has a strong selectivity against 5-LOX versus a number of other arachidonic acid processing enzymes. As controls, Setileuton and Zileuton also displayed excellent selectivity [25,26,34] whereas baicalein did not [43].

A few inhibitors were then tested for efficacy in whole human blood, which is known to express 5-LOX upon activation by an ionophore. Compounds 1 and 13 displayed roughly 50% inhibition at 10 μM drug dosing in whole blood, while the positive control, Setileuton, was found to inhibit 100% at 10 μM (Table 2.4). Compound 15 was also tested, but the potency was shown to be further reduced, with less than 10% inhibition at 10 μM (Table 4). The cellular inhibition values for

compounds 1 and 13 and Setileuton were diminished relative to the isolated-enzyme inhibitor values. This result, along with results of other analogues failing to display high potency, could indicate either non-specific interactions or metabolism of the inhibitors by the cell. Ketaminazole (16) was also tested in whole human blood and was shown to display reduced potency relative to in-vitro. However, its potency was higher than that of ketoconazole, with the former displaying approximately 20-fold reduction in potency, a similar trend was observed with Setileuton. Interestingly, ketoconazole displayed a similar potency to the modified ketaminazole, improved efficacy of anti-fungals may result from this enhanced anti-inflammatory property.

The determination of the reductive phenylenediamine core being the key potency component and the fact that addition of large functionalities to either side of the phenylenediamine core were well tolerated, led us to consider the similarity between the chemotype discussed herein and ketoconazole (Table 3.5). Ketoconazole is a CYP51 inhibitor with an azole that targets the active site heme and is a potent antifungal, anti-dandruff medication [9,14]. In addition, ketoconazole was previously determined to inhibit 5-LOX, although weakly [17]. Considering the similarity of ketoconazole to our chemotype, we hypothesized that the low potency of the former was most likely due to the absence of the phenylenediamine core, and thus inability in reducing the active site ferric ion in 5-LOX. Thus, we modified the structure of ketoconazole to include a diamine core (16, ketaminazole) and found that its potency against 5-LOX increased over 70-fold compared to ketoconazole and that it became a

reductive inhibitor, as seen by its activity in the pseudoperoxidase assay (Table 2.5). The selectivity of the ketaminazole (16) was also investigated and found to preferentially inhibit 5-LOX over 200 times better than that of 12-LOX, 15-LOX-1, 15-LOX-2, COX-1 and COX-2 (Table 5). This is most likely due to the large active site of 5-LOX compared to the other human LOX isozymes.

The importance of the phenylenediamine core for reductive inhibition was further verified using computational methods. Molecular modeling of possible inhibitor binding modes within the active site of ketoconazole and ketaminazole was initiated by deprotonating the amine groups at the phenylenediamine core and energy minimization of the compounds with LigPrep. The inhibitors listed in Tables 3.1 and 3.2 were then docked against the crystal structure of the modified protein, Stable-5-LOX (3O8Y), using Glide's "XP" (extra-precision) mode. Different trials, with varying van der Waals scaling factors and alternating positional or hydrophobic constraints linking the inhibitor to the active site, resulted in high-ranking binding poses for several inhibitors depicting the deprotonated amine nitrogen within 10 Å of the catalytic iron. The docking results of these inhibitors support the hypothesis that the reduction of the ferric iron could be caused by the phenylenediamine core, either through an inner sphere or outer sphere mechanism. Docking of the larger inhibitors, ketoconazole and ketaminazole (16), generated poses with similar Glide docking scores to the other inhibitors studied, suggesting a comparable binding mode despite the differences in IC₅₀ values. In several high-ranking binding poses, the amine/ester

core was observed to be within 5 Å of the catalytic iron (Figure 3.1), suggesting that inhibition is weaker in ketoconazole than in ketaminazole (16) because it is lacking the phenylenediamine core and thus it is not able to reduce the active site iron.

The docking poses of the phenylenediamine inhibitors not only suggest the amine as a potential conduit of iron reduction, but they also suggest the active site iron-hydroxide moiety could possibly abstract a hydrogen atom from the amine by an inner sphere mechanism, as is seen in the natural mechanism of LOX with its fatty acid substrate. To test this hypothesis, compound 13 was incubated in buffer constituted with D₂O to deuterate the phenylenediamine core amine, and its IC₅₀ value compared to the protonated amine, in H₂O. A 2.4-fold increase in the IC₅₀ for 13 was observed in D₂O, which is well below the kinetic isotope effect expected for hydrogen atom abstraction [44], suggestive of a proton independent outer sphere reductive mechanism. To further verify this proton independent reductive mechanism, compounds 1 and 7 (containing the protonated and methylated amine, respectively) were investigated. Both were shown to have a similar increase in IC₅₀ values in D₂O and H₂O, suggesting the effect does not involve the proton.

In order to evaluate the concept of improved 5-LOX inhibition for an anti-inflammatory effect combined with antifungal potency we examined the effect of ketaminazole (16) and ketoconazole for selectivity against which the human and *C. albicans* proteins. Binding ketaminazole (16) and ketoconazole with both *C. albicans* CYP51 (CaCYP51) and *H. sapiens* CYP51 (HsCYP51) produced strong type II

difference spectra (Figure 2) signifying direct coordination of the compounds as the sixth ligand of the heme prosthetic group of CYP51 [45,46]. Ketoconazole and ketaminazole (16) both bound tightly to CaCYP51 with K_d values of 44 ± 7 and 70 ± 6 nM, respectively. Tight binding is observed when the K_d for the ligand is similar to or less than the concentration of CYP51 present [47]. The similar K_d values obtained for ketoconazole and ketaminazole (16) suggest that both azoles would be equally effective as antifungal agents against wild-type CaCYP51. This is understandable as the CYP51 potency of this class of molecules is predominantly due to their azole moiety, which is quite distant from the ketaminazole (16) modification of the phenylenediamine core. This compares with reported K_d values of 10 to 50 nM previously obtained for other azole antifungals against CaCYP51 [48]. Ketoconazole bound 3.6-fold more tightly to HsCYP51 ($K_d = 211\pm 39$ nM) compared to ketaminazole (16) ($K_d = 761\pm 41$ nM). The increased selectivity of ketaminazole (16) for the fungal CYP51 over the host CYP51 homolog (10.9-fold based on K_d values) is more than twice that of ketoconazole (4.8-fold), suggesting the potential for less off-target activity for ketaminazole (16) (e.g. CYPs). Other reported azole-containing anti-fungal agents have K_d values <100 nM for clotrimazole, econazole and miconazole, ~180 nM for ketoconazole and ~70 μ M for fluconazole with HsCYP51 [49].

The IC_{50} CYP51 assay was performed to verify the azole binding data (Figure 3), and both results were found to be consistent with differential binding between

ketoconazole and ketaminazole (16). CaCYP51 was strongly inhibited by both ketoconazole and ketaminazole (16), with IC_{50} values of ~ 0.5 and ~ 0.9 μM , respectively, confirming that both azoles bind tightly to CaCYP51. Interestingly, at 4 μM ketaminazole (16) CaCYP51 retained $\sim 15\%$ CYP51 activity, suggesting that lanosterol can displace ketaminazole (16) but not ketoconazole from CaCYP51. HsCYP51 was less severely inhibited by both ketoconazole and ketaminazole (16) with IC_{50} values of ~ 5 and ~ 16 μM , respectively, indicating less tight azole binding and suggested that lanosterol can displace ketoconazole, and especially ketaminazole (16), from HsCYP51. At 95 μM ketoconazole, HsCYP51 was inactivated, this is in contrast to the $\sim 30\%$ CYP51 activity remaining in the presence of 155 μM ketaminazole (16). The 3-fold higher IC_{50} value for ketaminazole (16) over ketoconazole with HsCYP51 confirmed that ketaminazole (16) would be less disruptive to the CYP51 function of the host homolog than ketoconazole, conferring a therapeutic advantage of the former for use as a topical/surface-contact antifungal agent. These results indicate that the minor modification of ketoconazole to ketaminazole (16) not only retains the fungal CYP51 potency of ketaminazole and improves its selectivity but also increases its 5-LOX potency selectivity over 40-fold, thus making it a potent dual CYP51 / 5-LOX inhibitor. This is significant as it is widely regarded that dandruff has two medical consequences, fungal infection and inflammation response [14,17]. Therefore, the dual nature of ketaminazole (16) could potentially increase its effectiveness against the disease and for other mycoses.

3.3 Conclusion

In conclusion, the current data indicate that the phenylenediamine chemotype is a robust inhibitor against 5-LOX, demonstrating high potency, enzyme selectivity and cellular activity. The mechanism of action is via the reduction of the active site ferric ion, similar to that seen for Zileuton, the only FDA-approved LOX inhibitor. It is interesting to note that unlike Zileuton, which chelates the iron through the N-hydroxyurea, the phenylenediamine chemotype lacks an obvious chelating moiety. Structural modification around the phenylenediamine core was well tolerated, while, even relatively minor changes to the phenylenediamine moiety resulted in a loss of activity, presumably due to changes in its reduction potential. This attribute was utilized to modify the structure of ketoconazole to include the phenylenediamine moiety and produce a novel inhibitor, ketaminazole (16). This compound demonstrated a 40-fold increase in potency against 5-LOX, comparable potency against fungal CYP51, and improved selectivity against the human CYP51, relative to ketoconazole. This dual anti-fungal and anti-inflammatory of ketaminazole (16), could potentially have therapeutic uses for anti-dandruff therapy.

3.4 Acknowledgement

The SAR synthesis was performed at the NCGC by Ganesha Rai, Ajit Jadhav, Anton Simeonov, and David J. Maloney.

The fungal screens were performed by Andrew G. S. Warrilow, Josie E. Parker, Diane E. Kelly, S. L. Kelly.

3.5 Methods

3.5.1 Overexpression and Purification of 5-Human Lipoxygenase, 12-Human Lipoxygenase, and the 15-Human Lipoxygenases.

Human reticulocyte 15-lipoxygenase-1 (15-LOX-1) [50], human platelet 12-lipoxygenase (12-LOX) [50], human prostate epithelial 15-lipoxygenase-2 (15-LOX-2) [51] were expressed as N-terminally, His6-tagged proteins and purified to greater than 90% purity [52]. Human leukocyte 5-lipoxygenase was expressed as a non-tagged protein and used as a crude ammonium sulfate protein fraction, as published previously [22].

3.5.2 Lipoxygenase UV-Vis-based Manual Assay.

The initial one-point inhibition percentages were determined by following the formation of the conjugated diene product at 234 nm ($\epsilon = 25,000 \text{ M}^{-1}\text{cm}^{-1}$) with a Perkin-Elmer Lambda 40 UV vis spectrophotometer at one inhibitor concentration. All reaction mixtures were 2 mL in volume and constantly stirred using a magnetic stir bar at room temperature (23°C) with approximately 40 nM for 12-LOX and 20 nM of 15-LOX-1 (by iron content). Reactions with crude ammonium sulfate precipitated 5-LOX were carried out in 25 mM HEPES (pH 7.3), 0.3 mM CaCl₂, 0.1 mM EDTA, 0.2 mM ATP, 0.01% Triton X-100, 10 μM AA and with 12-hLO in 25 mM Hepes buffer (pH 8.0), 0.01% Triton X-100, and 10 μM AA. Reactions with 15-LOX-1 and 15-LOX-2 were carried out in 25 mM Hepes buffer (pH 7.5), 0.01% Triton X-100, and 10 μM AA. The concentration of AA (for 5-LOX and 12- LOX)

and LA (for 15-LOX-1) were quantitatively determined by allowing the enzymatic reaction to go to completion. IC_{50} values were obtained by determining the enzymatic rate at various inhibitor concentrations and plotting the rates against inhibitor concentration, followed by a hyperbolic saturation curve fit. The data used for the saturation curves were performed in duplicate or triplicate, depending on the quality of the data. It should be noted that all of the potent inhibitors displayed greater than 80% maximal inhibition unless otherwise stated in the tables. Inhibitors were stored at $-20^{\circ}C$ in DMSO. As a result of screening with a semi-purified protein the question arose whether the 5-LOX concentration was approaching the inhibitor concentration for our most potent inhibitors, which would affect the Henri-Michaelis-Menten approximation. In order to answer this question, we compared the IC_{50} values of two high potency 5-LOX inhibitors to that in the literature. Setileuton displayed an IC_{50} value of 60 ± 6 nM, in good agreement with the literature value of 45 ± 10 nM, and Zileuton displayed an IC_{50} value of 560 ± 80 nM, in good agreement with the literature value of 500 ± 100 nM [2,13]. The solvent isotope effect of the inhibitor IC_{50} was investigated utilizing the same conditions and methods as stated above. The pH of the buffered D_2O , was established using standard methods.

3.5.3 Steady-State Inhibition Kinetics.

Lipoxygenase rates were determined by monitoring the formation of the conjugated product, 5-HPETE, at 234 nm ($\epsilon = 25\ 000\ M^{-1}\ cm^{-1}$) with a Perkin-Elmer Lambda 40 UV/vis spectrophotometer. Reactions were initiated by the addition of 5-

LOX to a constantly stirring, 2mL cuvette containing 40 μM AA in 25 mM HEPES (pH 7.3), 0.3 mM CaCl_2 , 0.1 mM EDTA, and 0.2 mM ATP, at varied inhibitor concentrations in the presence of 0.01% Triton X-100. The substrate concentration was determined by allowing the enzymatic reaction to proceed to completion. Kinetic data were obtained by recording initial enzymatic rates at varied inhibitor concentrations, and subsequently fitting the data to the Henri-Michaelis-Menten equation, using KaleidaGraph (Synergy) to determine the microscopic rate constants, V_{max} ($\mu\text{mol}/\text{min}/\text{mg}$) and V_{max}/K_M ($\mu\text{mol}/\text{min}/\text{mg}/\mu\text{M}$). These kinetic parameters were subsequently reported, $1/V_{\text{max}}$ and K_M/V_{max} versus inhibitor concentration, to yield K_i and $K_{i'}$, respectively.

3.5.4 Cyclooxygenase Assay.

Ovine COX-1 (Cat. No. 60100) and human COX-2 (Cat. No. 60122) were purchased from Cayman Chemical. Approximately 2 μg of either COX-1 or COX-2 were added to 0.1 M Tris-HCl buffer (pH 8.0) buffer containing 100 μM AA, 5 mM EDTA, 2 mM phenol and 1 μM hematin at 37 $^{\circ}\text{C}$. Data were collected using a Hansatech DW1 oxygen electrode chamber, as described previously [53]. Inhibitor or carrier solvent were mixed with the respective COX within the electrode cell. The reaction was initiated by the addition of arachidonic acid, followed by monitoring of the rate of oxygen consumption. Ibuprofen, aspirin and indomethacin, and the carrier solvent, DMSO, were used as positive and negative controls, respectively.

3.5.5 Human Blood LTB₄ Inhibition Assay.

Whole human blood was dispensed in 150 uL samples, followed by addition of inhibitor or control (vehicle, DMSO), and incubated for 15 min at 37 °C. The leukocytes were activated by introduction of the calcium ionophore, A23817 (freshly diluted from a 50 mM DMSO stock to 1.5 mM in Hanks balanced salt solution), and incubated for 30 min at 37 °C. Samples were then centrifuged at 1,500 rpm (300 g) for 10 min at 4 °C and the supernatant diluted 20-50-fold (batch dependent) for LTB₄ detection, using an ELISA detection kit (Cayman Chemicals Inc.). Inhibitors were added at 10 μM or 15 μM concentrations (0.5 μM for control Setileuton) [54-56]. IC₅₀ values were generated using an IC₅₀ estimation equation.

3.5.6 Pseudoperoxidase activity assay.

The reductive properties of the inhibitors were determined by monitoring the pseudoperoxidase activity of lipoxygenase in the presence of the inhibitor and 13-HPODE. Activity is characterized by direct measurement of the product degradation by following the decrease of absorbance at 234 nm using a Perkin-Elmer Lambda 40 UV/Vis spectrometer (50 mM sodium phosphate (pH 7.4), 0.3 mM CaCl₂, 0.1 mM EDTA, 0.01% Triton X100, 10 μM 13-HPODE). All reactions were performed in 2 mL of buffer and constantly stirred with a rotating stir bar (22 °C). The reaction was initiated by addition of 10 μM inhibitor (a 1:1 ratio to product); A loss of greater than 40% of product absorption at 234 nm signified a positive activity result. The control

inhibitors for this assay were Setileuton and Zileuton, known non-reductive and reductive inhibitors, respectively.

3.5.7 Inhibitor modeling.

Grid generation and flexible ligand docking were performed using Glide, while energy minimization and ligand preparation of inhibitors were done with LigPrep. LigPrep and Glide are both products of Schrodinger, Inc., and utilize energy functions to generate and rank models of ligand 3D structures and ligand-protein interactions, respectively. The crystal structure of stable human 5-lipoxygenase (PDB ID: 3O8Y) was used to generate a Glide grid in which to carry out docking algorithms with our inhibitors. This structure contains several point mutations that remove destabilizing sequences, but because none of these are located at the active site of the enzyme, we find it reasonable to assume the mutant structure holds as an accurate model of the wild-type active site. Positional constraints at the catalytic iron and at hydrophobic pockets within the active site were established and utilized intermittently during different docking calculations. Poses generated from ligand docking were ranked according to their GlideScores.

3.5.8 CYP51 protein studies.

C. albicans CYP51 (CaCYP51) and *Homo sapiens* CYP51 (HsCYP51) proteins were expressed in *E. coli* using the pCWori⁺ vector, isolated and purified to over 90% purity as previously described [48,49]. Native cytochrome P450 concentrations were determined by reduced carbon monoxide difference spectra⁵⁷ based on an extinction

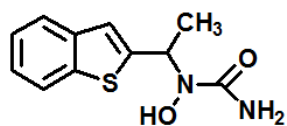
coefficient of $91 \text{ mM}^{-1} \text{ cm}^{-1}$ ^{58, 59}. Absorption measurements of azole antifungal agents to $5 \text{ }\mu\text{M}$ CaCYP51 and $5 \text{ }\mu\text{M}$ HsCYP51 were performed as previously described [48,60] using 0.1 , 0.2 and 0.5 mg ml^{-1} stock solutions of ketoconazole and ketaminazole (16) in DMSO. Azole antifungal agents were progressively titrated against CYP51 protein in 0.1 M Tris-HCl (pH 8.1) and 25% (w/v) glycerol, with the spectral difference determined after each incremental addition of azole. The dissociation constant (K_d) of the enzyme-azole complex was determined by nonlinear regression (Levenberg-Marquardt algorithm) of a plot of $\Delta A_{\text{peak-trough}}$ against azole concentration using a rearrangement of the Morrison equation fitted by the computer program ProFit 6.1.12 (QuantumSoft, Zurich, Switzerland).

IC_{50} determinations were performed using the CYP51 reconstitution assay system previously described [61,62] containing $1 \text{ }\mu\text{M}$ CaCYP51 or $0.3 \text{ }\mu\text{M}$ HsCYP51, $2 \text{ }\mu\text{M}$ human cytochrome P450 reductase, $50 \text{ }\mu\text{M}$ lanosterol, $50 \text{ }\mu\text{M}$ dilaurylphosphatidylcholine, 4.5% (wt/vol) 2-hydroxypropyl- β -cyclodextrin, 0.4 mg ml^{-1} isocitrate dehydrogenase, 25 mM trisodium isocitrate, 50 mM NaCl, 5 mM MgCl_2 and 40 mM MOPS (pH ~ 7.2). Azole antifungal agents were added in $5 \text{ }\mu\text{l}$ DMSO followed by 5 minutes incubation at $37 \text{ }^\circ\text{C}$ prior to assay initiation with 4 mM β -NADPH with shaking for a further 10 minutes at $37 \text{ }^\circ\text{C}$. Sterol metabolites were recovered by extraction with ethyl acetate, followed by derivatization with *N,O*-bis(trimethylsilyl)trifluoroacetamide and tetramethylsilane prior to analysis by gas chromatography mass spectrometry [63]. IC_{50} in this study is defined as the inhibitor

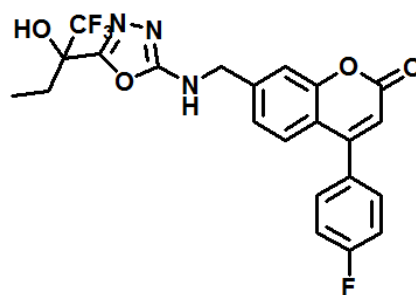
concentration required for 50% inhibition of the CYP51 reaction under the stated assay conditions.

3.6 Figures

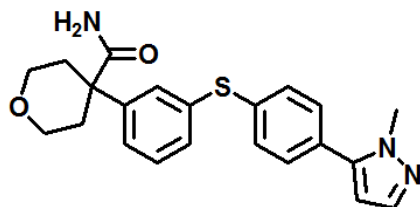
Figure 3.1 Structures of various types of LOX inhibitors.



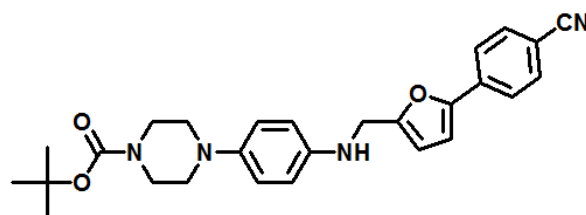
Zileuton
Reductive, Chelative



Setileuton (MK-0633)
Competitive, Non-reductive



PF-4191834
Competitive, Non-reductive



1
Reductive

Figure 3.2 Docking ketoconazole and ketaminazole to the crystal structure of the Stable-5-LOX. Glide docking scores and poses were similar to other high-ranking docked inhibitors.

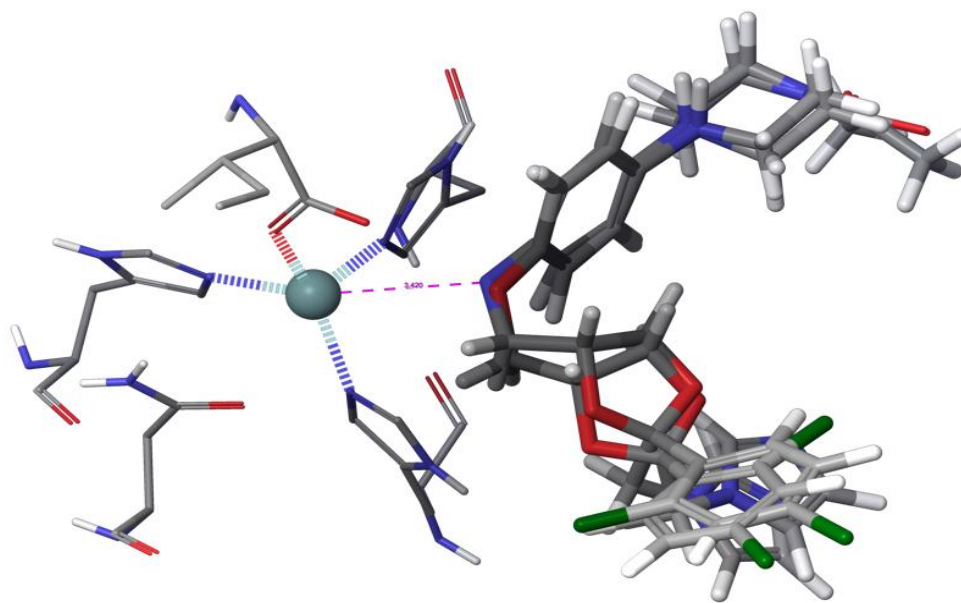


Figure 3.3 Binding properties of ketoconazole and ketaminazole with CaCYP51 and HsCYP51. Azole antifungals were progressively titrated against 5 μM CaCYP51 (filled circles) and 5 μM HsCYP51 (hollow circles). The resultant type II difference spectra are shown for ketoconazole (A) and ketaminazole (B). Saturation curves for ketoconazole (C) and ketaminazole (D) were constructed and a rearrangement of the Morrison equation was used to fit the data¹. The data shown represent one replicate of the three performed.

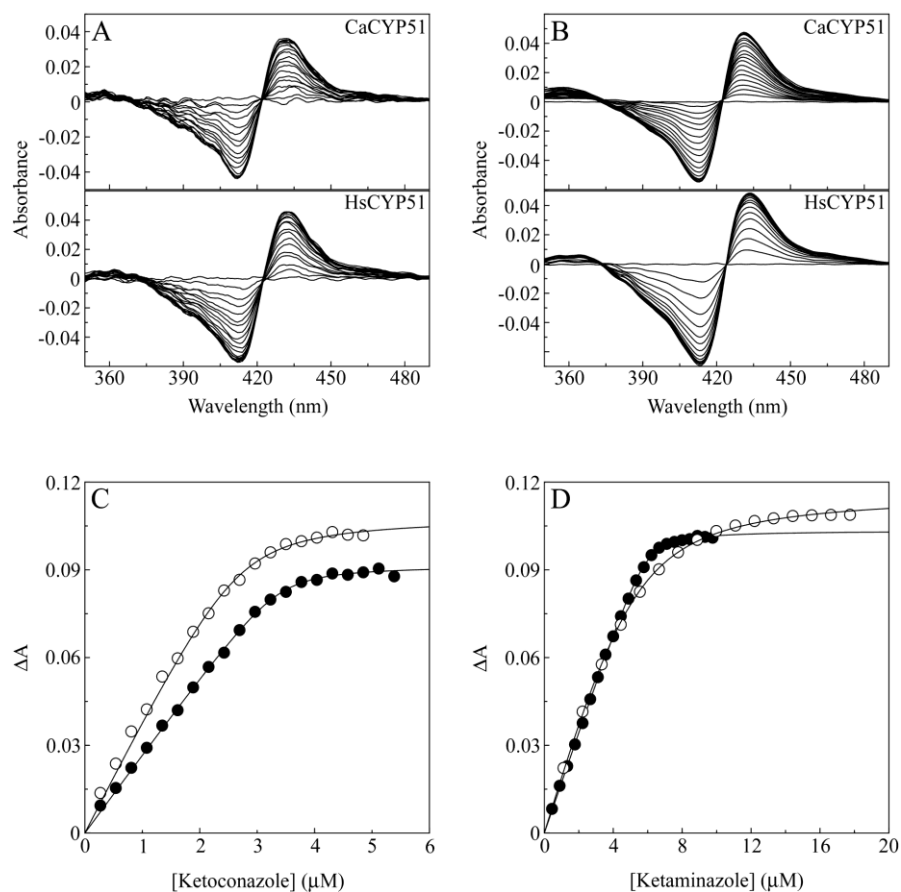
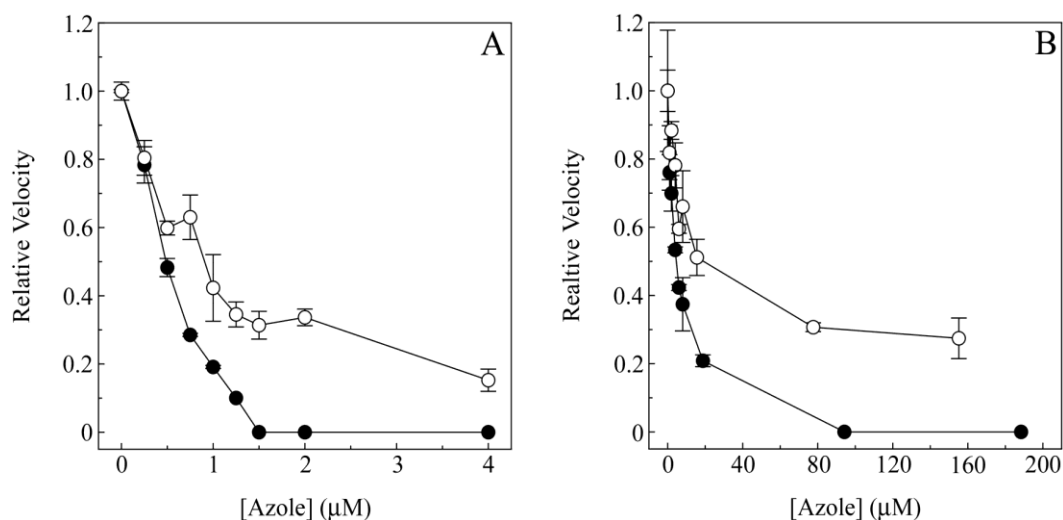
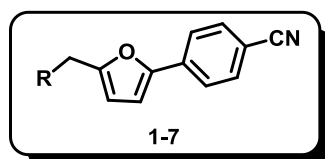


Figure 3.4 Determination of IC_{50} values for ketoconazole and ketaminazole with CaCYP51 and HsCYP51. CYP51 reconstitution assays (0.5-ml total volume) containing 1 μ M CaCYP51 (A) or 0.3 μ M HsCYP51 (B) were performed as detailed in Materials and Methods. Ketoconazole (solid circles) and ketaminazole (hollow circles) concentrations were varied from 0 to 4 μ M for CaCYP51 and up to 190 μ M for HsCYP51 with the dimethylsulfoxide concentration kept constant at 1% (vol/vol). Mean values from two replicates are shown along with associated standard deviation bars. Relative velocities of 1.0 were equivalent to 1.04 and 2.69 nmoles 14 α -demethylated lanosterol produced per minute per nmole CYP51 (min^{-1}) for CaCYP51 and HsCYP51, respectively.



3.7 Tables

Table 3.1 Representative analogues evaluated for pseudoperoxidase activity. The UV-Vis-based mauanl inhibition data (3 replicates) were fit as described in the methods section.



Compound	R	Reductive Activity	IC ₅₀ (μM) [± SD (μM)]
Zilueton	NA	Yes	0.56 [0.08]
Setileuton	NA	No	0.06 [0.007]
1		Yes	0.17 [0.05]
2		No	>150
3		No	>150
4		No	>150
5		No	>150
6		Yes	1.1 [0.2]
7		Yes	2.7 [0.4]

Table 3.2 5-LOX inhibition of Representative Analogues. The UV-Vis-based mauanl inhibition data (3 replicates) were fit as described in the methods section.

Compound	R	5-LOX IC ₅₀ (μM) [± SD (μM)]
1		0.17 [0.05]
8		0.10 [0.06]
9		1.5 [0.2]
10		>150
11		1.1 [0.10]
12		2.6 [0.3]
13		0.52 [0.07]
14		0.33 [0.07]
15		0.6 [0.1]

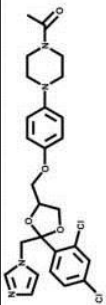
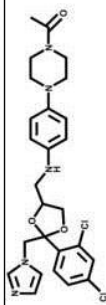
Table 3.3 Selectivity profile of representative analogues. The UV-Vis-based manual inhibition data (3 replicates) were fit as described in the methods section.

Compound	5- LOX	12- LOX	15- LOX-1	15- LOX-2	COX-1	COX-2
1	0.17	>150	>150	>150	>25	>50
13	0.52	>50	>50	>50	>150	>150
14	0.33	>150	>25	10	>150	Na
15	0.60	>50	>150	>50	Na	Na
Setileuton	0.060	>150	>150	>150	>150	>50
Zileuton	0.56	>150	>50	>150	>150	Na
Baicalein	0.84	3.3 ^a	12 ^a	>150	>150	Na

Table 3.4 Whole human blood activity profile of representative analogues. The Elisa absorption Vis-based inhibition data (3 replicates) were fit as described in the methods section, drugs were assayed at 10 μ M .

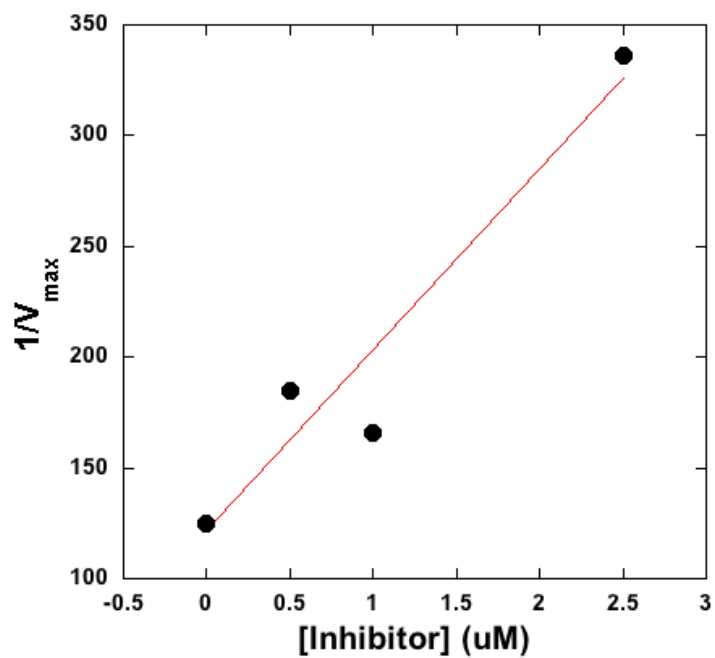
Compound	Inhibition (%)
Setileuton	100 (11)
Cicloproxin	34 (2)
Ketaminazole	45 (10)
Ketoconazole	25 (3)
13	54 (11)
1	65 (14)
15	8 (1)

Table 3.5 Reductive property (Red. act.) and IC50 values (μM), with error in parenthesis. The UV-Vis-based manual inhibition data (3 replicates) were fit as described in the methods section.

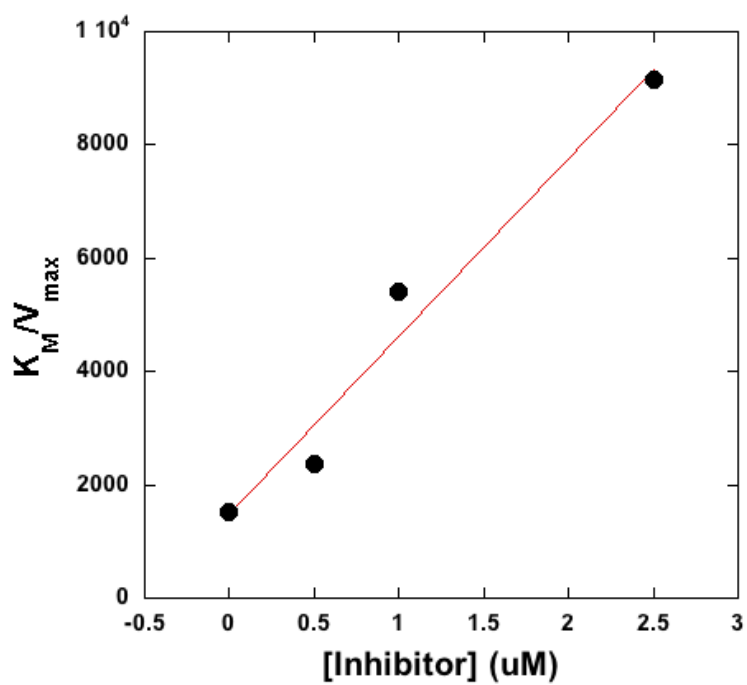
Structure	Compound	Red. act.	5- LOX	12- LOX	15- LOX-1	15- LOX-2	COX- 1	COX- 2
	ketoconazole	No	>50	>150	>50	>150	>150	>25
	ketaminazole	Yes	0.70 (0.01)	>150	>150	>150	>150	>150
NA	ciclopirox	NA	10.5 (1.1)	>100	>100	NA	>100	>150

3.8 Supporting Materials

Supplementary Figure 3.1 The $1/V_{\max}$ versus inhibitor fit with compound **13**, determining K_i . The enzyme assay was performed in 40 μM AA in 25 mM HEPES (pH 7.3), 0.3 mM CaCl_2 , 0.1 mM EDTA, 0.2 mM ATP at 22° C.



Supplementary Figure 3.2 The K_M/V_{max} versus inhibitor fit with compound **13**, determining K_I' . The enzyme assay was performed in 40 μM AA in 25 mM HEPES (pH 7.3), 0.3 mM CaCl₂, 0.1 mM EDTA, 0.2 mM ATP at 22° C.



3.9 References

1. Lutz, J. D.; Dixit, V.; Yeung, C. K.; Dickmann, L. J.; Zelter, A.; Thatcher, J. E.; Nelson, W. L.; Isoherranen, N. Expression and Functional Characterization of Cytochrome P450 26a1, a Retinoic Acid Hydroxylase. *Biochem Pharmacol* **2009**, *77*, 258-68.
2. Rubin, P.; Mollison, K. W. Pharmacotherapy of Diseases Mediated by 5-Lipoxygenase Pathway Eicosanoids. *Prostaglandins Other Lipid Mediat* **2007**, *83*, 188-97.
3. O'Byrne, P. M.; Israel, E.; Drazen, J. M. Antileukotrienes in the Treatment of Asthma. *Annals of Internal Medicine* **1997**, *127*, 472-480.
4. Radmark, O. P. The Molecular Biology and Regulation of 5-Lipoxygenase. *American Journal of Respiratory and Critical Care Medicine* **2000**, *161*, S11-S15.
5. Ford-Hutchinson, A. W.; Gresser, M.; Young, R. N. 5-Lipoxygenase. *Annu. Rev. Biochem* **1994**, *63*, 383-417.
6. Werz, O.; Steinhilber, D. Therapeutic Options for 5-Lipoxygenase Inhibitors. *Pharmacology & Therapeutics* **2006**, *112*, 701-718.
7. Pergola, C.; Werz, O. 5-Lipoxygenase Inhibitors: A Review of Recent Developments and Patents. *Expert Opinion on Therapeutic Patents* **2010**, *20*, 355-375.
8. Zouboulis Ch, C.; Saborowski, A.; Boschnakow, A. Zileuton, an Oral 5-Lipoxygenase Inhibitor, Directly Reduces Sebum Production. *Dermatology* **2005**, *210*, 36-8.
9. Faergemann, J. Management of Seborrheic Dermatitis and Pityriasis Versicolor. *Am J Clin Dermatol* **2000**, *1*, 75-80.
10. Kerr, K.; Darcy, T.; Henry, J.; Mizoguchi, H.; Schwartz, J. R.; Morrall, S.; Filloon, T.; Wimalasena, R.; Fadayel, G.; Mills, K. J. Epidermal Changes Associated with Symptomatic Resolution of Dandruff: Biomarkers of Scalp Health. *Int J Dermatol* **50**, 102-13.
11. Kuhns, D. B.; Nelson, E. L.; Alvord, W. G.; Gallin, J. I. Fibrinogen Induces Il-8 Synthesis in Human Neutrophils Stimulated with Formyl-Methionyl-Leucyl-Phenylalanine or Leukotriene B(4). *J Immunol* **2001**, *167*, 2869-78.

12. Aoki, Y.; Qiu, D.; Zhao, G. H.; Kao, P. N. Leukotriene B4 Mediates Histamine Induction of Nf-Kappab and Il-8 in Human Bronchial Epithelial Cells. *Am J Physiol* **1998**, 274, L1030-9.
13. Ryu, S.; Choi, S. Y.; Acharya, S.; Chun, Y. J.; Gurley, C.; Park, Y.; Armstrong, C. A.; Song, P. I.; Kim, B. J. Antimicrobial and Anti-Inflammatory Effects of Cecropin a(1-8)-Magainin2(1-12) Hybrid Peptide Analog P5 against Malassezia Furfur Infection in Human Keratinocytes. *J Invest Dermatol* **2011**, 131, 1677-83.
14. Faergemann, J.; Borgers, M.; Degreef, H. A New Ketoconazole Topical Gel Formulation in Seborrhoeic Dermatitis: An Updated Review of the Mechanism. *Expert Opinion on Pharmacotherapy* **2007**, 8, 1365-1371.
15. Borgers, M.; Degreef, H. The Role of Ketoconazole in Seborrhoeic Dermatitis. *Cutis* **2007**, 80, 359-63.
16. Scheinfeld, N. Ketoconazole: A Review of a Workhorse Antifungal Molecule with a Focus on New Foam and Gel Formulations. *Drugs Today (Barc)* **2008**, 44, 369-80.
17. Beetens, J. R.; Loots, W.; Somers, Y.; Coene, M. C.; de Clerck, F. Ketoconazole Inhibits the Biosynthesis of Leukotrienes in Vitro and in Vivo. *Biochemical Pharmacology* **1986**, 35, 883-891.
18. Steel, H. C.; Tintinger, G. R.; Theron, A. J.; Anderson, R. Itraconazole-Mediated Inhibition of Calcium Entry into Platelet-Activating Factor-Stimulated Human Neutrophils Is Due to Interference with Production of Leukotriene B4. *Clin Exp Immunol* **2007**, 150, 144-50.
19. Koeberle, A.; Zettl, H.; Greiner, C.; Wurglics, M.; Schubert-Zsilavec, M.; Werz, O. Pirinixic Acid Derivatives as Novel Dual Inhibitors of Microsomal Prostaglandin E2 Synthase-1 and 5-Lipoxygenase. *Journal of Medicinal Chemistry* **2008**, 51, 8068-8076.
20. McMillan, R. M.; Walker, E. R. Designing Therapeutically Effective 5-Lipoxygenase Inhibitors. *Trends Pharmacol Sci* **1992**, 13, 323-30.
21. Musser, J. H.; Kreft, A. F. 5-Lipoxygenase: Properties, Pharmacology, and the Quinolinyl(Bridged)Aryl Class of Inhibitors. *J. of Med. Chem.* **1992**, 35, 2501 - 2524.

22. Robinson, S. J.; Hoobler, E. K.; Riener, M.; Loveridge, S. T.; Tenney, K.; Valeriote, F. A.; Holman, T. R.; Crews, P. Using Enzyme Assays to Evaluate the Structure and Bioactivity of Sponge-Derived Meroterpenes. *Journal of Natural Products* **2009**, *72*, 1857-63.
23. Falgueyret, J. P.; Hutchinson, J. H.; Riendeau, D. Criteria for the Identification of Non-Redox Inhibitors of 5-Lipoxygenase. *Biochemical Pharmacology* **1993**, *45*, 978-81.
24. Young, R. N. Inhibitors of 5-Lipoxygenase: A Therapeutic Potential yet to Be Fully Realized? *European Journal of Medicinal Chemistry* **1999**, *34*, 671-685.
25. Carter, G. W.; Young, P. R.; Albert, D. H.; Bouska, J.; Dyer, R.; Bell, R. L.; Summers, J. B.; Brooks, D. W. 5-Lipoxygenase Inhibitory Activity of Zileuton. *J Pharmacol Exp Ther* **1991**, *256*, 929-37.
26. McGill, K. A.; Busse, W. W. Zileuton. *The Lancet* **1996**, *348*, 519-524.
27. Bell, R. L.; Young, P. R.; Albert, D.; Lanni, C.; Summers, J. B.; Brooks, D. W.; Rubin, P.; Carter, G. W. The Discovery and Development of Zileuton: An Orally Active 5-Lipoxygenase Inhibitor. *Int J Immunopharmacol* **1992**, *14*, 505-10.
28. Stewart, A. O.; Bhatia, P. A.; Martin, J. G.; Summers, J. B.; Rodrigues, K. E.; Martin, M. B.; Holms, J. H.; Moore, J. L.; Craig, R. A.; Kolasa, T.; Ratajczyk, J. D.; Mazdiyasi, H.; Kerdesky, F. A.; DeNinno, S. L.; Maki, R. G.; Bouska, J. B.; Young, P. R.; Lanni, C.; Bell, R. L.; Carter, G. W.; Brooks, C. D. Structure-Activity Relationships of N-Hydroxyurea 5-Lipoxygenase Inhibitors. *J Med Chem* **1997**, *40*, 1955-68.
29. Walenga, R. W.; Showell, H. J.; Feinstein, M. B.; Becker, E. L. Parallel Inhibition of Neutrophil Arachidonic Acid Metabolism and Lysosomal Enzyme Secretion by Nordihydroguaiaretic Acid. *Life Sciences* **1980**, *27*, 1047-1053.
30. Kemal, C.; Louis-Flamberg, P.; Krupinski-Olsen, R.; Shorter, A. Reductive Inactivation of Soybean Lipoxygenase-1 by Catechols. *Biochemistry* **1987**, *26*, 7064-7072.
31. Whitman, S.; Gezginci, M.; Timmermann, B. N.; Holman, T. R. Structure-Activity Relationship Studies of Nordihydroguaiaretic Acid Inhibitors toward Soybean, 12-Human, and 15-Human Lipoxygenase. *J. Med. Chem.* **2002**, *45*, 2659-2661.

32. Pham, C.; Jankun, J.; Skrzypczak-Jankun, E.; Flowers, R. A.; Funk, M. O. Structural and Thermochemical Characterization of Lipoxygenase-Catechol Complexes. *Biochemistry* **1998**, *37*, 17952-17957.
33. Nelson, M. J.; Cowling, R. A.; Seitz, S. P. Structural Characterization of Alkyl and Peroxyl Radicals in Solutions of Purple Lipoxygenase. *Biochemistry* **1994**, *33*, 4966-4973.
34. Ducharme, Y.; Blouin, M.; Brideau, C.; Châteauneuf, A.; Gareau, Y.; Grimm, E. L.; Juteau, H. I. N.; Laliberté, S. B.; MacKay, B.; Massé, F. D. R.; Ouellet, M.; Salem, M.; Styhler, A.; Friesen, R. W. The Discovery of Setileuton, a Potent and Selective 5-Lipoxygenase Inhibitor. *ACS Medicinal Chemistry Letters* **2010**, *1*, 170-174.
35. Masferrer, J. L.; Zweifel, B. S.; Hardy, M.; Anderson, G. D.; Dufield, D.; Cortes-Burgos, L.; Pufahl, R. A.; Graneto, M. Pharmacology of Pf-4191834, a Novel, Selective Non-Redox 5-Lipoxygenase Inhibitor Effective in Inflammation and Pain. *J Pharmacol Exp Ther* **334**, 294-301.
36. Lo, H. Y.; Man, C. C.; Fleck, R. W.; Farrow, N. A.; Ingraham, R. H.; Kukulka, A.; Proudfoot, J. R.; Betageri, R.; Kirrane, T.; Patel, U.; Sharma, R.; Hoermann, M. A.; Kabcenell, A.; Lombaert, S. D. Substituted Pyrazoles as Novel 5-Lipoxygenase Antagonists: Investigation of Key Binding Interactions within the Catalytic Domain. *Bioorg Med Chem Lett* **20**, 6379-83.
37. Itoh, T.; Nagata, K.; Miyazaki, M.; Ishikawa, H.; Kurihara, A.; Ohsawa, A. A Selective Reductive Amination of Aldehydes by the Use of Hantzsch Dihydropyridines as Reductant. *Tetrahedron* **2004**, *60*, 6649-6655.
38. Ito, S.; Kubo, T.; Morita, N.; Ikoma, T.; Tero-Kubota, S.; Kawakami, J.; Tajiri, A. Azulene-Substituted Aromatic Amines. Synthesis and Amphoteric Redox Behavior of N,N-Di(6-Azulenyl)-P-Toluidine and N,N,N',N'-Tetra(6-Azulenyl)-P-Phenylenediamine and Their Derivatives. *The Journal of Organic Chemistry* **2005**, *70*, 2285-2293.
39. Vouros, P.; Biemann, K. The Structural Significance of Doubly Charged Ion Spectra. Phenylenediamine Derivatives. *Organic Mass Spectrometry* **1969**, *2*, 375-386.
40. Sakurai, H.; Ritonga, M. T. S.; Shibatani, H.; Hirao, T. Synthesis and Characterization of P-Phenylenediamine Derivatives Bearing an Electron-Acceptor Unit. *The Journal of Organic Chemistry* **2005**, *70*, 2754-2762.

41. Gilbert, N. C.; Bartlett, S. G.; Waight, M. T.; Neau, D. B.; Boeglin, W. E.; Brash, A. R.; Newcomer, M. E. The Structure of Human 5-Lipoxygenase. *Science* **2011**, 331, 217-9.
42. Mogul, R.; Johansen, E.; Holman, T. R. Oleyl Sulfate Reveals Allosteric Inhibition of Soybean Lipoxygenase-1 and Human 15-Lipoxygenase. *Biochemistry* **2000**, 39, 4801-4807.
43. Deschamps, J. D.; Kenyon, V. A.; Holman, T. R. Baicalein Is a Potent in Vitro Inhibitor against Both Reticulocyte 15-Human and Platelet 12-Human Lipoxygenases. *Bioorg Med Chem* **2006**, 14, 4295-301.
44. Lewis, E. R.; Johansen, E.; Holman, T. R. Large Competitive Kinetic Isotope Effects in Human 15-Lo Catalysis Measured by a Novel Hplc Method. *J. Am. Chem. Soc.* **1999**, 121, 1395-1396.
45. Jefcoate, C. R. Measurement of Substrate and Inhibitor Binding to Microsomal Cytochrome P-450 by Optical-Difference Spectroscopy. *Methods Enzymol* **1978**, 52, 258-79.
46. Jefcoate, C. R.; Gaylor, J. L.; Calabrese, R. L. Ligand Interactions with Cytochrome P-450. I. Binding of Primary Amines. *Biochemistry* **1969**, 8, 3455-63.
47. Copeland, R. A. Evaluation of Enzyme Inhibitors in Drug Discovery. A Guide for Medicinal Chemists and Pharmacologists. *Methods Biochem Anal* **2005**, 46, 1-265.
48. Warrilow, A. G.; Martel, C. M.; Parker, J. E.; Melo, N.; Lamb, D. C.; Nes, W. D.; Kelly, D. E.; Kelly, S. L. Azole Binding Properties of Candida Albicans Sterol 14-Alpha Demethylase (Cacyp51). *Antimicrob Agents Chemother* **2010**, 54, 4235-45.
49. Strushkevich, N.; Usanov, S. A.; Park, H. W. Structural Basis of Human Cyp51 Inhibition by Antifungal Azoles. *J Mol Biol* **2010**, 397, 1067-78.
50. Amagata, T.; Whitman, S.; Johnson, T. A.; Stessman, C. C.; Loo, C. P.; Lobkovsky, E.; Clardy, J.; Crews, P.; Holman, T. R. Exploring Sponge-Derived Terpenoids for Their Potency and Selectivity against 12-Human, 15-Human, and 15-Soybean Lipoxygenases. *J Nat Prod* **2003**, 66, 230-5.
51. Deschamps, J. D.; Gautschi, J. T.; Whitman, S.; Johnson, T. A.; Gassner, N. C.; Crews, P.; Holman, T. R. Discovery of Platelet-Type 12-Human Lipoxygenase Selective Inhibitors by High-Throughput Screening of Structurally Diverse Libraries. *Bioorganic & Medicinal Chemistry* **2007**, 15, 6900-8.

52. Vasquez-Martinez, Y.; Ohri, R. V.; Kenyon, V.; Holman, T. R.; Sepulveda-Boza, S. Structure-Activity Relationship Studies of Flavonoids as Potent Inhibitors of Human Platelet 12-Hlo, Reticulocyte 15-Hlo-1, and Prostate Epithelial 15-Hlo-2. *Bioorganic & Medicinal Chemistry* **2007**, *15*, 7408-25.
53. Rai, G.; Kenyon, V.; Jadhav, A.; Schultz, L.; Armstrong, M.; Jameson, J. B.; Hoobler, E.; Leister, W.; Simeonov, A.; Holman, T. R.; Maloney, D. J. Discovery of Potent and Selective Inhibitors of Human Reticulocyte 15-Lipoxygenase-1. *J Med Chem* **2010**, *53*, 7392-7404.
54. Hutchinson, J. H.; Li, Y.; Arruda, J. M.; Baccei, C.; Bain, G.; Chapman, C.; Correa, L.; Darlington, J.; King, C. D.; Lee, C.; Lorrain, D.; Prodanovich, P.; Rong, H.; Santini, A.; Stock, N.; Prasit, P.; Evans, J. F. 5-Lipoxygenase-Activating Protein Inhibitors: Development of 3-[3-Tert-Butylsulfanyl-1-[4-(6-Methoxy-Pyridin-3-Yl)-Benzyl]-5-(Pyridin-2-Yl-methoxy)-1h-Indol-2-Yl]-2,2-Dimethyl-Propionic Acid (Am103). *Journal of Medicinal Chemistry* **2009**, *52*, 5803-5815.
55. Fogh, J.; Poulsen, L. K.; Bisgaard, H. A Specific Assay for Lukotriene B4 in Human Whole Blood. *Journal of Pharmacological and Toxicological Methods* **1992**, *28*, 185-190.
56. Spaethe, S. M.; Snyder, D. W.; Pechous, P. A.; Clarke, T.; VanAlstyne, E. L. Guinea Pig Whole Blood 5-Lipoxygenase Assay: Utility in the Assessment of Potential 5-Lipoxygenase Inhibitors. *Biochemical Pharmacology* **1992**, *43*, 377-382.
57. Estabrook, R. W.; Peterson, J. A.; Baron, J.; Hildebrandt, A. G. The Spectrophotometric Measurement of Turbid Suspensions of Cytochromes Associated with Drug Metabolism. *Methods Pharmacol.* **1972**, *2*, 303-350.
58. Omura, T.; Sato, R. The Carbon Monoxide-Binding Pigment of Liver Microsomes. II. Solubilization, Purification, and Properties. *J Biol Chem* **1964**, *239*, 2379-85.
59. Omura, T.; Sato, R. The Carbon Monoxide-Binding Pigment of Liver Microsomes. I. Evidence for Its Hemoprotein Nature. *J Biol Chem* **1964**, *239*, 2370-8.
60. Lamb, D. C.; Kelly, D. E.; Waterman, M. R.; Stromstedt, M.; Rozman, D.; Kelly, S. L. Characteristics of the Heterologously Expressed Human Lanosterol 14 α -Demethylase (Other Names: P45014dm, Cyp51, P45051) and Inhibition of the Purified Human and *Candida Albicans* Cyp51 with Azole Antifungal Agents. *Yeast* **1999**, *15*, 755-63.

61. Lipesheva, G. I.; Ott, R. D.; Hargrove, T. Y.; Kleshchenko, Y. Y.; Schuster, I.; Nes, W. D.; Hill, G. C.; Villalta, F.; Waterman, M. R. Sterol 14alpha-Demethylase as a Potential Target for Antitrypanosomal Therapy: Enzyme Inhibition and Parasite Cell Growth. *Chem Biol* **2007**, *14*, 1283-93.
62. Lipesheva, G. I.; Zaitseva, N. G.; Nes, W. D.; Zhou, W.; Arase, M.; Liu, J.; Hill, G. C.; Waterman, M. R. Cyp51 from *Trypanosoma Cruzi*: A Phyla-Specific Residue in the B' Helix Defines Substrate Preferences of Sterol 14alpha-Demethylase. *J Biol Chem* **2006**, *281*, 3577-85.
63. Venkateswarlu, K.; Denning, D. W.; Manning, N. J.; Kelly, S. L. Resistance to Fluconazole in *Candida Albicans* from Aids Patients Correlated with Reduced Intracellular Accumulation of Drug. *FEMS Microbiol Lett* **1995**, *131*, 337-41.

Chapter 4

Pseudoperoxidase investigations of hydroperoxides and inhibitors of human lipoxygenases

4.1 Introduction

The inflammatory response in humans is regulated by fatty acid signaling cascades, which are initiated by the oxidation of polyunsaturated fatty acids. Three classes of enzymes catalyze this oxidation: cyclooxygenase (COX) [1]; cytochrome P450 [2]; and lipoxygenase (LOX) [3], the last one is the focus of this study. Lipoxygenases (LOXs) are a family of iron-containing metalloenzymes that utilize a non-heme iron center to incorporate molecular oxygen into a variety of fatty acids. There are three main LOXs of pharmacological importance, 5-LOX, 12-LOX and 15-LOX. They are named according to their oxygenation position on arachidonic acid (AA) [4], which generates the hydroperoxyeicosatetraenoic acid (HPETE) product [5]. HPETEs are responsible for maintaining the homeostasis of the inflammatory response [6], and have also been implicated in many human diseases, such as asthma [7], psoriasis [8], atherosclerosis [9], cancer [10], heart disease [11,12] and diabetes [13] to name a few.

Considering the important role LOX plays in human disease, numerous inhibitors of LOX have been reported [14-28]. These can generally be classified into three

categories, reductive inhibitors, such as Zileuton [21,22], BWb70c [19,20,26], and nordihydroguaiaretic acid (NDGA) [27,28], chelative inhibitors (such as compound **1** [29] and competitive/mixed inhibitors such as compound **2** [30])(**Figure 4.1**). Nevertheless, only one of these compounds, has been approved as a drug, Zileuton [21,22], which is a potent and selective 5-LOX inhibitor [20,23]. It contains an *N*-hydroxyurea moiety, which chelates to the active ferric ion and reduces it to the inactive ferrous ion [23-25]. Many other reductive inhibitors of LOX have been found, such as *N*-hydroxyureas, hydroxybenzofurans, hydroxamic acids, hydroxylamines, and catechols [18-20,26], indicating the ease by which LOX isozymes can be inhibited in this manner. However, it is challenging to determine whether a particular inhibitor of LOX is reductive because it is difficult to concentrate human LOX isozymes to high enough concentration for the direct visualization of the active site iron by electron paramagnetic resonance (EPR). Interestingly, Zileuton and other hydroxamic acids were initially designed to chelate the iron center of LOX [21,25], but it was later determined, using the UV pseudoperoxidase assay, that Zileuton also reduced the active site iron of 5-LOX [18]. Nordihydroguaiaretic acid (NDGA), found in the *Larrea tridentata* plant, is another example of a non-specific LOX inhibitor, which possesses a dual mode of inhibition [27,31,32]. NDGA contains a catechol moiety, which binds to the active site ferric ion, but it also reduces metal center to the ferrous form, with the concomitant oxidation of the catechol moiety to the semiquinone. This reactivity is also seen with the non-heme iron

enzyme, catechol dioxygenase, whose catechol substrate is activated to the semiquinone by the active site ferric ion for oxidation by molecular oxygen [32-34].

Considering that direct detection by EPR is not practical for many human LOX isozymes, the typical method for determining whether an inhibitor is reductive in nature is the pseudoperoxidase assay. This assay measures the reduction of the fatty acid hydroperoxide product by the ferrous ion to the alkoxy radical, generating the active ferric form of LOX (**Figure 4.2**). However, for this process to be catalytic, a reducing inhibitor is required to reduce the ferric ion back to its ferrous form. This cycling results in the degradation of both the hydroperoxide product and the reducing inhibitor. The reaction is typically monitored by the reduced absorbance at 234 nm [35-37], which is due to the decomposition of the resulting alkoxy radical, triggering a loss in the conjugation of the hydroperoxide product. However, this assay is not without difficulties, and Riendeau and coworkers observed that NDGA and 13-(S)-HPODE did not support the pseudoperoxidase assay with 5-LOX [37]. An alternative method for investigating reductive inhibitors is to monitor their ability to quench the free radical of 1,1-diphenyl-2-picrylhydrazyl (DPPH); however this method is not reliable for predicting the reductive activity of LOX inhibitors. DPPH is considered a general indicator of the cellular reduction potential [38,39], which is distinct from the reduction potential of the various LOX isozymes. Alternative methods detect the loss of the hydrogenperoxide product directly through iodine oxidation [40], radiolabeling [41], thiobarbituric acid (TBA) [42], enzymatic oxidation of dyes [43], or coupled

oxidation of NADH [44]. Unfortunately, these assays are tedious and subject to various confounding factors. Simplified methods have been developed, such as those based on the fluorescent indicator, diphenyl-1-pyrenylphosphine (DPPP) [45], and the visible indicator, iron-xylene orange (XO) [46,47], both of which are oxidized by the hydroperoxy-lipids, changing their spectroscopic properties. These methods are robust and have been successfully utilized for high-throughput inhibitor screening of LOX inhibitors [29,30,45,48].

Given the need for a robust pseudoperoxidase procedure to determine the mechanism of reducing inhibitors in these studies, we utilized both the conjugated diene decomposition (UV) and iron-xylene orange (XO) pseudoperoxidase assays to determine the best hydroperoxides for the pseudoperoxidase reaction against the human isozymes, 5-LOX, 12-LOX, 15-LOX-1 and 15-LOX-2. In addition, the reductive nature of a variety of disease-related LOX inhibitors were determined utilizing the aforementioned conditions for the UV and XO assays.

4.2 Results and discussion

4.2.1 Evaluation of hydroperoxides as pseudoperoxidase substrates.

To further understand the pseudoperoxidase activity of the various LOXs, the primary products from AA and LA, 13-(S)-HPODE, 12-(S)-HPETE and 15-(S)-HPETE, were screened to determine if they were substrates for the XO pseudoperoxidase assay (**Table 4.1**). It was observed that 13-(S)-HPODE was the most effective substrate for all the LOX isozymes tested, as seen by the large

consumption of the hydroperoxide product. Interestingly, 12-(S)-HPETE and 15-(S)-HPETE were not effective pseudoperoxidase substrates, especially with 12-LOX and 15-LOX-2. We attribute this to the fact that these LOX products can also be oxygenation substrates, resulting in doubly oxygenated products (i.e. di-HETEs). For both 12-LOX and 15-LOX-2, the oxygenation rates were comparable to the pseudoperoxidase rates, making measurements difficult. For these two isozymes, the HPETE concentration was increased to 40 μ M to obtain more reliable data. In the case of 15-LOX-2, this increase in concentration allowed for a measurable pseudoperoxidase rate, above that of the oxygenation rate. However, these conditions did not allow for measurable pseudoperoxidase rates for 12-LOX. Therefore, 13-(S)-HPODE is the most reliable substrate for all of the LOX isozymes with the XO pseudoperoxidase assay.

4.2.2 Iron-xylene orange pseudoperoxidase inhibitor assay.

LOX inhibitors were screened against 5-LOX, 12-LOX, 15-LOX-1 and 15-LOX-2 to evaluate their ability to reduce the active ferric form of the isozyme. Initially the iron-xylene orange (XO) pseudoperoxidase assay with 13-(S)-HPODE was utilized with the well-characterized reductive inhibitors, Zileuton and BWB70c (**Figure 4.1**). These two inhibitors were active against all isozymes screened, indicating that each isozyme is capable of oxidizing these two inhibitors and reducing 13-(S)-HPODE to complete the pseudoperoxidase cycle (**Figure 4.2** and **Table 4.2**). 5-LOX and 15-LOX-1 displayed the most consistent pseudoperoxidase activities, displaying the

greatest total consumption of 13-(S)-HPODE. Compound **1** does not support the assay, indicating that it is not a reductive inhibitor [29]. Compound **1** is a potent and selective 12-LOX inhibitor that is currently being investigated for its effectiveness against diabetes and heart disease [29]. It has been proposed that compound **1** chelates the active site iron, similarly to Zileuton, however, it was not known at the time whether this inhibition was reductive in nature because EPR spectroscopy was not possible. The current data indicate that compound **1** is distinct from Zileuton in that it does not reduce the ferric ion to the inactive ferrous state. The 15-LOX-1 inhibitor, compound **2**, also does not display antioxidant activity. Compound **2** is a potential therapeutic for stroke, and these results are consistent with its inability to reduce the standard free radical 1,1-diphenyl-2-picrylhydrazyl (DPPH) [30]. Interestingly, ascorbic acid (**Figure 4.1**), a known reductant with high concentrations in the cell, also supported the XO pseudoperoxidase assay. This is consistent with its chelative structure and reductive nature and suggests that ascorbic acid may facilitate the conversion of LOX isozymes to their inactive ferrous form in the cell. NDGA, however, did not support the XO pseudoperoxidase assay with any of the LOX isozymes. These results are in contrast with our previous work, which demonstrated that NDGA and its various derivatives displayed reductive activity against soybean LOX-1 [27]. These apparently “conflicting” data suggest that the human LOX isozymes may interact differently with NDGA than soybean LOX-1, as previously seen with 5-LOX [37].

4.2.3 UV pseudoperoxidase activity assay.

As mentioned above, an alternative method to the XO pseudoperoxidase assay is to measure the decomposition of the hydroperoxide by monitoring the decrease in absorbance, at 234 nm. Unlike the XO pseudoperoxidase assay, in which the signal is produced by the hydroperoxide reacting directly with the ferrous xylenol orange complex, the UV pseudoperoxidase assay follows the decrease in absorbance (234 nm), due to a secondary decomposition of the alkoxy radical after the hydroperoxide oxidation of the ferrous center [35,37]. Even though the UV pseudoperoxidase assay does not directly measure the decomposition of the hydroperoxide, it does have the advantage of being a continuous assay, allowing for the rate determination pseudoperoxidase activities amongst the various human isozymes. Utilizing this method, BWb70c was screened against the lipoxygenase isozymes. It was observed that 15-LOX-1 had the greatest V_{\max} at 20 μM 13-(S)-HPODE, with a rate of 3.3 +/- 0.06 mole/sec/mole, ~20 times the velocity of 12-LOX, and ~250 times that of 15-LOX-2 (**Table 4.3**). NDGA, however, did not display UV pseudoperoxidase activity with any of these three LOX isozymes, which is consistent with the results of the XO pseudoperoxidase assay. It should be noted that the low percent decomposition of 13-(S)-HPODE in the UV assay is due to the fact that this assay is detecting the secondary decomposition of the alkoxy radical, and not the primary decomposition of the hydroperoxide, monitored in the XO assay.

4.2.4 Residual oxygenase activity after the pseudoperoxidase reaction.

Prior to this study, NDGA was shown to be a reductive inhibitor against soybean LOX-1 [27], which is consistent with its catechol structure however, it was inactive in the 5-LOX pseudoperoxidase assay [37]. In this investigation, NDGA also did neither support the pseudoperoxidase assay with 5-LOX nor with 12-LOX, 15-LOX-1 and 15-LOX-2. A possible explanation for this lack of pseudoperoxidase activity by NDGA could be due to its radical chemistry and the auto-inactivation of the human LOX isozymes. It is known that human LOX isozymes auto-inactivate [52], presumably through oxidation of active site residues by radical intermediates generated in the catalytic process, but this has not been proven conclusively [53]. Considering that the pseudoperoxidase assay generates both hydroperoxide and inhibitor radicals (the one-electron-reduced hydroperoxide and the one-electron-oxidized inhibitor, **Figure 4.2**), it is possible that either radical could inactivate LOX. Therefore, the activity of the LOX isozymes were determined by adding AA, after a significant amount of 13-(S)-HPODE and reducing inhibitor were consumed via the pseudoperoxidase activity, and measuring the residual LOX activity (**Table 4.4**). In this method, LOX treated with a BWB70c/13-(S)-HPODE mixture showed significant activity after the pseudoperoxidase assay, relative to BWb70c alone. Note that the addition of BWB70c does inhibit the enzyme, but enough residual activity is observed to establish the relative activity of the LOX isozyme with and without product present. The competitive inhibitors, compounds **1** and **2**, also retained

residual activity, which would be expected from non-reducing inhibitors. In contrast, 12-LOX, 15-LOX-1 and 15-LOX-2 did not demonstrate any oxygenase activity after the pseudoperoxidase turnover when 13-(S)-HPODE and NDGA were added, relative to NDGA alone. As mentioned above, because the inactivity of LOX observed with 13-(S)-HPODE and NDGA is relative to inhibitor alone, this lack of activity is not due to the inherent inhibitory activity of NDGA, but rather due to the cycling of the pseudoperoxidase activity with both 13-(S)-HPODE and NDGA being present. These data are consistent with the inactivation of human LOX isozymes being due to the presence of NDGA radicals generated through the pseudoperoxidase activity.

These data also indicate that NDGA is a reducing inhibitor, but that a secondary radical is possibly the potent inhibitor to the human LOX isozymes. This is consistent with the work of Riendeau and coworkers, which showed that NDGA and 13-(S)-HPODE did not support the pseudoperoxidase assay with 5-LOX [37]. We are currently investigating the nature of this radical and how it inactivates LOX, possibly through a suicide-inhibitor mechanism. It should be noted that it is unlikely that the 13-(S)-HPODE radicals, generated during the pseudoperoxidase assay, inactivate the LOX isozymes. The reaction of various reductive inhibitors (e.g. BWb70c, Zileuton and ascorbic acid) and 13-(S)-HPODE does not affect the oxygenase activity of LOX, even though 13-(S)-HPODE radicals are generated in all of these reactions.

4.3 Conclusion.

These results demonstrate that both the UV and XO assays are effective methods of detecting pseudoperoxidase activity for 5-LOX, 12-LOX, 15-LOX-1 and 15-LOX-2, if 13-(S)-HPODE is used as the hydroperoxide substrate. The AA products, 12-(S)-HPETE and 15-(S)-HPETE, are not consistent hydroperoxide substrates since they undergo a competing transformation to the di-HETE products. These two assays are also effective methods for determining whether a particular inhibitor is reductive in nature with 5-LOX, 12-LOX, 15-LOX-1 and 15-LOX-2 but there is a caveat. Reductive inhibitors generate radicals during the pseudoperoxidase assay, which in the case of NDGA can inactivate human LOX isozymes. Therefore inhibitors, which do not support the pseudoperoxidase assay, should also be investigated for rapid inactivation of the LOX isozyme in order to clarify the negative pseudoperoxidase result. In comparison, both assays do not measure hydroperoxide levels directly, with the UV assay measuring a side reaction that records only partial degradation of the hydroperoxide. However, both assays do possess particular advantages, with the XO assay allowing for a high-throughput approach, as previously reported [46,47]. In contrast, the UV assay requires less set-up time, provides pseudoperoxidase rates and allows for the determination of enzyme inactivation. Given these advantages and disadvantages of the two assays, careful thought should be given when utilizing either method. Finally, the fact that ascorbic acid supports both the UV and XO pseudoperoxidase assays may imply wider consequences of the biological reactive

state of LOX since ascorbic acid could help maintain the inactive ferrous form of LOX isozymes in the cell.

4.4 Acknowledgement

The inhibitor synthesis was performed at the NCGC by Ganesha Rai and David J. Maloney.

4.5 Methods.

4.5.1 Materials.

All commercial fatty acids (Sigma-Aldrich Chemical Company, and NuCheck) were stored at $-80\text{ }^{\circ}\text{C}$ for a maximum of 6 months. LOX products were generated by reacting substrate with the appropriate LOX isozyme (13-(S)-HPODE from soybean LOX-1 and LA, 15-(S)-HPETE from 15-LOX-2 and AA, and 12-(S)-HPETE from 12-LOX and AA). The reaction to generate product was carried out as follows. 2 liter solution of 50-100 μM substrate in the appropriate buffer (50 mM Borate pH 9.2 for soybean LOX-1, 25 mM HEPES pH 7.5 for 15-LOX-2 and 25 mM HEPES pH 8 for 12-LOX) was run to completion and quenched with 10 mL acetic acid. The products were extracted three times with dichloromethane and the resulting solution evaporated to dryness, and reconstituted with MeOH for HPLC purification. The products were HPLC-purified using an isocratic elution of 55% acetonitrile: 45% H_2O : 0.1% acetic acid. All products were tested with enzyme to show that no residual substrate was present and subjected to analytical HPLC to test for purity. Zileuton, BWb70c and NDGA were purchased from Sigma/Aldrich Chemicals. The inhibitors, compounds **1** and **2** were previously characterized and kindly provided by the NCGC. All other chemicals were reagent grade or better and were used without further purification.

4.5.2 Overexpression and purification of 5-human lipoxygenase, 12-human lipoxygenase, and the 15-human lipoxygenases.

Human reticulocyte 15-lipoxygenase-1 (15-LOX-1) [49], human platelet 12-lipoxygenase (12-LOX) [49] and human prostate epithelial 15-lipoxygenase-2 (15-LOX-2) [50] were expressed as N-terminally, His6-tagged proteins and purified to greater than 90% purity. Human leukocyte 5-lipoxygenase was expressed as a non-tagged protein and used as a crude ammonium sulfate protein fraction, as published previously [51].

4.5.3 Evaluation of hydroperoxides as pseudoperoxidase substrates.

The ability of various HPETEs to serve as substrates to the pseudoperoxidase activity was investigated with 20 μM BWb70c and the LOX isozymes. Pseudoperoxidase activity measurements were conducted on a Perkin-Elmer Lambda 40 UV/Vis spectrometer using a universal assay buffer for all human LOXs screened (50 mM Sodium Phosphate (pH 7.4), 0.3 mM CaCl_2 , 0.1 mM EDTA, and 0.01% Triton X100). The hydroperoxide concentration was 20 μM of 13-(S)-HPODE for all LOX isozymes investigated. However, in the case of 12-HPETE and 15-HPETE, 20 μM was used for 5-LOX and 15-LOX-1, whereas 40 μM was used in the case of 12-LOX and 15-LOX-2. This higher concentration of hydroperoxide was due to competing reactions for these two LOX isozymes (*vide infra*). The following concentrations of each isozyme were used (400 nM of 12-LOX, 300 nM of 15-LOX-1, 2 μM of 15-LOX-2) to 2 mLs of buffer on an oscillating shaker (22 $^\circ\text{C}$). The

reaction was initiated by addition of 20 μM BWb70c, a known reductive inhibitor. The reaction was incubated for 30 minutes and quenched with two parts of the iron-xylene orange solution (25 mM H_2SO_4 , 100 mM xylene orange, and 250 mM ferrous sulfate, solubilized in 90:10 methanol:water) [46,47]. In order to determine if any competing reactions degraded the hydroperoxide, the hydroperoxide stability (i.e. maximal absorption at 590 nm) was determined through the use of two controls. The first control measured an inhibitor/hydroperoxide solution with iron-xylene orange added, to account for any degradation of the hydroperoxide by the inhibitor. The second control measured an enzyme/hydroperoxide solution with iron-xylene orange added, to account for any breakdown of the hydroperoxide by the LOX isozyme, without the inhibitor present. These two controls allowed for the determination of the background percentage, which was subsequently subtracted from the measured percentage. In all cases, the inhibitors did not degrade a significant amount of hydroperoxide product, however, some LOX isozymes did degrade 12-(S)-HPETE and 15-(S)-HPETE by increasing their absorbance at 280 nm, presumably through converting the HPETEs to di-HETEs. Due to this slow consumption of hydroperoxide by 12-LOX and 15-LOX-2, higher concentrations of hydroperoxides (40 μM) were required to ensure a sufficient rate of the pseudoperoxidase reaction, relative to that of the aforementioned background reactions. In all assays, the primary absorption peaks for the hydroperoxide lipids and their oxidized metabolites were confined to the UV region, resulting in no overlap between their absorption bands and that of the 590 nm

oxidized iron-xylenol orange product. Controls to establish the endpoint of the pseudoperoxidase reaction (i.e. 100% degradation of the hydroperoxide) were conducted by measuring an iron-xylenol orange solution with enzyme and inhibitor, but no hydroperoxide added. Given the large error for these results, 20% or less, a positive result for pseudoperoxidase activity, after the subtraction of control rates, was considered a loss of greater than 45% absorption at 590 nm in 30 minutes. The amount of enzyme varied for each LOX isozyme, so this minimal level of detection corresponds to approximately 1.3 mol/min/mol for 12-LOX, 1.5 mol/min/mol for 15-LOX-1 and 0.25 mol/min/mol for 15-LOX-2.

4.5.4 Iron-xylenol orange pseudoperoxidase inhibitor assay.

The reductive properties of the inhibitors were determined by monitoring the pseudoperoxidase activity of lipoxygenase in the presence of 40 μ M inhibitor and 20 μ M 13-(S)-HPODE. Increased concentrations of inhibitors were used in this assay to drive the reaction to completion. Pseudoperoxidase activity measurements were conducted as described above. All inhibitors were run alone with 13-(S)-HPODE to account for direct breakdown of 13-(S)-HPODE, and to account for absorbance changes from individual inhibitors. The control inhibitors for this assay were Zileuton and BWb70c, known reductive inhibitors.

4.5.5 UV pseudoperoxidase activity assay.

The pseudoperoxidase activity rates were determined with BWb70c as the reducing inhibitor, 13-(S)-HPODE as the oxidizing product and the following

isozymes; 12-LOX, 15-LOX-1 and 15-LOX-2. Activity for all isozymes was determined by monitoring the decrease at 234 nm (product degradation) in buffer (50 mM sodium phosphate (pH 7.4), 0.3 mM CaCl₂, 0.1 mM EDTA, 0.01% Triton X100, and 20 μM 13-(S)-HPODE), with a Perkin-Elmer Lambda 40 UV/Vis spectrometer. The following concentrations of each isozyme were used (400 nM of 12-LOX, 300 nM of 15-LOX-1, 2 μM of 15-LOX-2) in 2 mLs of buffer and constantly stirred with a rotating stir bar (22 °C). The reaction was initiated by the addition of 20 μM inhibitor (at a 1:1 ratio to product), and the initial rate recorded. The percent consumption of 13-(S)-HPODE was recorded for each of the isozymes, with a loss of product less than 35% not being considered as significant activity. Individual controls were conducted with inhibitor alone with product and enzyme alone with product. These negative controls established the baseline for the assay, reflecting non-pseudoperoxidase dependent hydroperoxy product decomposition.

4.5.6 Residual oxygenase activity after the pseudoperoxidase reaction.

To evaluate whether inactivation occurred as a result of pseudoperoxidase cycling, the LOX residual activity was measured after a set amount of pseudoperoxidase turnover was completed. The activity was characterized by an increase in absorbance at 234 nm due to product formation using a Perkin-Elmer Lambda 40 UV/Vis spectrometer for all human isozymes was utilized. The same buffer (50 mM Sodium Phosphate (pH 7.4), 0.3 mM CaCl₂, 0.1 mM EDTA, and 0.01% Triton X100) and reaction mixture constantly stirred with a rotating stir bar in

2 mLs of buffer (22 °C). Pseudoperoxidase reactions were initiated as described above, except in the case of 15-LOX-1, where compound **2** (**Figure 4.1**) was screened at lower inhibitor concentration (10 μ M), due to the high potency of this inhibitor (compound **5** in our previous publication [30], $IC_{50} = 19$ nM). Oxygenase activity was evaluated 2 min post initiation of the pseudoperoxidase assay by the addition of 20 μ M AA to the reaction mixture. This time interval was determined to be sufficient to inactivate the isozymes with NDGA. Residual activity was determined by comparing the initial rates with inhibitor and 13-(S)-HPODE versus inhibitor alone, because the inhibitor itself lowers the rate of the oxygenation.

4.6 Figures

Figure 4.1. Classifications of general LOX inhibitors.

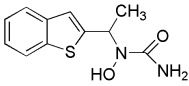
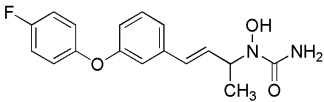
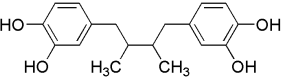
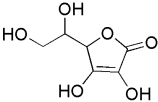
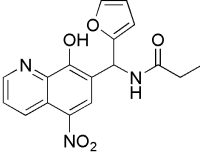
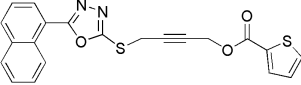
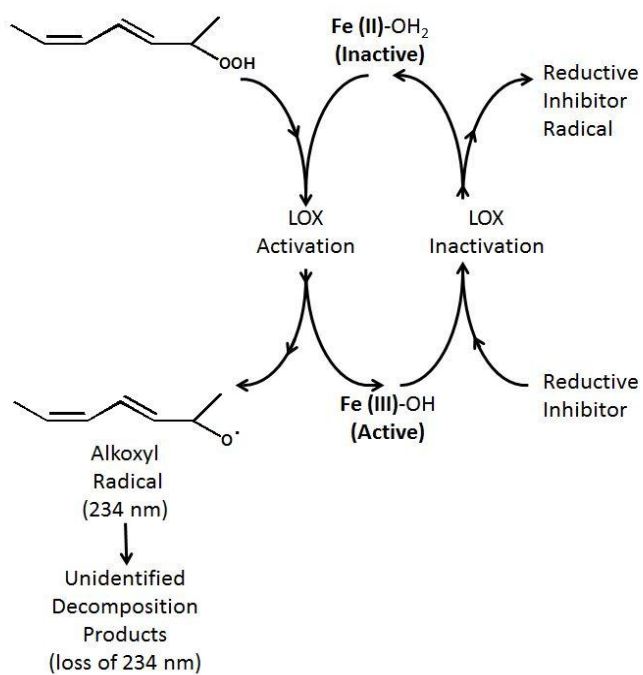
	Zileuton Chelative Reductive
	BWb70c Chelative Reductive
	NDGA Chelative Reductive
	Ascorbic acid
	1 Chelative
	2 Competitive

Figure 4.2. The LOX pseudoperoxidase reaction scheme.



4.7 Tables

Table 4.1 Product decomposition percentages with the XO pseudoperoxidase assay. ^a Assay was conducted over a 30 minute turnover period, using 20 μ M hydroperoxide and 20 μ M BWb70c within 50 mM Sodium Phosphate (pH 7.4), 0.3 mM CaCl₂, 0.1 mM EDTA, and 0.01% Triton X100. ^b All values had an error of 20% or less. ^c Due to the oxygenation reaction, 40 μ M hydroperoxide was used in these reactions.

	13-(S)-HPODE	12-(S)-HPETE	15-(S)-HPETE
5-LOX	75% ^b	80%	100%
12-LOX	50%	<20% ^c	<20% ^c
15-LOX-1	100%	100%	75%
15-LOX-2	100%	50% ^c	50% ^c

Table 4.2 XO assay percent conversion results of LOX isozymes with various inhibitors. ^b Assay was conducted over a 30 minute turnover period, using 20 μ M hydroperoxide and 40 μ M inhibitor within 50 mM Sodium Phosphate (pH 7.4), 0.3 mM CaCl₂, 0.1 mM EDTA, and 0.01% Triton X100. ^b All values had an error of 20% or less.

Compound	5-LOX	12-LOX	15-LOX-1	15-LOX-2
Zileuton	100% ^b	50%	100%	100%
BWb70c	100%	50%	100%	100%
NDGA	0%	0%	0%	0%
Ascorbic acid	50%	50%	85%	75%
1	0%	0%	0%	0%
2	0%	0%	0%	0%

Table 4.3 Rate comparison of LOX isozymes with the UV pseudoperoxidase activity. Enzyme assays were conducted using 20 μM hydroperoxide and 20 μM BWb70c within 50 mM sodium phosphate (pH 7.4), 0.3 mM CaCl_2 , 0.1 mM EDTA, and 0.01% Triton X100. The percent conversion was evaluated over a 30 minute time period.

	12-LOX	15-LOX-1	15-LOX-2
V_{max} (mole/sec/mole)	0.14	3.3	0.013
Conversion (%)	40%	50%	40%

Table 4.4 Residual activity after completion of the pseudoperoxidase assay. Enzyme was incubated for 2 min in 20 μ M hydroperoxide and 20 μ M inhibitor within 50 mM sodium phosphate (pH 7.4), 0.3 mM CaCl₂, 0.1 mM EDTA, and 0.01% Triton X100. Residual activity was measured by addition of 20 μ M AA, following the increase in absorbance at 234 nm.

Enzyme	13-(S)- HPODE/ NDGA	13-(S)- HPODE/ BWb70c	13-(S)- HPODE/ Compound #1	13-(S)- HPODE / Compound #2
12-LOX	0%	80%	100%	100%
15-LOX-1	0%	50%	100%	100%
15-LOX-2	10%	50%	100%	100%

4.8 References

1. Vane, J. R.; Bakhle, Y. S.; Botting, R. M., Cyclooxygenases 1 and 2. *Annu. Rev. Pharmacol. Toxicol.* **1998**, 38, 97-120.
2. Capdevila, J. H.; Falck, J. R.; Estabrook, R. W., Cytochrome P450 and the arachidonate cascade. *FASEB J* **1992**, 6 (2), 731-736.
3. Haeggstrom, J. Z.; Wetterholm, A., Enzymes and receptors in the leukotriene cascade. *Cell Mol Life Sci* **2002**, 59 (5), 742-753.
4. Yamamoto, S., Mammalian lipoxygenases : molecular structures and functions. *Biochim. Biophys. Acta* **1992**, 1128 (2-3), 117-131.
5. Solomon, E. I.; Zhou, J.; Neese, F.; Pavel, E. G., New Insights from Spectroscopy into the structure/function relationships of lipoxygenases. *Chem. Biol.* **1997**, 4 (11), 795-808.
6. Serhan, C. N., Lipoxin biosynthesis and its impact in inflammatory and vascular events. *Biochim Biophys Acta* **1994**, 1212 (1), 1-25.
7. Nakano, H.; Inoue, T.; Kawasaki, N.; Miyataka, H.; Matsumoto, H.; Taguchi, T.; Inagaki, N.; Nagai, H.; Satoh, T., Synthesis and biological activities of novel antiallergic agents with 5-lipoxygenase inhibiting action. *Bioorg. Med. Chem.* **2000**, 8 (2), 373-380.
8. Fogh, K.; Kragballe, K., Eicosanoids in inflammatory skin diseases. *Prostaglandins & other lipid mediators* **2000**, 63 (1-2), 43.
9. Capra, V.; Bäck, M.; Barbieri, S. S.; Camera, M.; Tremoli, E.; Rovati, G. E., Eicosanoids and Their Drugs in Cardiovascular Diseases: Focus on Atherosclerosis and Stroke. *Medicinal research reviews* **2012**.
10. Rao, C. V.; Janakiram, N. B.; Mohammed, A., Lipoxygenase and Cyclooxygenase Pathways and Colorectal Cancer Prevention. *Current colorectal cancer reports* **2012**, 1-9.
11. Yeung, J.; Apopa, P. L.; Vesci, J.; Kenyon, V.; Rai, G.; Jadhav, A.; Simeonov, A.; Holman, T. R.; Maloney, D. J.; Boutaud, O., Protein kinase C regulation of 12-lipoxygenase-mediated human platelet activation. *Molecular pharmacology* **2012**, 81 (3), 420-430.

12. Ikei, K. N.; Yeung, J.; Apopa, P. L.; Ceja, J.; Vesci, J.; Holman, T. R.; Holinstat, M., Investigations of human platelet-type 12-lipoxygenase: role of lipoxygenase products in platelet activation. *Journal of Lipid Research* **2012**.
13. Weaver, J. R.; Holman, T. R.; Imai, Y.; Jadhav, A.; Kenyon, V.; Maloney, D. J.; Nadler, J. L.; Rai, G.; Simeonov, A.; Taylor-Fishwick, D. A., Integration of pro-inflammatory cytokines, 12-lipoxygenase and NOX-1 in pancreatic islet beta cell dysfunction. *Molecular and Cellular Endocrinology* **2012**.
14. Koeberle, A.; Zettl, H.; Greiner, C.; Wurglics, M.; Schubert-Zsilavecz, M.; Werz, O., Pirinixic Acid Derivatives as Novel Dual Inhibitors of Microsomal Prostaglandin E2 Synthase-1 and 5-Lipoxygenase. *Journal of Medicinal Chemistry* **2008**, 51 (24), 8068-8076.
15. McMillan, R. M.; Walker, E. R., Designing therapeutically effective 5-lipoxygenase inhibitors. *Trends Pharmacol Sci* **1992**, 13 (8), 323-30.
16. Deschamps, J. D.; Kenyon, V. A.; Holman, T. R., Baicalein is a potent in vitro inhibitor against both reticulocyte 15-human and platelet 12-human lipoxygenases. *Bioorg Med Chem* **2006**, 14 (12), 4295-301.
17. Segraves, E. N.; Shah, R. R.; Segraves, N. L.; Johnson, T. A.; Whitman, S.; Sui, J. K.; Kenyon, V. A.; Cichewicz, R. H.; Crews, P.; Holman, T. R., Probing the activity differences of simple and complex brominated aryl compounds against 15-soybean, 15-human, and 12-human lipoxygenase. *J Med Chem* **2004**, 47 (16), 4060-5.
18. Falgueyret, J. P.; Hutchinson, J. H.; Riendeau, D., Criteria for the identification of non-redox inhibitors of 5-lipoxygenase. *Biochemical Pharmacology* **1993**, 45 (4), 978-81.
19. Pergola, C.; Werz, O., 5-Lipoxygenase inhibitors: a review of recent developments and patents. *Expert Opinion on Therapeutic Patents* **2010**, 20 (3), 355-375.
20. Robert N, Y., Inhibitors of 5-lipoxygenase: a therapeutic potential yet to be fully realized? *European Journal of Medicinal Chemistry* **1999**, 34 (9), 671-685.
21. Carter, G. W.; Young, P. R.; Albert, D. H.; Bouska, J.; Dyer, R.; Bell, R. L.; Summers, J. B.; Brooks, D. W., 5-lipoxygenase inhibitory activity of zileuton. *J Pharmacol Exp Ther* **1991**, 256 (3), 929-37.
22. McGill, K. A.; Busse, W. W., Zileuton. *The Lancet* **1996**, 348 (9026), 519-524.

23. Bell, R. L.; Young, P. R.; Albert, D.; Lanni, C.; Summers, J. B.; Brooks, D. W.; Rubin, P.; Carter, G. W., The discovery and development of zileuton: an orally active 5-lipoxygenase inhibitor. *Int J Immunopharmacol* **1992**, 14 (3), 505-10.
24. Musser, J. H.; Kreft, A. F., 5-Lipoxygenase: properties, pharmacology, and the quinolinyl(bridged)aryl class of inhibitors. *Journal of Medicinal Chemistry* **1992**, 35 (14), 2501-2524.
25. Lewis, A. J.; Glaser, K. B.; Sturm, R. J.; Molnar-Kimber, K. L.; Bansbach, C. C., Strategies for the development of new antiarthritic agents. *International journal of immunopharmacology* **1992**, 14 (3), 497-504.
26. Yeadon, M.; Dougan, F.; Petrovic, A.; Beesley, J.; Payne, A., Effect of BW B70C, a novel inhibitor of arachidonic acid 5-lipoxygenase, on allergen-induced bronchoconstriction and late-phase lung eosinophil accumulation in sensitised guinea-pigs. *Inflammation Research* **1993**, 38, 8-18.
27. Whitman, S.; Gezginici, M.; Timmermann, B. N.; Holman, T. R., Structure-activity relationship studies of nordihydroguaiaretic acid inhibitors toward soybean, 12-human, and 15-human lipoxygenase. *J. Med. Chem.* **2002**, 45 (12), 2659-2661.
28. Reddanna, P.; Krishna Rao, M.; Channa Reddy, C., Inhibition of 5-lipoxygenase by vitamin E. *FEBS letters* **1985**, 193 (1), 39-43.
29. Kenyon, V.; Rai, G.; Jadhav, A.; Schultz, L.; Armstrong, M.; Jameson, J. B., 2nd; Perry, S.; Joshi, N.; Bougie, J. M.; Leister, W.; Taylor-Fishwick, D. A.; Nadler, J. L.; Holinstat, M.; Simeonov, A.; Maloney, D. J.; Holman, T. R., Discovery of potent and selective inhibitors of human platelet-type 12- lipoxygenase. *J Med Chem* **2011**, 54 (15), 5485-97.
30. Rai, G.; Kenyon, V.; Jadhav, A.; Schultz, L.; Armstrong, M.; Jameson, J. B.; Hoobler, E.; Leister, W.; Simeonov, A.; Holman, T. R.; Maloney, D. J., Discovery of potent and selective inhibitors of human reticulocyte 15-lipoxygenase-1. *J Med Chem* **2010**, 53 (20), 7392-7404.
31. Walenga, R. W.; Showell, H. J.; Feinstein, M. B.; Becker, E. L., Parallel inhibition of neutrophil arachidonic acid metabolism and lysosomal enzyme secretion by nordihydroguaiaretic acid. *Life Sciences* **1980**, 27 (12), 1047-1053.

32. Kemal, C.; Louis-Flamberg, P.; Krupinski-Olsen, R.; Shorter, A., Reductive Inactivation of Soybean Lipoxygenase-1 by Catechols. *Biochemistry* **1987**, *26*, 7064-7072
33. Nelson, M. J.; Cowling, R. A.; Seitz, S. P., Structural Characterization of Alkyl and Peroxyl Radicals in Solutions of Purple Lipoxygenase. *Biochemistry* **1994**, *33* (16), 4966-4973.
34. Pham, C.; Jankun, J.; Skrzypczak-Jankun, E.; Flowers, R. A.; Funk, M. O., Structure of the Soybean Lipoxygenase-NitroCatechol Complex. *Biochemistry* **1998**, *37*, 17952-17957.
35. Zheng, Y.; Brash, A. R., On the Role of Molecular Oxygen in Lipoxygenase Activation. *Journal of Biological Chemistry* **2010**, *285* (51), 39876-39887.
36. Chamulitrat, W.; Hughes, M. F.; Eling, T. E.; Mason, R. P., Superoxide and peroxy radical generation from the reduction of polyunsaturated fatty acid hydroperoxides by soybean lipoxygenase. *Archives of biochemistry and biophysics* **1991**, *290* (1), 153-159.
37. Riendeau, D.; Falgueyret, J. P.; Guay, J.; Ueda, N.; Yamamoto, S., Pseudoperoxidase Activity of 5-Lipoxygenase Stimulated by Potent Benzofuranol and N-Hydroxyurea Inhibitors of the Lipoxygenase Reaction. *Biochem. J.* **1991**, *274*, 287-292.
38. Wang, H.; Li, J.; Follett, P. L.; Zhang, Y.; Cotanche, D. A.; Jensen, F. E.; Volpe, J. J.; Rosenberg, P. A., 12-Lipoxygenase plays a key role in cell death caused by glutathione depletion and arachidonic acid in rat oligodendrocytes. *European Journal of Neuroscience* **2004**, *20* (8), 2049-58.
39. van Leyen, K.; Arai, K.; Jin, G.; Kenyon, V.; Gerstner, B.; Rosenberg, P. A.; Holman, T. R.; Lo, E. H., Novel lipoxygenase inhibitors as neuroprotective reagents. *Journal of Neuroscience Research* **2008**, *86* (4), 904-9.
40. Mair, R.; Graupner, A. J., Determination of organic peroxides by iodine liberation procedures. *Analytical Chemistry* **1964**, *36* (1), 194-204.
41. Girotti, A. W., Photosensitized oxidation of membrane lipids: reaction pathways, cytotoxic effects, and cytoprotective mechanisms. *Journal of Photochemistry and Photobiology B: Biology* **2001**, *63* (1), 103-113.

42. Jiang, Z. Y.; Woollard, A. C. S.; Wolff, S. P., Lipid hydroperoxide measurement by oxidation of Fe 2+ in the presence of xylenol orange. Comparison with the TBA assay and an iodometric method. *Lipids* **1991**, 26 (10), 853-856.
43. Ferrer, A. S.; Santema, J. S.; Hilhorst, R.; Visser, A. J. W. G., Fluorescence detection of enzymatically formed hydrogen peroxide in aqueous solution and in reversed micelles. *Analytical biochemistry* **1990**, 187 (1), 129-132
44. Frew, J. E.; Jones, P.; Scholes, G., Spectrophotometric determination of hydrogen peroxide and organic hydroperoxides at low concentrations in aqueous solution. *Analytica Chimica Acta* **1983**, 155, 139-150.
45. Dahlström, M.; Forsström, D.; Johannesson, M.; Huque-Andersson, Y.; Björk, M.; Silfverplatz, E.; Sanin, A.; Schaal, W.; Pelcman, B.; Forsell, P. K. A., Development of a fluorescent intensity assay amenable for high-throughput screening for determining 15-lipoxygenase activity. *Journal of biomolecular screening* **2010**, 15 (6), 671-679.
46. Waslidge, N. B.; Hayes, D. J., A colorimetric method for the determination of lipoxygenase activity suitable for use in a high throughput assay format. *Anal Biochem* **1995**, 231 (2), 354-8.
47. Gay, C.; Collins, J.; Gebicki, J. M., Hydroperoxide assay with the ferric-xylenol orange complex. *Anal Biochem* **1999**, 273 (2), 149-55.
48. Deschamps, J. D.; Gautschi, J. T.; Whitman, S.; Johnson, T. A.; Gassner, N. C.; Crews, P.; Holman, T. R., Discovery of platelet-type 12-human lipoxygenase selective inhibitors by high-throughput screening of structurally diverse libraries. *Bioorganic & Medicinal Chemistry* **2007**, 15 (22), 6900-8.
49. Amagata, T.; Whitman, S.; Johnson, T. A.; Stessman, C. C.; Loo, C. P.; Lobkovsky, E.; Clardy, J.; Crews, P.; Holman, T. R., Exploring sponge-derived terpenoids for their potency and selectivity against 12-human, 15-human, and 15-soybean lipoxygenases. *J Nat Prod* **2003**, 66 (2), 230-5.
50. Vasquez-Martinez, Y.; Ohri, R. V.; Kenyon, V.; Holman, T. R.; Sepulveda-Boza, S., Structure-activity relationship studies of flavonoids as potent inhibitors of human platelet 12-hLO, reticulocyte 15-hLO-1, and prostate epithelial 15-hLO-2. *Bioorganic & Medicinal Chemistry* **2007**, 15 (23), 7408-25.
51. Robinson, S. J.; Hoobler, E. K.; Riener, M.; Loveridge, S. T.; Tenney, K.; Valeriote, F. A.; Holman, T. R.; Crews, P., Using enzyme assays to evaluate the

structure and bioactivity of sponge-derived meroterpenes. *Journal of Natural Products* **2009**, 72 (10), 1857-63.

52. Reynolds, C. H., Inactivation of soybean lipoxygenase by lipoxygenase inhibitors in the presence of 15-hydroperoxyeicosatetraenoic acid. *Biochemical Pharmacology* **1988**, 37 (23), 4531-7.

53. Gan, Q. F.; Witkop, G. L.; Sloane, D. L.; Straub, K. M.; Sigal, E., Identification of a Specific Methionine in Mammalian 15-Lipoxygenase which is Oxygenated by the Enzyme Product 13-HPODE - Dissociation of Sulfoxide Formation from Self-Inactivation. *Biochemistry* **1995**, 34 (21), 7069-7079.